2022

BACTERIOPHAGE INFECTION INDUCES INTRACELLULAR POLYAMINE ACCUMULATION AS A DEFENSE MECHANISM IN PSEUDOMONAS AERUGINOSA

Camilia Dornelles de Mattos

BACTERIOPHAGE INFECTION INDUCES INTRACELLULAR POLYAMINE ACCUMULATION AS A DEFENSE MECHANISM IN PSEUDOMONAS AERUGINOSA

By

Camilla Dornelles de Mattos

BS Biochemistry and Molecular Biology, University of California-Davis, Davis, CA, USA
2012

Dissertation

presented in partial fulfillment of the requirements for the degree of

Doctor of Philosophy

in Cellular, Molecular, and Microbial Biology

The University of Montana, Missoula, MT, USA

December 2022

Approved By:

Scott Whittenburg, Dean of The Graduate School

Graduate School

Patrick R. Secor

Division of Biological Sciences

Michael F. Minnick

Division of Biological Sciences

Beverly J. Piggott

Division of Biological Sciences

Brandon S. Cooper

Division of Biological Sciences

Scott Wetzel

Division of Biological Sciences

Stephen Lodmell

Division of Biological Sciences

Table of Contents

List of Figures

List of Tables

Acknowledgments

There are not enough words to describe how thankful I am to all the people who helped make this marathon expedition to a doctorate possible, but special shout outs go out to:

Patrick R. Secor – I felt like I hit the lottery, as I could not have wished for a more patient, supportive, enthusiastic, and encouraging Ph.D. mentor. I will be forever grateful for your expertise, humor, and unyielding support throughout my graduate career.

My committee members, Mike Minnick, Stephen Lodmell, Scott Wetzel, Brandon Cooper, and Beverley Piggott – Thank you for keeping me accountable and on my toes to refine my skills and get me to the level of researcher I am today.

My lab mates – A million thanks for making all the research enjoyable, keeping my spirits up, and the moral support. Appreciation goes to Margie Kinnersley, Alison Coluccio, Lia Michaels, Laura Jennings, Diane Brooks, Amelia Schmidt, Dominick Faith, Jared McGourty, Autumn Robinson, Robert Brzozowski, Conner Copeland, Madilyn Head, Eleni Wohl, Tyrza Lamma, Alex Joyce, DeAnna Bublitz, Elise Wells, Shelby Cole, Aubrey Schwartzkopf, Audrey Dozier, Devin Hunt, and Jake Cohen.

Caleb Schwartzkopf and Valery Roman-Cruz – To my best friends through this grad school experience, thank you for being my confidantes, for all the laughs, and sharing your hopes and dreams with me. You will not be forgotten.

Elizabeth Catudio-Garrett, Luke White, Lewis Sherer, Miyuki Hayashi, Aaron Held, and Adam Drobish – some of the many graduate students I got to know. Seeing how your work flourished before my eyes was an inspiration.

Sarah Weldon, David Xing, Jill Burke, and Catherine Filardi – some of the most helpful and knowledgeable people I met while I was getting my bearings at the start and getting me through the last part of this journey. Your support was invaluable.

My family – Angelo, Cristina, Pedro, Melissa, Isabella, Vera and cats Zoe, Milo, Lyra, Caspian, and Mia. Thanks for being so supportive during these years away, I wish it was easier to see you all more often. Thanks for always being in my corner.

Abstract

Cells are constantly monitoring their extracellular environment for danger signals that warn of imminent threats. When cells are killed by physical or other non-infectious injuries, they release concentrated intracellular molecules into the surrounding area. These danger-associated molecules alert other cells that danger is nearby. When cells are killed by pathogens, they release both damage-associated and pathogen-associated signals. Both eukaryotic and bacterial cells sense these molecules and make threat assessments of cellular injury. Here, I show that lysis of *Pseudomonas aeruginosa* and other bacterial species releases high concentrations of polyamines that are in turn taken up by surviving cells in a process mediated by Gac/Rsm and cyclic-di-GMP signaling. Intracellular polyamine levels spike in neighboring cells, with the duration of the high polyamine levels dictated by the infection status of the cell. In bacteriophage-infected cells, intracellular polyamine levels remain high, resulting in inhibition of bacteriophage genome replication. Linear DNA, whether in the form of packaged bacteriophage DNA or damage-induced linearized host DNA, was sufficient to induce intracellular polyamine accumulation, indicating that linear DNA is interpreted as a secondary danger signal. In addition, we discovered a group of N4-like bacteriophage that have evolved a means to disrupt intracellular polyamine accumulation and to allow for unencumbered phage replication. Because polyamines are ubiquitous to cellular life and Gac/Rsm and cyclic-di-GMP signaling are widespread amongst γ-proteobacteria, we propose that intracellular polyamine accumulation is a general strategy employed by bacteria to defend against bacteriophage infection and allow *P. aeruginosa* to make threat assessments of cellular injury.

Chapter 1: Introduction and Context

1.1 *Pseudomonas aeruginosa*, a major human pathogen

Pseudomonads are Gram-negative, γ-proteobacteria that colonize a wide assortment of environments due to versatile metabolic and physiological attributes. Being prevalent in nature, pseudomonads occupy soil, water systems, decaying organic matter, can act as a plant growth-promoting bacterium, and can be pathogenic to mammalian and plant cells [1, 2]. *Pseudomonas aeruginosa* is an opportunistic pathogenic strain that specifically presents significant problems in medical settings, as it is a leading cause of nosocomial infections in burn wounds, urinary tract infections, and pneumonia [1], as it can persist on hospital surfaces and equipment like floors, respiratory devices, dialysis machinery, and medical devices like hip replacements [3].

P. aeruginosa has a relatively large genome (5.5-7 Mbp) when compared to other free-living bacteria such as *Escherichia coli* (4.6-5.5 Mbp), *Bacillus subtilis* (4.2 Mbp), *Staphylococcus aureus* (2.8 Mbp), and *Mycobacterium tuberculosis* (4.4 Mbp) [4]. *P. aeruginosa* encodes a large number of regulatory enzymes that permit it to have great metabolic diversity and adaptability to environmental changes. Because of this enhanced coding capacity, treatment of *P. aeruginosa* infections has become a challenge as this bacterium has an increased capacity to resist many currently available antibiotics [4]. Further, excessive antibiotic usage only accelerates multidrug-resistant *P. aeruginosa* development, resulting in antibiotic therapies becoming ineffective against this bacterium [4]. Because of its prevalence in human infections and high rate of multidrug resistances, it has been deemed a major human pathogen by the World Health Organization (WHO) [5].

P. aeruginosa infection persistence is partially due to its ability to form biofilms to help attach the bacterium to surfaces. The biofilm matrix is composed of exopolysaccharides, DNA, and proteins that encapsulate bacteria, shielding them from harsh conditions like antibiotics, antibacterial agents, and immune system effectors [3, 6]. To exacerbate the issue, *P. aeruginosa* has a strong ability to develop antibiotic resistance, leading to difficulty in treating infections [3]. *P. aeruginosa* is of particular

concern to patients with cystic fibrosis (CF), as it is a predominant cause of morbidity and mortality. CF patients have abnormal airway epithelial linings that make it highly suitable for bacterial colonization, with chronic infections that can lead to pulmonary failure and death [3]. *P. aeruginosa* infections can be acute or chronic, and the type of infection determines the virulence factors, or molecules synthesized by bacteria that allow it to survive and establish within a host [7]. Acute infections are commonly associated with high mortality rates, rapid spread, tissue damage, and sepsis [8]. Acute infections are associated with expression of motility appendages like flagellum, type-IV-pili, and virulence factors like exotoxin A and lipase [9]. Chronic infections are associated with days to months-long persistence, and usually develop in CF patients [8]. During chronic infections, biofilm-related virulence factors are overexpressed to aid in persistence and antibiotic tolerance, such as exopolysaccharide expression (Psl/Pel, alginate, and elastase) [10] (**Fig 1-1**). The mechanisms that control the acute-to-chronic switch is governed by many regulatory modules. Examples include quorum sensing, bis-(3',5')-cyclic dimeric guanosine monophosphate (cyclic-di-GMP), cyclic-AMP (cAMP), and two-component systems like Gac/Rsm signaling [9-11].

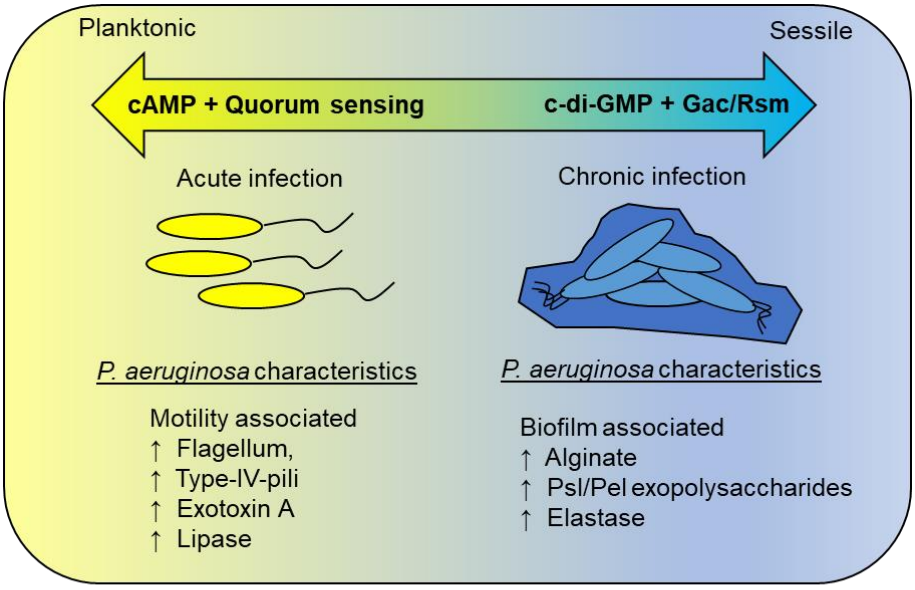

Figure 1-1. Differential virulence expression based on lifestyle in *P. aeruginosa*. Global regulators like cAMP, quorum sensing, c-di-GMP, or two-component regulator systems control the acute-to-chronic transitions, leading to differential expression of virulence factors.

1.2 Two-component regulatory systems (TCSs)

Two-component systems are a mechanism to sense and respond to environmental changes by recognizing environmental signals and, through a signal cascade, convert it into transcriptional activation [12]. The first component of the system consists of inner membrane-bound histidine kinases (HK) that sense extracellular stimuli through their sensor domains [12]. HK induction induces a conformational change that induces autophosphorylation by a bound ATP, one HK subunit donating the γ-phosphate to another HK subunit, followed by a phosphotransfer to the cognate cytoplasmic response regulator (RR) [13]. HKs are categorized by the mode of phosphoryl group transfer domains: classical, unorthodox, and hybrid (**Fig 1-2**). The classical mechanism involves a two-step phosphorelay mechanism where the HK senses a specific signal, causing an autophosphorylation of a conserved histidine residue in its H1 domain, followed by a phosphate group transfer to the cognate RR [14] (**Fig 1-2 A**). Unorthodox HK systems have a four-step phosphorelay mechanism where there is an aspartic acid residue (D1) and H2 domain in the HK and another residue in the receiver (D2) domain in the RR. Thus, the phosphate is transferred by H1-D1-H2-D2 (**Fig 1-2 B**). Lastly, a hybrid system shares similarities to the unorthodox system, but the H2 domain acts as an individual protein rather than part of the HK [14] (**Fig 1-2 C**). The two-step phosphorelay system is a rapid regulatory mechanism, whereas unorthodox and hybrid systems allow for alternate strategies to fine tune TCS activity. The RR consists of an aspartate-containing receiver domain to accept γ-phosphates and DNA binding domains [13]. The phosphotransfer to the RR activates the output domain that initiates protein-DNA or protein-protein interactions [15]. An example of an RR exerting their function through protein-protein interactions includes the chemotaxis protein CheV in *B. subtilis*, where phosphorylation of the RR CheV combines with the protein binding CheW domain and regulates the activity of chemotaxis receptor kinase complexes, which is vital for *B. subtilis* chemotaxis to attractants [16]. Other two-component systems induce expression of small non-coding regulatory RNAs (sRNAs), which affect mRNA translation in several ways, including binding to target mRNAs to either block ribosome binding and translation or stabilizing mRNA secondary structures to increase translation rates.

sRNAs can also affect post-transcriptional gene expression by binding and sequestering global post-transcriptional regulators [17].

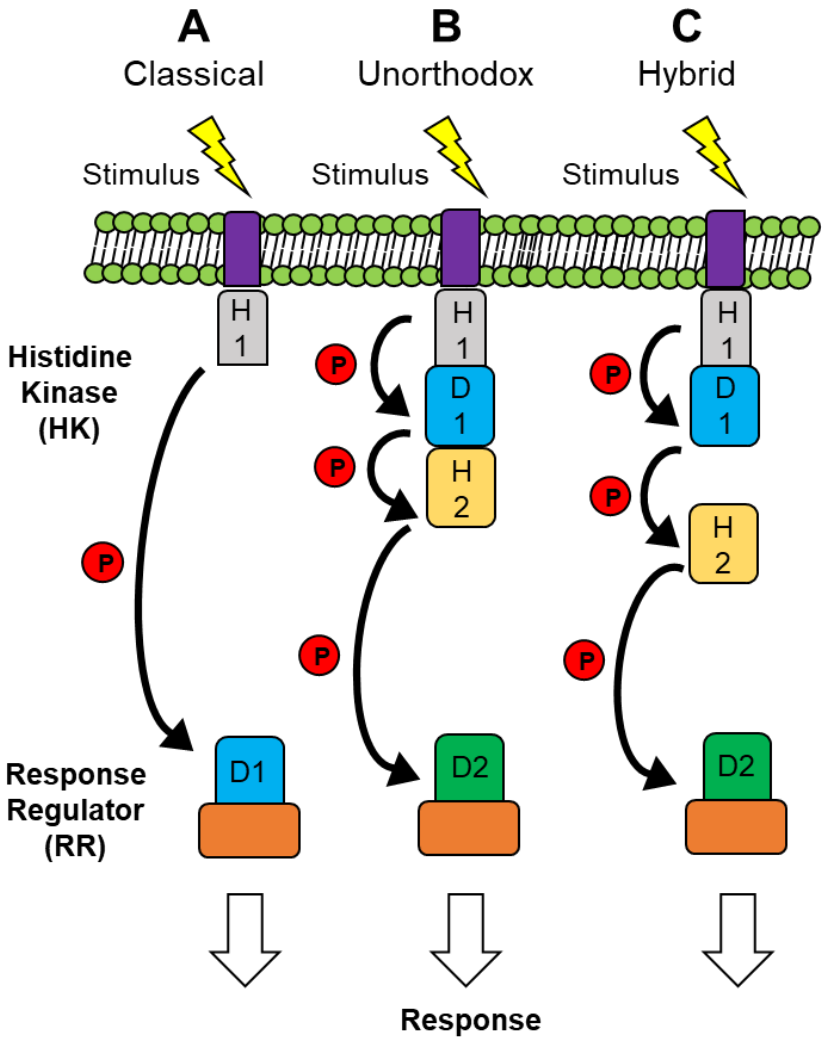

Figure 1-2. Schematic of two-component systems. Histidine kinases (HKs) sense stimulus using their sensor domains, causing one HK to donate its phosphate to a response regulator (RR). The RR triggers downstream responses. (A) Classical systems consist of a stimulus interacting with the input domain (purple), followed by transmitter domain (H1, gray) autophosphorylation and transfer to the receiver (D1, blue) domain of the RR. (B) Unorthodox systems consists of the H1 domain (gray) being followed by an additional aspartic domain (D1, blue) and a H2 (yellow) domain of HK. The phosphate group is transferred to the receiver domain (D2, green) of the RR. (C) Hybrid systems are similar to unorthodox but have the H2 domain (yellow) act as an external phosphotransfer protein as opposed to being part of the HK.

Finally, to reset the system for another round of signal transduction, the RR is dephosphorylated by the phosphatase-activity of the cognate sensor or an unrelated phosphatase [18]. One of the biggest challenges in characterizing two-component systems is identifying the stimuli that the histidine kinases sense. There are a number of indications that signals such as light, temperature, pH, osmolarity, oxygen pressure, specific ions, redox states, and quorum sensing molecules could be possible candidates, but two-component input signals are largely unknown [19].

1.3 The Gac/Rsm two-component signaling pathway

The focus of this thesis is on the two-component system (TCS) called Gac/Rsm (named such for global activation and regulator of secondary metabolism) that modulates a wide range of virulence and stress-responsive genes, such as extracellular enzyme production, toxin secretion, quorum sensing molecules, motility, biofilm formation, and the acute-to-chronic infection transition [20]. This TCS has homologous systems in other γ-proteobacteria and are referred to LemA (GacS)/GacA in *Pseudomonas*, *Erwinia,* and *Vibrio fisherii* species, CsrA/CsrB in *E. coli*, VarS/VarA in *Vibrio cholerae,* BarA/SirA in *Salmonella*, and LetS/LetA in *Legionella* [21]. The first two of three sensor kinases for this system are RetS and LadS, which compete for binding with the last sensor kinase GacS. RetS and LadS act in opposing manners, where LadS stimulates the system and RetS forms inactive heterodimers with GacS, preventing phosphorylation of the response regulator GacA [9, 22] (**Fig 1-3**). Gac/Rsm signaling begins when the sensor kinase GacS is activated by an unknown ligand. The response regulator GacA is phosphorylated by GacS, inducing the transcription of small RNAs *rsmY* and *rsmZ* [23, 24]. These sRNAs contain GGA motifs in the exposed stem loops of their predicted secondary structures, which allows for binding to RNA-binding proteins acting as global posttranscriptional repressors [21]. In *P. aeruginosa*, sRNAs RsmY/RsmZ will bind to RsmA, the RNA-binding protein that specifically recognizes and binds to conserved GGA motifs in 5'-untranslated regions (5'-UTRs) of their target mRNAs, preventing ribosome binding and translation [23, 24]. Of note, RsmA controls second messenger cyclic-di-GMP levels through repression of the *sadC* gene, which can control biofilm formation and responses to external stimuli [6]. An inactive Gac/Rsm

system is associated with acute infection gene expression, whereas an active system is associated with chronic infection, such as biofilm formation [25]. There are many studies aiming to characterize the activating ligand for Gac/Rsm, but to date the only agreement is that the molecule is small, water-soluble, and possibly nonpolar, but there are conflicting studies for the latter [19, 20, 26].

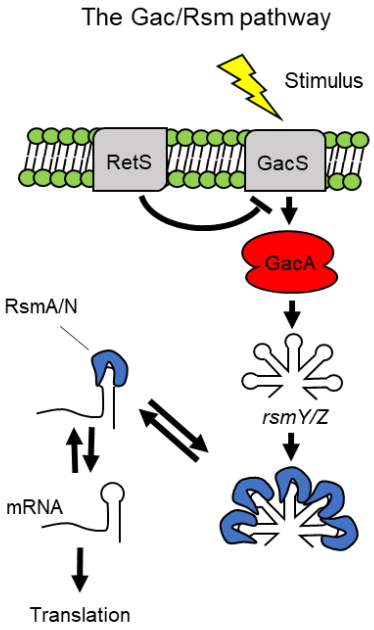

Figure 1-3. Schematic of Gac/Rsm signaling pathway in *P. aeruginosa*.
Gac/Rsm signaling is initiated by the activation of the sensor histidine kinase GacS by unknown ligands. GacS phosphorylates the response regulator GacA, which induces the transcription of the small RNAs *rsmY* and *rsmZ*. These sRNAs bind and sequester the mRNA-binding proteins RsmA or RsmN away from their target mRNAs, allowing the translation of hundreds of different mRNAs.

1.4 Bacteriophages

Bacteriophages (or phages) are viruses that infect bacteria. Phages are the most abundant biological entities on Earth, with an estimated 10^{31} phage particles on the planet, outnumbering bacteria by about 10-fold [27]. Phages range in diversity, from those with DNA or RNA and single-stranded or double-stranded genomes packaged and condensed in linear form [27]. Phage infection starts at the adsorption/attachment of phage on the cell surface. Through random collisions between phage and host, the receptor-binding proteins on the phage surface bind to cell surface receptors on the host. Common host receptors include lipopolysaccharides (LPS), type-IV-pili, or flagella

[28]. Following successful attachment, phage will then inject their genome into the host cytoplasm [28]. At that point, the phage genome will enter into one of two life cycles: lytic or lysogenic, with phages that can transition between the two life cycles being deemed as temperate and those that cannot referred to as lytic (**Fig 1-4**) [28]. During the lytic cycle, the phage shunts the host cell's replication machinery to initiate replication, transcription, and translation of phage proteins and nucleic acids. Once complete, phage virions are assembled from the individual phage proteins and the replicated genome is packaged into a proteinaceous head. Once enough virions are constructed, phage-encoded endolysins translocate to the periplasm and cleave host peptidoglycan, causing cell lysis, virion release, and host death. Burst size, or the number of virions that exit a host cell, varies from phage to phage [29]. In the lysogenic

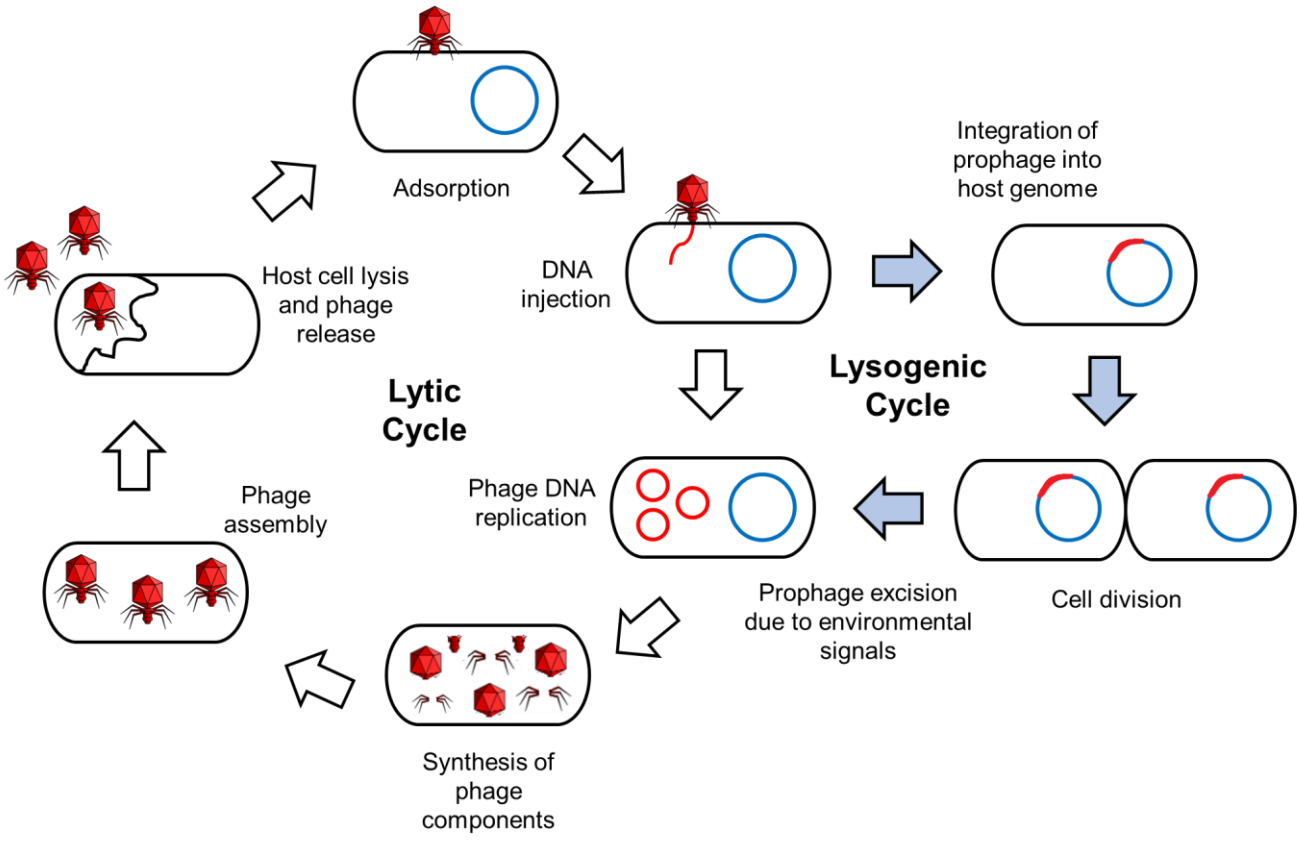

Figure 1-4. Bacteriophage lifecycle overview. (Left side cycle) In the lytic cycle, phage injects its genome into the host cell after attachment to the host. The phage DNA replicates, followed by translation of new virion components. The replicated genomes are combined with the phage components to assemble new virions. When all is complete, the host cell is lysed and new phage are released into the extracellular space. (Right side cycle) In the lysogenic cycle, the phage genome integrates into the host chromosome and replicates when the host undergoes cell division. If the appropriate signals are sensed by the prophage, it will excise and shift into the lytic cycle.

life cycle, viral genomes remain in the host either as an extrachromosomal plasmid or integrated into the bacterial chromosome as a prophage. The bacterial host carrying a prophage is termed a lysogen, with the prophage replicating along with the bacterial genome as it divides. Phage genes are silenced by phage repressor proteins, keeping the phage from converting to the lytic cycle. These repressor proteins can also confer repressor-mediated immunity, where the repressor prevents superinfection by other phages with similar repressors, silencing their lytic genes too [29]. The systems described above are relevant to well-studied phages like *E. coli* phages λ and T7, as phage biology is vast and diverse.

1.5 Bacterial phage defense systems

The co-interaction between bacteria and phage induced a mutual adaptation and counter adaptation (also called coevolution) caused by selection pressure. Bacteria evolved adaptations to prevent phage infection using defense systems. Examples include cleaving invading viral DNA within the cell, blocking phage genome replication, and halting of viral assembly [28]. In response, phages have evolved means to overcome these defense systems, such as modifying their receptor-binding proteins to allow for adsorption and overcoming targeted nucleic acid cleaving by encoding anti-restriction–modification, anti-CRISPR systems, and point mutations in specific sequences [30]. The most researched bacterial defense systems include innate-system like restriction modification systems (RMs), abortive infection (Abi), and adaptive-immune systems like CRISPR-Cas [31].

RM systems are composed of a restriction endonuclease (RE) and a methyltransferase (MT). The methyltransferase recognizes self/host DNA and subsequently methylates specific DNA sequences, protecting the modified host DNA from the RE, as it targets the same sequences but only cleaves unmodified DNA (perceived as non-self) [32]. By these means, incoming viral DNA that arrives unmodified is cleaved by the RE due to lack of modification. RM systems are grouped into four types based on their substrate specificity, cofactor requirements, subunit composition, sequence recognition, and cleavage position. Type I enzymes form a protein complex that has both restriction and modification capabilities and cleave a distance away from the target site (~100 bp to

10,000 bp). Type II systems are the most well studied and are composed of separate RE and MT enzymes and cleave DNA close to the target site. Type III systems are heterotrimers (MT_2RE_1) or heterotetramers (MT_2RE_2) and compete among themselves for modification or restriction in the same catalytic cycle. Recognition is achieved when two recognition sequences are in an inverse position relative to each other. Finally, type IV systems cleave DNA substrates at specific methylated sequences. However, these systems are recent discoveries and as such are not well studied [32]. Examples of RM-like defense systems that use methylation for self/non-self-discrimination include the defense island associated with restriction modification system (DISARM) and bacteriophage exclusion system (BREX) [28, 33].

In abortive infection (Abi), the cell recognizes phage infection and the cell metabolically shuts down, becomes dormant, or kills itself. Abortive infections have varying activating signals to allow for cell death to interrupt phage at multiple lifecycle stages during infection [33]. These systems are composed of at least two modules: one that senses the phage infection and one that shuts down metabolism or kills the cell upon infection detection. Abi systems can recognize a variety of phage-associated intermediates including phage genome replication and transcription, structural phage proteins, or inhibition of other defense systems. Examples of Abi system mechanisms include degrading inner membranes, indiscriminate degradation (whether it be host or phage) of genomes and messenger RNAs (mRNAs), transfer RNA (tRNA) degradation, and host translation machinery degradation. Many times the Abi-induced growth arrest leads to eventual host death, but sometimes it is reversible [34]. Some examples of Abi systems include the RexAB system that senses phage protein-DNA complexes and forms an ion channel in the inner membrane, causing a loss of membrane potential and drastic drop in cellular ATP levels, ultimately inhibiting cellular growth and phage production [33]. Another Abi system includes toxin-antitoxin (TA) systems that consist of two genes; one encoding a toxin and one encoding an antitoxin granting immunity to the toxin protein. TA systems are divided into six types, but the most common type seen is type II TA systems where the toxin and antitoxins are proteins that physically bind to one another, preventing toxicity. The antitoxin is less stable than the toxin and is more likely to be degraded by cellular proteases, so production of the antitoxin must be maintained.

During times of cellular stress, protein production slows and the antitoxin is degraded, freeing the stable toxin and causing cell death through indiscriminate degradation of host and phage mRNAs [33].

Lastly, some bacteria have an adaptive-immune system called CRISPR-Cas (clustered repeated interspaced palindromic repeats - CRISPR associated genes) [31]. In this system, previous exposure to infection is archived to allow for any subsequent infections with phage nucleic acids to be cleaved in a sequence-specific manner. The system provides a memory of previous infection through spacer acquisition of phage protospacers, recognition of similar sequences by crRNA-Cas protein complexes, and silencing of viral nucleic acids through base-pairing and nuclease activity. The bacterial genome contains the CRISPR array (short 30-40bp unique spacer sequences that may or may not be palindromic that alternate with repeats). The spaces serve as DNA templates for CRISPR RNAs (crRNAs). The spacer sequences feature phage- or plasmid-derived genetic material, making CRISPR a specific defense mechanism [35]. Cas proteins target invading DNA by pairing with the crRNA from the CRISPR loci to form the CRISPR-Cas effector complex that screens and cleaves matching (foreign) nucleic acids [35]. Bacterial phage defense systems are able to recognize phage infection, but how these systems make threat assessments is not well studied. My dissertation delves into this gap using *P. aeruginosa* as a model organism.

1.6 Bacterial threat assessment

An immune system traditionally consists of specialized cells that detects the presence of threats and mounts an appropriate response. The uncovering of the adaptive immune-like system CRISPR-Cas in prokaryotes revealed that adaptive immunity is present in single-celled organisms [36-38]. It stands to reason that organisms as ancient as prokaryotes would also have evolved the capability to sense threats and orchestrate protective procedures, not unlike the innate immune system of eukaryotes. Eukaryotic cells detect threats using conserved pattern recognition receptors (PRRs), with examples of danger-associated signals including ATP, oxidized lipids, microbial-derived molecules, and intracellular proteins, as these molecules are normally located inside cells and are indicative of cellular damage [37, 38]. Cells can then make threat

assessments based on the nature of the danger signal to initiate appropriate responses. Examples include leukocyte recruitment during cellular injury to modify immune and coagulation systems to protect the area as a whole, whereas an infectious injury would mount a defensive response by recruiting immune cells to destroy infected cells and extracellular pathogens [39].

Like eukaryotic cells, bacteria can also sense and respond to molecules released by lysed cells. More often than not, bacterial danger sensing mechanisms that have been characterized are often mediated through two-component regulatory systems, but other types of regulatory pathways have also been described. For example, *P. aeruginosa* and *Salmonella enterica* detect molecules released by lysed bacteria, inducing an upregulation of antibacterial and antimicrobial pathways to protect themselves from imminent threats like competing bacterial species. These defensive responses were mediated through the two-component systems Gac/Rsm and PhoPQ, respectively [26, 36, 40]. One difficulty in characterizing bacterial danger sensing mechanisms is that many of these defense systems are regulated by two-component systems, and the identities of the danger signal molecules are not characterized. Further, many danger signal response pathways only look into the cellular responses to bacterial competition and less so on the effects of phage infection. My dissertation investigates the cellular responses in the context of phage infection as a result of cell lysis.

1.7 Polyamines

Polyamines are polycations that consist of aliphatic hydrocarbon chains with various amine groups [41, 42]. Polyamines are found in nearly all lifeforms on Earth, with some Archaea and certain bacteria like *Staphylococcus aureus* being exceptions [43]. Polyamines interact directly and indirectly with various molecules such as DNA, RNA and proteins to modulate gene expression [44]. Downstream effects of polyamine interactions include enhancing or inhibiting transcription and translation, cell growth stimulation or stalling, and inducing stress responses [45, 46]. The most common types of polyamines found in bacteria are putrescine, spermidine, spermine, and cadaverine [47]. Further, the intracellular concentrations of polyamines range from 0.1 mM to 30

mM in bacteria [43, 47]. As polyamines can enhance or hinder cellular functions, polyamine level homeostasis needs to be tightly controlled.

1.7.1 Biological functions of polyamines

Polyamines have many uses in bacterial cells. They can be used as nitrogen and carbon sources in times of scarcity, which allows for persistence [44]. As polyamines are protonated at cellular pH, they act as counter ions to negatively-charged DNA and RNA. Polyamines are crucial for cell homeostasis, as their functions include modulating transcription and translation, stimulating cell growth, biofilm formation, and virulence factor expression [41, 48]. For example, polyamines can bind to ribosomes and increase codon usage accuracy, causing upregulation of genes involved in energy metabolism, tRNA/mRNA expression, and transport protein production on cell membranes [49]. Polyamines can also spur stress response activation, as they have roles in activating SOS systems and resistance mechanisms in response to acidic compounds, antibiotics, and oxidative stress [46]. Polyamines have been reported to coat bacterial surfaces, shielding the bacterium from cationic peptides, aminoglycosides, and quinolone antibiotics [46]. Depending on the species, intracellular polyamines can enhance or inhibit DNA gyrase activities [43]. While polyamines can increase cellular processes, high intracellular levels of polyamines can inhibit cellular functions, either by blocking access sites or inducing conformational changes due to charge neutralization [44, 50]. Finally, while polyamines are crucial for growth in many bacterial species, there is evidence that many Gram-positive bacteria subsist on very low levels of polyamines and can grow and form biofilms in polyamine-independent ways, although the means by which this is done is poorly characterized [51, 52].

Polyamines are also vital for many viral infections. As polyamines are polycationic, they are frequently bound to negatively-charged phage nucleic acids to allow for charge neutralization to allow for condensing of the genome for packaging [53, 54]. Further, many phages manipulate intracellular polyamine levels to enhance viral DNA replication and protein translation by promoting polyamine accumulation or synthesis [55, 56]. As mentioned earlier, polyamines are able to coat bacterial cell surfaces, which can block

phage attachment by competing for binding receptors or reducing receptor expression on the cell surface [57]. Lastly, high polyamine levels can cause phage DNA aggregation, making the template DNA unavailable for transcription or replication by RNA or DNA polymerases, respectively [58, 59].

1.7.2 Polyamine biosynthesis

Intracellular polyamine levels can be altered by either *de novo* biosynthesis or importing exogenous polyamines from the extracellular space. Polyamines can be synthesized from the amino acids ornithine and methionine, with arginine and lysine serving as secondary sources [45]. Putrescine can be made through two pathways: from ornithine through ornithine decarboxylase (ODC) and from arginine via arginine decarboxylase (ADC) and agmatinase [60]. Spermidine and spermine can be made from putrescine by adding aminopropyl groups by spermidine and spermine synthases that are sourced from the methionine derivative—decarboxylated S-adenosylmethionine (dcAdoMet or dSAM) produced by a S-adenosylmethionine decarboxylase (AdoMetDC) [60].

1.7.3 Polyamine catabolism

As excessive polyamines are cytotoxic, bacteria must oxidize or acetylate polyamines to ensure their cellular activities remain active. In *P. aeruginosa*, polyamine catabolism is directed by three kinds of reactions: γ-glutamylation, aminotransferase activity, and spermine/spermidine dehydrogenases [45]. In *P. aeruginosa*, the most versatile polyamine catabolism pathway is through the γ-glutamylation pathway (GGP). This pathway consists of four consecutive reactions whose enzymes are encoded by the *pauABCD* locus with redundant specificities for different polyamines [61]. GGP genes include six *pauA* (*pauA1* to *pauA6*), four *pauB* (*pauB1* to *pauB4*), one *pauC* (*pauC*), and two *pauD* (*pauD1* and *pauD2*) homologues [61, 62]. Specific combinations of *pauA* genes are specific for catabolism of putrescine, spermidine, and spermine [61]. Other less described catabolic reactions include putrescine cleavage using aminotransferases (possibly *kauB* or *spuC*) and dehydrogenases (example *spdH*) to produce succinate as a nitrogen source, but these studies are still preliminary [45, 61, 63, 64]. Further, there are indications that spermidine and spermine catabolism are also performed by the first

three genes in the *spuABCDEFGH* operon, but the biochemical functions of the gene products of *spuA* and *spuB* are not well characterized [63].

1.7.4 Polyamine uptake/import

There are some bacteria (but not *P. aeruginosa*) that lack polyamine biosynthetic pathways and must import polyamines from the extracellular environment. Polyamine import is more energetically economical than biosynthesis, in terms of ATP consumption. Polyamine uptake is important for optimizing cell growth, metabolism, and environmental adaptation, and deficiencies in a system leads to attenuated virulence and type II secretion system expression [45, 65]. *P. aeruginosa* encodes at least three ATP-binding cassette (ABC)-type polyamine transport systems: the second half of the *spuABCDEFGH* operon (*spuEFGH*), *potABCD* and *potFGHI* operons. All three systems are made up of one periplasmic polyamine binding proteins, two transmembrane channel forming proteins, and a membrane-associated ATPase [65]. The *spuEFGH* portion of the operon uptakes spermidine and other polyamines, in which SpuE is a periplasmic spermidine-binding protein, SpuG and SpuH constitute the transmembrane channel, and SpuF is a cytoplasmic ATPase [65]. PotABCD is a spermidine importer that consists of a membrane-associated ATPase (PotA), two transmembrane channel-forming proteins (PotB and PotC), and a periplasmic substrate-binding protein for spermidine (PotD) [50]. PotFGHI is a putrescine importer consisting of a periplasmic substrate binding protein for putrescine (PotF), membrane-associated ATPase (PotG), and two transmembrane channel-forming proteins (PotH and PotI) [63, 66]. As the three transport systems have overlapping polyamine preferences, the loss of one system can be compensated by a different system.

1.8 Aims of this dissertation

My dissertation focuses on (1) characterizing the molecule (later on identified as being polyamines) that upon high enough exposure triggers a reduction in phage titers in *P. aeruginosa*, (2) linking the exposure to extracellular polyamines to a Gac/Rsm-dependent intracellular polyamine accumulation (IPA) that inhibits phage DNA replication and transcription, and (3) identifying specific characteristics of IPA triggers and point out a family of phages that overcome this tolerance phenotype despite high

intracellular polyamine levels. This research adds to the knowledge base on how polyamines affect phage replication in the model organism *P. aeruginosa*. This research spotlights danger signaling as a common feature across biological domains, and can highlight general means that cells respond to viral infection and cellular injury.

Chapter 2: Bacterial lysate induces Gac/Rsm-dependent phage tolerance

2.1 Introduction

Bacteria face a multitude of threats to their survival, ranging from abiotic stressors (temperature, moisture, UV radiation, nutrient availability, etc.), overt antagonism by other bacteria, and bacteriophage (phage) infection [36]. When these events occur, cellular injury can occur, which results in the release of bacterial contents into the extracellular space. Similar to how eukaryotic cells sense danger signals to raise appropriate immune responses through pattern recognition receptors (PRRs), bacterial cells also can detect and respond to molecules released by lysed bacteria [26, 36, 67, 68]. For example, *Pseudomonas aeruginosa* can sense substances in lysed neighboring bacteria through the Gac/Rsm pathway [26, 36]. In response to kin cell lysis exposure, Gac/Rsm is upregulated and antibacterial pathways initiate to shield *P. aeruginosa* from competing bacterial species. Nevertheless, the identity of molecules that act as danger signals in bacteria are scantily characterized and effects on bacterial responses to viral infection are poorly understood.

In *P. aeruginosa*, the Gac/Rsm pathway is a two-component system that has a wide-ranging regulon that modulates multiple virulence factors, such as biofilm formation, quorum sensing, motility, and lifestyle decisions [22, 69]. Gac/Rsm signaling induction occurs when the sensor histidine kinase GacS is activated and phosphorylates the response regulator GacA, which regulates the expression of *rsmZ*/*rsmY* by directly binding to the sequence upstream of these sRNA genes. The sRNAs bind and sequester the RsmA protein from its target mRNA (**See Fig 1-3 and 2-6**). Furthermore, an additional sensor kinase, RetS (regulator of exopolysaccharide and type III

secretion) works with GacS to modulate GacA [25]. The sensor kinase RetS counteracts GacS activity and inactivation of the *retS* gene constitutively activates Gac/Rsm signaling [9, 70, 71]. As of yet, the activating ligand for Gac/Rsm system activation is still unknown [19]. While the mechanisms and downstream effects of many two-component systems are well investigated, the biggest challenge is identifying the stimulating signal. A variety of signals such as light, temperature, pH, osmolarity, oxygen species or concentration, pressure, ions, redox states, and quorum sensing molecules have been identified as candidates, a majority of two-component system input signals have yet to be confirmed as the principal signal [19].

Gac/Rsm signaling modulate lifestyle decisions in *P. aeruginosa* through a few mechanisms. One process occurs upon activation of Gac/Rsm signaling, causing an increase in intracellular levels of the second messenger cyclic-di-GMP through SadC expression [6]. Cyclic-di-GMP, a cyclic dinucleotide signaling molecule, regulates processes involved in the transition between motile (low cyclic-di-GMP) and sessile (high cyclic-di-GMP) lifestyles in response to external stimuli [72]. High cyclic-di-GMP levels are associated with biofilm formation, which has been shown to be protective against antibiotics or antibacterial treatments [73]. However, whether the high cyclic-di-GMP state could also confer protection against phage infection is not well explored. To that end, we sought to investigate the role of cyclic-di-GMP and Gac/Rsm signaling in protecting against infectious threats in the face of nearby cellular death.

In this chapter, experiments are described testing the hypothesis that lysed bacterial cells release danger signals that triggers a transient phage tolerance phenotype in surviving cells. We used RNA-sequencing and microbial genetics to characterize cellular responses of *P. aeruginosa* to cell lysates and phage infection. Using purification techniques to characterize the activating signal, we determined that the activating molecule is small, heat-stable, and water soluble. We also determined that Gac/Rsm and cyclic-di-GMP signaling is required for lysate-induced phage tolerance to be triggered, indicating a role for it in maintaining cellular integrity in response to infectious phage threats. Lastly, because Gac/Rsm signaling is conserved across γ-proteobacteria and other species' cell lysates induced phage tolerance, this response

may indicate a broad strategy that bacteria utilize to defend themselves against bacteriophage infections.

2.2 Materials and Methods

2.2.1 Bacterial Strains, bacteriophages, and culture conditions

Bacterial strains, phages, and plasmids are listed in Table 2-1. Deletion mutants were constructed using allelic exchange and Gateway technology, as described previously [74]. Unless indicated otherwise, bacteria were grown in lysogeny broth (LB) at 37°C with shaking and supplemented with antibiotics (Sigma) or 0.1% arabinose when appropriate. Unless otherwise noted, antibiotics were used at the following concentrations: gentamicin (10 or 30 μg ml^{-1}), ampicillin (100 μg ml^{-1}), and carbenicillin (300 μg ml^{-1}).

Table 2-1. List of bacterial strains, phages, and plasmids used in this study

Strain	Description	Source
Escherichia coli		
DH5α	Plasmid maintenance/propagation	New England Biolabs
S17	λpir-positive strain used for conjugation	New England Biolabs
NC101	AIEC isolate	[75]
Staphylococcus aureus		
JP1	Serotype-8 human blood isolate	[76]
Burkholderia cenocepacia		
K56-2	Epidemic CF isolate	[77]
Pseudomonas aeruginosa		
PAO1	Wild type	[78]
PAO1 Δ*retS*	Clean deletion of *retS* from PAO1	[71]
PAO1 Δ*gacS*	Clean deletion of *gacS* from PAO1	[79]
PAO1 Δ*rsmY/Z*	Clean deletion of *rsmY* and *rsmZ* from PAO1	This study
PAO1 Δ*retS/rsmY/Z*	Clean deletion of *rsmY* and *rsmZ* from PAO1 Δ*retS*	This study
PAO1 Δ*pilA*	Clean deletion of *pilA* from PAO1	[80]
PAK	*P. aeruginosa* strain K Wild type	[81]
Bacteriophage		
Pf4	Inoviridae	[82]
JBD26	Siphoviridae	[83]
CMS1	Podoviridae	[78]

DMS3vir	Siphoviridae	[84]
F8	Myoviridae	[85]
KPP21	Podoviridae	[86]
Plasmids		
pEX18Gm	Allelic exchange suicide vector	[87]
pJN105	araC-PBAD cassette cloned in pBBR1MCS-5, GmR; empty vector	[88]
pJN105::PA2133	PA2133 in pJN105; degrades cyclic-di-GMP, GmR	This study

2.2.2 Primers table

The oligonucleotides used to develop *P. aeruginosa* deletion mutants are listed in Table 2-2

Table 2-2. List of oligonucleotides used in this study

Name	Sequence 5' - 3'
Δ*rsmY*-out F	CGGCGAGCGGAACTATTACA
Δ*rsmY*-out R	AGGCGGAACTGAACCACATG
Δ*rsmZ*-out F	CCAGGCGATTTTCTCCGAAGA
Δ*rsmZ*-out R	GCCAAAAACGCTCGGTGAAT

2.2.3 Plaque assay

Plaque assays were performed using lawn overlays of the indicated strains grown on the indicated plates. Phages in filtered supernatants were serially diluted ten-fold in PBS and spotted onto lawns of the indicated strain. Plaques were imaged after 18 h of growth at 37°C.

2.2.4 Cell lysate preparation (phage infection or sonication)

Overnight cultures of *P. aeruginosa* PAO1 cells were pelleted, washed in PBS, and resuspended in fresh LB. Bacteria were then lysed by infecting with DMS3vir (MOI = 1) or sonication. Cell debris was removed by centrifugation and any virions removed by filtering through a 100 kDa MWCO membrane. Agar plates were prepared by adding agar powder (1.5% w/vol) to the bacterial lysate and then autoclaving.

2.2.5 Chloroform extraction

Bacterial cell lysates from 2.2.4 were transferred to a separation funnel or 50 mL conical tube. 10% v/v of chloroform was added to the lysate, vortexed, and allowed to separate

undisturbed for 2-3 hours. If done in a conical tube, the lysate was centrifuged to condense the interphase layer, and the top aqueous layer was collected. If done in a separation funnel, the top aqueous layer was collected using an automatic serological pipette and a slow steady sterile air stream was placed into the bottom of the collected container to drive off any residual chloroform.

2.2.6 Molecular weight cut off filtration

Overnight cultures of *P. aeruginosa* PAO1 cells were pelleted, washed in PBS, and resuspended in fresh LB. Bacteria were then lysed by sonication. Cell debris was removed by centrifugation (21.0 xg, 10 minutes, 20C). Cell lysate was then passed through spin columns (Sigma) ranging from 100, 10, 5, 3 kDa filter sizes. Both the retentate and the flow-through were collected. Agar plates were prepared by adding agar powder (1.5% w/vol) to the filtered bacterial lysate.

2.2.7 Growth curve assays

Overnight cultures were diluted to an OD_{600} of 0.05 in 96-well plates containing LB and, if necessary, the appropriate antibiotics, cell lysate, or polyamines. Three biological replicates with three technical replicates were used per condition. After 2 h of growth, strains were infected with the indicated phage and growth measurements resumed. OD_{600} was measured using a CLARIOstar (BMG Labtech) plate reader at 37°C every 15 minutes with shaking prior to each measurement.

2.2.8 Lyophilization

Lyophilization was carried out using a Labcono 8-port capacity lyophilizer. Cell lysate samples were frozen in 10.0 mL aliquots to -80°C in 50 mL conical tubes. Once frozen, the tops were covered with two layers of parafilm and three holes were poked into the parafilm using a sterile needle. Samples were loaded into the lyophilizer and samples were freeze dried for 20-24 hours, or until all the liquid has been removed from the sample. The parafilm was removed, tubes were capped, and samples were stored at room temperature. To rehydrate, dried sublimate was resuspended in 10.0 mL of LB.

Agar plates were prepared by adding equal volume of molten LB with agar powder (1.5% w/vol) to the dried sublimate.

2.2.9 Twitch motility assay

Overnight cultures of indicated strains were used to inoculate a subculture in 3.0 mL of LB and set to grow in a shaker (220 rpm, 37°C) for 6-8 hours. Either LB or cell lysate plates were warmed to 37°C before using. Bacterial subcultures were resuspended using a 200 µL pipette tip, with the goal of coating the tip with the bacterial culture. The tip was then used to stab the agar through to the bottom of the plate, with three replicates per strain. Stabbed plates were inverted and incubated at 37°C for 2-3 days. The agar was then discarded and the plate was stained with Coomassie Twitch stain (1.25 g dye in 500 mL DI H_20 + 10% w/vol acetic acid). The dye was rinsed and the twitch growth was imaged and measured.

2.2.10 CFU/mL assay – Determination of colony forming units

During the course of experiments, 1.0 mL of bacterial culture was collected and serially diluted ten-fold in 1x PBS buffer. 5 µL of the dilution culture series was spotted on a sterile LB agar plate. Dilutions were done in three replicates. The plates were incubated overnight at 37°C. The following day, the colonies were counted and CFU/mL were back calculated using the dilution factor, volume dispensed onto the plate, and the count that was in the 20 to 200 colonies per spot range. Averages of the three replicates were determined as well.

2.2.11 PFU/mL assay – Determination of plaque-forming units

During the course of experiments in which exogenous phage were added to the culture, a 500 µL aliquot was collected. The sample was centrifuged and the supernatant was collected and passed through a 0.22-µM filter to produce a cell-free supernatant. A bacterial lawn overlay of PAO1 WT was prepared on LB plates. The cell-free supernatant was serially diluted ten-fold and 5 µL was spotted onto the bacterial lawn. Once dried, the plaques were enumerated and PFU/mL was back calculated using the dilution factor, volume dispensed onto the plate, and the plaque count that was in the

range of 20 to 200 plaques per spot. Three replicates per time point were collected and used to determine the average PFU/mL.

2.2.12 Enzymatic digestion of cell lysate

Aliquots of chloroform extracted *P. aeruginosa* PAO1 cell lysate that was resuspended in 1x PBS was prepared for enzyme digestion. Enzymatic conditions were prepared as described in Table 2-3. Cell lysates were mixed with enzymatic solutions and digested for 8 hours. Mixtures were then heat-treated at 80C for 10 minutes to halt enzymatic activity. Mixtures were then used for growth curve assays as described in section 2.2.7 in Chapter 2, plaque assays in section 2.2.3 in Chapter 2, and PFU/mL assay in section 2.2.11 in Chapter 2.

Table 2-3. Summary of optimized enzymatic digestion conditions

	Optimal Parameters					
Enzyme	**Concentration**	**Unit**	**pH**	**Temp (°C)**	**Source**	**CAS**
Lysozyme	1	mg/mL	5	20-30	Fisher	BP535
RNase A	0.9	mg/mL	7.6	60	Sigma	R5000
DNase	1	mg/mL	7.6	60	Thermo	EN0521
Endopeptidase A	50	µg/mL	7.4	25	Millipore	324762
Carboxypeptidase G	2.2	units/mL	7.3	30	Sigma	C9658
Lysostaphin	1	µg/mL	7.5	37	Sigma	L7386

2.3 Results

2.3.1 Exposure to cell lysate induces a tolerance phenotype against most phages

Phage infections are known to cause mass bacterial cell lysis, triggering the mounting of bacterial defenses. To test whether neighboring cells can sense a phage-induced cell lysis event through the detection of released lysate, cell lysates were generated from *P. aeruginosa* PAO1. Cell lysates were produced by resuspending overnight cultures of *P. aeruginosa* in fresh LB and then infecting the bacterial culture with a lytic phage. Cellular debris was removed through centrifugation and infectious virions were removed with a 100 kDa membrane filter. Agar plates were prepared using the lysate supernatant

to make LB-lysate plates. Fresh *P. aeruginosa* PAO1 lawns were then spread on the LB-lysate agar plates (along with regular LB agar plates as a control), followed by spotting of a panel of diluted phages of diverse groups, including Inoviridae (Pf4), Podoviridae (CMS1), Siphoviridae (JBD26, DMS3vir) and Myoviridae (F8). After an overnight incubation at 37 °C, phage titers on both plate conditions were compared and imaged. Replication of nearly all phages, barring CMS1, was inhibited on the LB-lysate agar plates; no inhibition was seen on the regular LB agar plates (**Fig 2-1**).

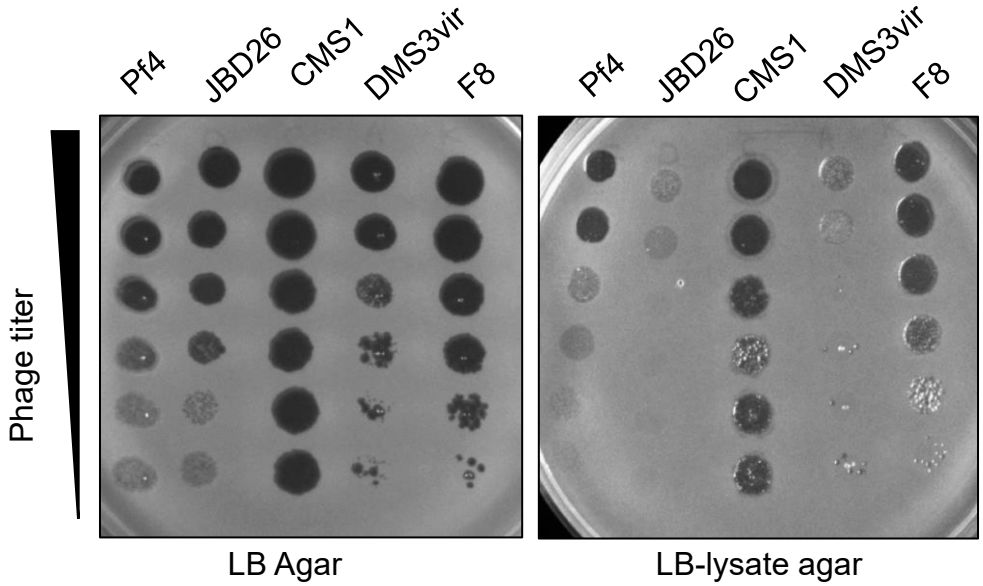

Figure 2-1. *P. aeruginosa* grown on kin cell lysate triggers a phage tolerance phenotype. *P. aeruginosa* PAO1 lawns grown on LB agar and LB-lysate agar plates and then challenged with a serially diluted phage panel. Representative images are after 18 hours of growth at 37°C.

Generation of cell lysate through sonication of overnight cultures resuspended in fresh LB instead of phage lysis produced similar inhibition of phage replication, suggesting that phage infection is not obligatory for phage suppression to occur. To determine whether the signal strength would be affected by concentration, cell lysates were prepared to be more or less concentrated than the normal protocol by altering the bacterial concentration present during sonication. More concentrated cell lysates were created by preparing overnight cultures and combining the bacterial pellets into a single volume of resuspended LB to produce a high bacterial concentration solution, which was then sonicated and prepared as described previously; less concentrated cell

lysates were made by diluting overnight cultures in LB to reduce the concentration of bacteria before sonication. When sonicated cell lysate was concentrated, phage plaquing decreased in a dose-dependent manner (**Fig 2-2**). This suggested that the concentration of the compound in cell lysate needed to reach a certain threshold to induce phage tolerance and increased amounts of lysate induced more protection.

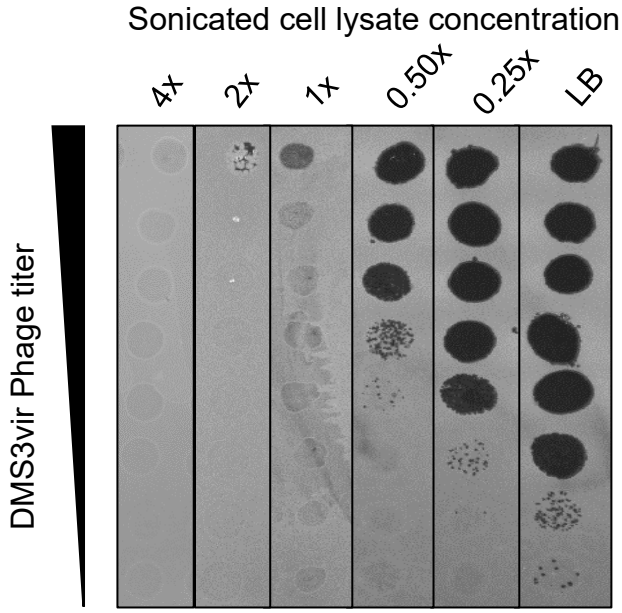

Figure 2-2. Increasing the concentration of cell lysate induces a greater phage tolerance phenotype. *P. aeruginosa* PAO1 lawns grown on LB agar and concentrated sonicated PAO1 WT cell lysate and then challenged with diluted DMS3vir phage. Representative images are after 18 hours of growth at 37°C.

Furthermore, when *P. aeruginosa* was transferred from the LB-lysate agar plate to a fresh LB plate and subsequently challenged with the phage panel, sensitivity to phage infection was restored **(Fig 2-3)**. This indicated that *P. aeruginosa* cell lysates triggered a transient phage tolerance phenotype rather than a phage resistance as would be conferred by genetic means.

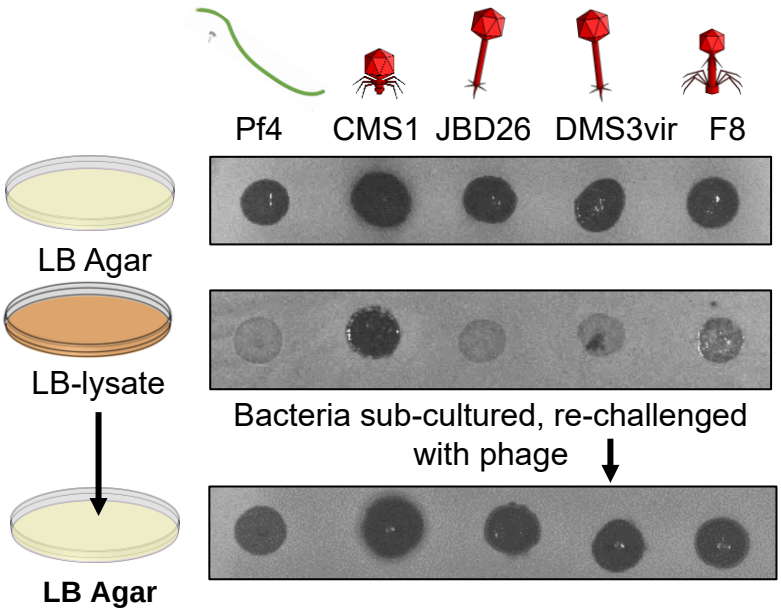

Figure 2-3. LB-lysate agar induces a phage tolerance phenotype in *P. aeruginosa*. PAO1 WT grown on LB agar and LB-lysate agar plates and then challenged with a phage panel at 10^6 PFU in 3 µL. Representative images are shown after 18 hours of growth at 37°C. PAO1 WT grown on lysate plates was then sub-cultured onto LB agar plates and challenged with the phage panel again, resulting in lysis. Representative images are shown.

To rule out the possibility that the signal in the cell lysate triggering phage tolerance was a species-specific response (i.e., *P. aeruginosa* PAO1 only responds to PAO1 lysate), cell lysates from other bacterial species (*S. aureus*, *E. coli*, *B. cenocepacia*, and *P. aeruginosa* PAK) were generated and plaque assays were performed. The inhibition of phage replication was similar in response to other bacterial species' lysates as with *P. aeruginosa* PAO1 lysates, indicating that there was a common signal in the lysates that induced the phage tolerance phenotype **(Fig 2-5)**.

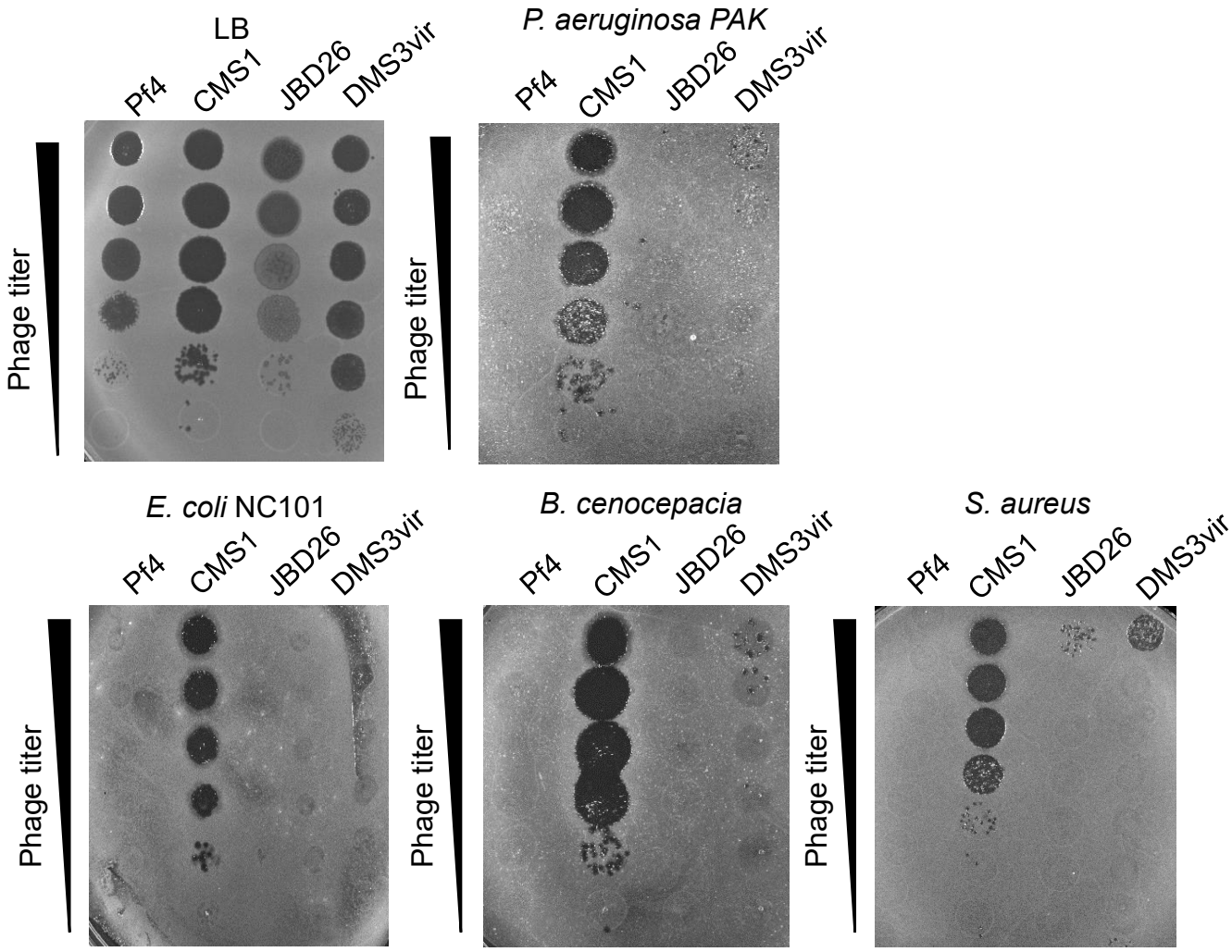

Figure 2-4. Cell lysates from other bacterial species triggers the phage tolerance phenotype in *P. aeruginosa*. Plaque assay panel using cell lysate from other bacterial species. *P. aeruginosa* PAO1 lawns grown on LB agar and LB-lysate agar plates from specified bacterial species and then challenged with a serially-diluted phage panel.

2.3.2 Cell lysate signal characterization

Based on the observation that a transient phage tolerance was being induced in response to the presence of cell lysate, it was hypothesized that a compound within the cell lysate served as a danger signal, which then triggered the mounting of phage defenses. The next step was to perform experiments to characterize the physical and chemical properties of the danger signal molecule(s) responsible for inducing phage tolerance. It was hypothesized that the active molecule(s) could be fragments of cell components that would remain in the supernatant after centrifugation, such as small fragments of the peptidoglycan cell wall, short nucleotide sequences, or short polypeptides. To rule out these molecules, cell lysates were digested with various enzymes and activity was verified through plaque assays **(Table 2-3)**. Peptidoglycan was digested with lysozyme and lysostaphin; polypeptides with endopeptidase and carboxypeptidase; and nucleotides were digested with RNase and DNase. All digested cell lysates retained activity, suggesting that the active molecule(s) were not nucleotides, small polypeptides, or peptidoglycan fragments.

To determine if the molecule(s) was hydrophobic or water-soluble, sonicated LB-lysate was extracted with chloroform ($CHCl_3$) and the top aqueous phase was used to produce $CHCl_3$-extracted LB-lysate plates. Plaque assays were repeated using DMS3vir, a well characterized lytic mutant of the *Mu*-like temperate *Pseudomonas* phage DMS3 [84]. Phage titers were quantified against a LB plate control to compare activities. The active molecule(s) was present in the aqueous layer, as phage titers were significantly lower in the $CHCl_3$-extracted LB-lysate plate (~10^9 PFU/mL) as compared to regular LB plates (~10^{11} PFU/mL) **(Fig 2-5)**. To identify the size range of the active molecule(s), the chloroform extracted cell lysate was passed through size-exclusion centrifuge columns, encompassing 100, 10, 5, and 3 kDa. Both the retentate and the flow-through were collected and mixed with molten agar (1.5%) to make LB-lysate plates and used in DMS3vir plaque assays to compare phage titers. The active fraction was retained in the flow-throughs of all the centrifuge sizes, indicating that the active molecule(s) were smaller than 3 kDa. Further, the smallest size fraction reduced PFUs to a greater extent than the $CHCl_3$-extracted LB-lysate (~10^7 PFU/mL) **(Fig 2-5)**. The $CHCl_3$-extracted LB-lysate was then lyophilized, stored, rehydrated with fresh LB, and used to make

rehydrated LB-lysate agar for another plaque assay. The rehydrated LB-lysate retained activity, and reduced DMS3vir plaquing to a similar degree as before lyophilization (~10^9 PFU/mL) (**Fig 2-5**). Collectively, these results suggested that the active molecule(s) was small and water-soluble.

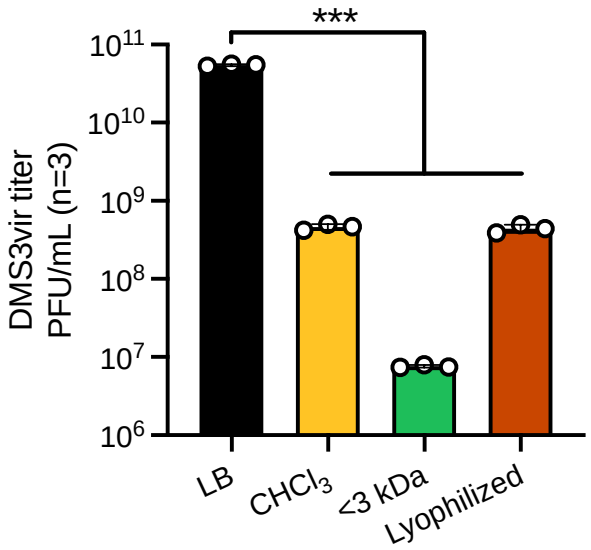

Figure 2-5. Purification of the active fraction of *P. aeruginosa* PAO1 cell lysate reduces phage plaquing titers. Phage DMS3vir was titered and spotted onto lawns of *P. aeruginosa* growing on LB agar or LB agar supplemented with the aqueous phase of CHCl3-extracted cell lysate, the aqueous phase passed through a 3 kDa MWCO membrane, or a lyophilized aqueous phase extract. Results are means ± SD of three experiments, ***P<0.001.

2.3.3 Gac/Rsm signaling pathway and cyclic-di-GMP signaling is vital for lysate-induced phage tolerance

RNA-seq was performed on *P. aeruginosa* PAO1 WT on LB-lysate agar and LB agar. By comparing the transcriptional profiles of both conditions, insights into identifying the signal in cell lysate that triggers phage tolerance would be highlighted. In *P. aeruginosa* grown on LB-lysate agar showed 394 genes that were differently regulated compared to cells grown on LB agar. Of note, small RNAs *rsmY* and *rsmZ* were upregulated suggesting that cell lysate activated Gac/Rsm signaling, consistent with previous work [26] **(Fig 2-6 A)**. It has been shown that a soluble signal sourced from lysed *P. aeruginosa* was detected by kin cells through the Gac/Rsm signaling pathway [26]. Gac/Rsm signaling modulates many bacterial behaviors, such as mobility, virulence

expression, biofilm formation, and quorum sensing, at the transcriptional level [22] **(Fig 2-6 B)**. To test the hypothesis that Gac/Rsm signaling and cell lysate-induced phage tolerance were linked, strains where the Gac/Rsm signaling pathway was either

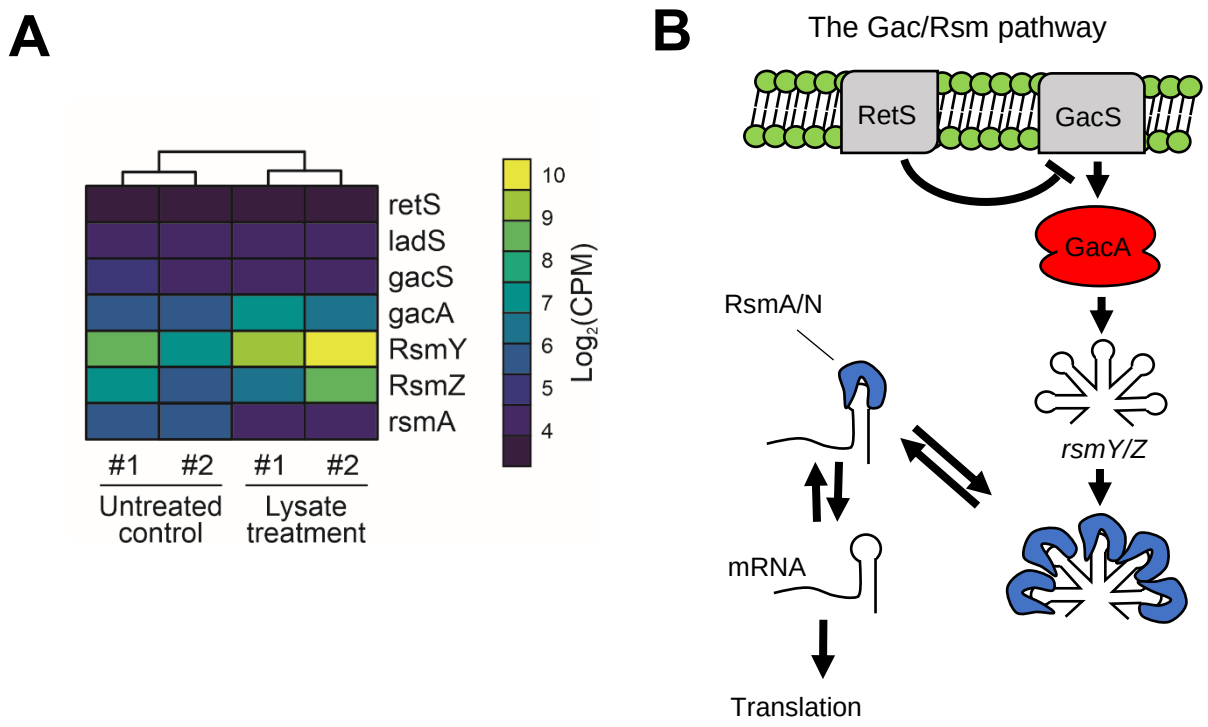

Figure 2-6. Exposure to cell lysate significantly upregulates Gac/Rsm gene expression. (A) Heatmap showing expression of genes in the Gac/Rsm pathway. Coloring indicates log2 of counts per million (CPM) reads. Two biological replicates for each treatment are shown. (B) Schematic of Gac/Rsm signaling pathway in *P. aeruginosa*.

disabled (Δ*gacS*, Δ*rsmY/Z*) or constitutively activated (Δ*retS*) were used. All strains showed no differences in growth on LB-lysate agar plates vs. LB agar plates **(Fig 2-7)**. On LB agar plates, phage DMS3vir formed clear plaques on wild type, Δ*gacS,* and Δ*rsmY/Z* lawns, but formed turbid plaques on Δ*retS* lawns **(Fig 2-8 A, top row)**, indicating that having an activated Gac/Rsm signaling was enough to inhibit DMS3vir replication. When the same strains were grown on LB-lysate agar plates, DMS3vir plaquing was reduced in wild-type lawns and completely inhibited on Δ*retS* lawns, whereas disabled Gac/Rsm signaling strains (Δ*gacS* and Δ*rsmY/Z*) were still susceptible to DMS3vir infection **(Fig 2-8 A, bottom row and 2-8 B)**. Moreover,

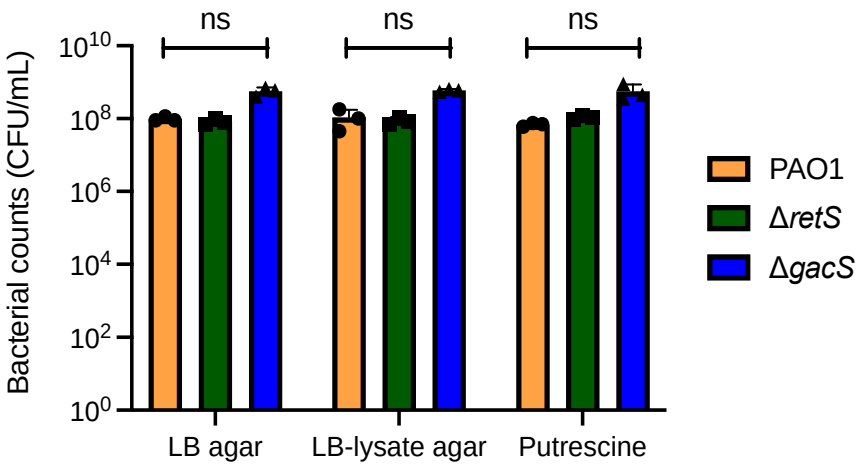

Figure 2-7. Growth of *P. aeruginosa* mutants on various plate conditions. Growth was measured by spotting serial dilutions of the indicated strains onto LB agar, LB-lysate agar, or LB agar supplemented with 50 mM putrescine. CFUs were counted after 18 h of growth at 37°C. N=3

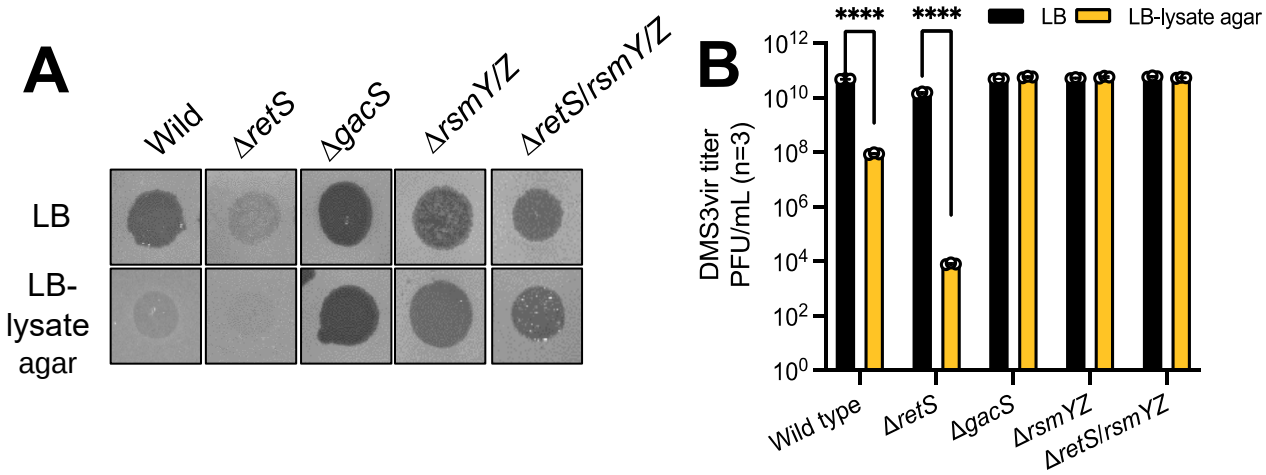

Figure 2-8. Lysate-induced phage tolerance is dependent on an active Gac/Rsm signaling pathway. Phage DMS3vir was spotted at 10^6 PFU in 3 µl onto lawns of the indicated strains grown on LB agar or LB lysate agar. Representative plaque images are shown. (F) DMS3vir PFU measurements on the indicated lawns growing on LB agar or LB-lysate agar are shown. Results are mean ± SD of three experiments, ****P<0.0001.

deleting *rsmY* and *rsmZ* from the phage-tolerant Δ*retS* background (Δ*retS/rsmY/Z*) restored susceptibility to phage infection on LB-lysate agar **(Fig 2-8)**.

DMS3vir uses Type IV pili as a cell surface receptor [47] and there are findings that link Gac/Rsm signaling with type IV pili repression to prevent phage infection [89]. To confirm whether LB-lysate agar had an effect on type IV pili expression, twitch assays were performed with wild-type, Δ*retS*, Δ*gacS*, and Δ*pilA P. aeruginosa*. Twitching motility was not reduced by lysate agar for any strains with active pili-dependent motility, indicating that Gac/Rsm signaling was essential for lysate induced-phage tolerance and

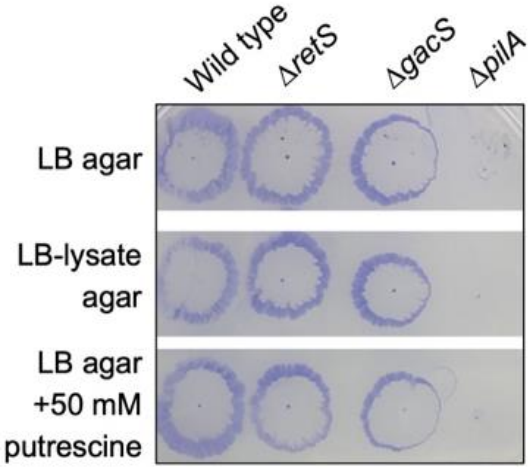

Figure 2-9. LB-lysate and putrescine does not affect type IV pili-dependent twitching motility. Twitch assays were performed with the indicated strains on the indicated lawns. Bacteria were stab-inoculated through the agar to the plastic dish below and grown for 24 h at 37°C. The agar was then removed and the adherent bacteria on the dish stained with Coomassie Blue. The Δ*pilA* strain is a twitch-deficient negative control. Representative images of triplicate experiments are shown.

was not mediated through Type-IV-pili phage receptor repression **(Fig 2-9)**.

In *P. aeruginosa*, activation of Gac/Rsm signaling increased intracellular levels of the second messenger cyclic-di-GMP, which regulates attributes like motility [11]. To test the hypothesis that high cyclic-di-GMP levels were required for lysate-induced phage tolerance, I expressed the phosphodiesterase PA2133, which rapidly degrades cyclic-di-GMP in *P. aeruginosa* [90], using an inducible plasmid. Expressing PA2133 in wild-type and Δ*retS P. aeruginosa* on lysate agar plates restored sensitivity to DMS3vir (**Fig 2-10**). These results also provide a link between cyclic-di-GMP signaling and phage defense in *P. aeruginosa*.

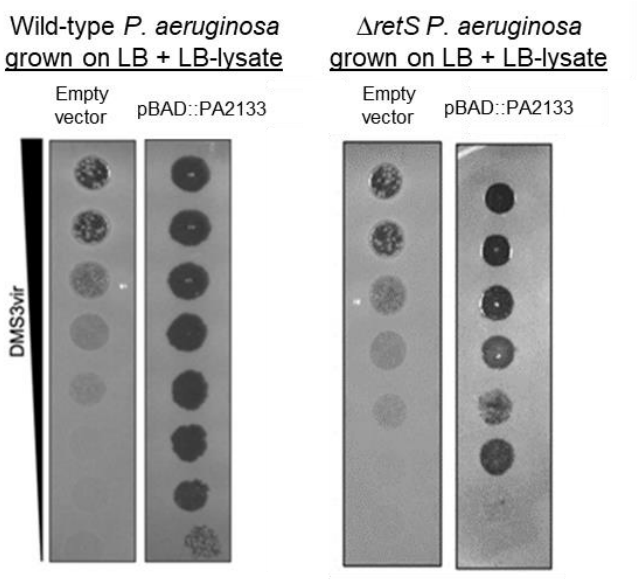

Figure 2-10. Phage tolerance is dependent upon cyclic-di-GMP signaling. Serial dilution plaque assays comparing the plating efficiency of phage DMS3vir on *P. aeruginosa* carrying an inducible c-di-GMP-degrading phosphodiesterase (pBAD::PA2133) or a control strain containing an empty vector. Bacterial lawns were grown on LB agar supplemented with $CHCl_3$-extracted lysate supplemented with 0.1% arabinose for 18 h.

2.4 Discussion

Cells are under constant threat of attack and have evolved various means to recognize threats, make assessments, and mount appropriate responses to ensure survival of the individual or the population as a whole. Eukaryotic cells are able to detect the presence of threats using conserved pattern recognition receptor (PRRs). These receptors can detect danger-associated signals such as free ATP, intracellular proteins, oxidized lipids, and other microbial-derived molecules [37, 38]. Consequently, bacteria also sense and respond to molecules released during lysis of neighboring cells [26, 36, 67, 68]. However, the characteristics of these danger-associated molecules and the effects on bacterial cell systems was poorly understood, particularly as it relates to responses to the threat of bacteriophage infection. Here, I described a transient phage tolerance phenotype in *P. aeruginosa* that was triggered by exposure to cell lysate. Further, the activating signal within the lysate was characterized to be a small, water-soluble, and heat-stable molecule that was not a nucleic acid, protein, or component of the peptidoglycan-containing cell wall. Lastly, I determined that this lysate-induced phage

tolerance required a functional Gac/Rsm signaling pathway, as engineered mutants that had a constitutively active Gac/Rsm pathway (Δ*retS*) were intrinsically more tolerant to phage, even without cell lysate exposure, and disabling the Gac/Rsm system by deleting downstream genes (Δ*gacS*, Δ*retS*/Δ*rsmYZ*) restored sensitivity to phage infection. Further, exposure to lysate did not confer protection if the Gac/Rsm system was disabled.

During a mass cell lysis event, bacterial contents are released into the extracellular space, which can contain molecules that serve as signals of an impending threat. Using techniques to collect cell-free bacterial lysates, we were able to induce a tolerance to various phage species when *P. aeruginosa* was exposed to lysate beforehand **(Fig 2-1)**. Further, as lysate generated through sonication or phage-lysis were equally as effective, this indicated that phage infection was not a requirement to induce phage tolerance. The activation of a transitory defense response upon cell lysate exposure was similar to other bacterial models, but other studies focused on antibacterial and antimicrobial defenses in *P. aeruginosa* and *Salmonella spp*. instead of anti-phage defenses [26, 40]. I observed that the lysate-induced phage tolerance phenotype was dose-dependent, as increasing the concentration of cell lysate increased the response, leading to more reduction in the plaquing ability of infecting phages **(Fig 2-2)**. This response shared elements with experiments where *B. subtilis* sensed phage-induced mass cell lysis areas. Here, *B. subtilis* broke down teichoic acid polymers, a major attachment site for Gram-positive infecting phages, and cells closest to the danger would line up along the lysis region, effectively forming a barrier of phage-tolerant cells to protect the population [68]. One chief difference between these results and ours was that *B. subtilis* responded to cell lysate by removing their phage attachment sites to shield themselves, but *P. aeruginosa* did not decrease the expression of their primary phage attachment moiety, the Type IV pilus **(Fig 2-9)**. This suggests that another mechanism of protection occurred to produce phage-tolerant *P. aeruginosa.* A novel perspective that came from our experiments was that *P. aeruginosa* exposed to cell lysate from different bacterial species triggered the phage-tolerance phenotype. This differed from previous research wherein *P. aeruginosa* sensed neighboring kin cell lysis, which in turn prompted the initiation of antibacterial defenses [26, 36]. The data suggest that the active molecule in

cell lysate is a common signal conserved across bacterial species and not a species-specific molecule.

Using purification techniques, we sought to characterize the active fraction that triggered the phage tolerance phenotype. A characteristic that was congruent with similar studies examining bacterial defenses was the small size of the active fraction. In different pseudomonads and *B. subtilis*, all previous characterizations suggested that their signaling factors were small enough to pass through their smallest filters and were low-molecular weight molecules, which lined up with the results that the active compound was smaller than 3 kDa [7, 19, 68]. Moreover, the results were unique to previously described work characterizing bacterial defense systems. On study showed that *Salmonella enterica* detected environmental DNA (eDNA) during cell lysis to mount defenses to produce a transient defense against antimicrobials [91]. This study differed from the results as DNase and RNase digestion did not abolish the induction capacity of our cell lysate, suggesting that eDNA nor a nucleic acid were not the identity of the phage tolerance molecule. It was documented that *P. aeruginosa* responds to peptidoglycan monomers GlcNAc from neighboring Gram-positive bacteria, mounting defenses against antagonistic bacteria [92]. However, our results conflicted with this finding as peptidoglycan-digested cell lysate was still able to activate tolerance against phage, suggesting that it was not a peptidoglycan component. While my characterization procedures showed similarities and disparities with previous work, the results suggested a molecule that was ubiquitous among bacteria, small, water soluble, and distinct from previously described molecules perceived as danger signals.

RNA-sequencing analysis showed that cell lysate significantly upregulated genes associated with the Gac/Rsm pathway **(Fig 2-6)**. In *P. aeruginosa*, the two-component system Gac/Rsm regulates various bacterial attributes, such as biofilm formation, virulence, and motility at the transcriptional level [22, 93]. Biofilms can serve as physical and chemical barriers to protect bacteria against phage infection and bacteria commonly use two-component systems to sense environmental changes to ensure their survival [89]. Since phage predation is an environmental stressor, we speculated that there could be a correlation with the Gac/Rsm sensor kinases RetS and GacS and

phage infection, where cell lysate could serve as the prelude to an incoming environmental stressor. For many two-component systems, the environmental triggers that activate the sensor kinases and the signaling cascade are unclear. The two-component systems characterized to date include biotic and abiotic factors with diverse structures [12]. It was found that there are two opposing schools of thought regarding importance of the sensor kinase RetS and its role in sensing cell lysate derived danger signals. Our results found that when we constitutively activated the Gac/Rsm system by deleting the sensor kinase RetS (Δ*retS*), the mutant was highly resistant to phage infection; the opposite was true when we deleted the other sensor kinase to disable the Gac/Rsm system (Δ*gacS*), producing a highly sensitive mutant. The results are consistent with studies that demonstrated the opposing effect of sensor kinases RetS and GacS on resistance to phages [89]. In opposition to our results, one study found that mutating a RetS signal sensing domain was crucial for cell lysate signal recognition, abolished response activation [9]. Their study indicated that RetS had a possible carbohydrate-binding module in its binding domain and that RetS was essential for response activation [9]. Peptidoglycan, comprising of a carbohydrate backbone with two alternating amino sugars bound by a β-(1,4)-glycosidic bond, would be a possible candidate for the activating ligand. However, our characterization experiments showed that peptidoglycan-free cell lysate still retained activity in wild-type PAO1, so it is unlikely that peptidoglycan acts as the activating ligand in our system. The results further contradict the study by Park et. al 2018, as lysate-induced tolerance was activated upon RetS deletion, suggesting our system is operating using a different mechanism that does not include RetS cell lysate signal recognition [94]. Downstream of the sensor kinase proteins in the signaling pathway are the small RNAs RsmY and RsmZ. Experiments showed that deletions of *rsmY* and *rsmZ* also abolished DMS3vir phage tolerance, even in the highly resistant Δ*retS* background **(Fig 2-8)**, and these results were also seen in similar experiments where RsmY and Rsm Z were deleted [89]. While complementation assays were not performed, it was previously demonstrated that complementation of *rsmY* and *rsmZ* in the Δ*gacS* background through plasmids increased resistance to phage as compared to the empty plasmid control in the Δ*gacS* background or the parent strain [89]. These results agree with

results demonstrating the importance of RsmY and RsmZ in lysate-induced phage tolerance. Experiments had established that a molecule in cell lysate was perceived as a danger signal and that the defense response prevented phage infection was dependent on an active Gac/Rsm pathway. The Gac/Rsm system activates ~300 genes [11, 22, 73]. Experiments identified the importance of specific genes (*gacS*, *rsmY*, and *rsmZ*) for phage tolerance response activation as well as genes that impeded the response when active (*retS*). All together this provides new insight into future research into finding the downstream responses that an active Gac/Rsm system confers, resulting in phage tolerance.

Bis-(3'5')-cyclic diguanosine monophosphate, or cyclic-di-GMP, is a cyclic dinucleotide that serves as a signaling molecule that transduces extra- or intracellular stimuli into metabolic changes by binding to allosteric molecules [95]. Cyclic-di-GMP regulates various processes such as motility and sessile lifestyle shifts, virulence, and biofilm formation [6]. Cyclic-di-GMP and the Gac/Rsm pathway work in tandem to modulate the transition to biofilms [6]. In *P. aeruginosa*, biofilm formation shields bacteria from antibiotic treatments and fosters resistance development, leading to cyclic-di-GMP targeting treatments gaining interest as an alternative target for antibacterial treatments [73]. To that end, we speculated that biofilms would also protect *P. aeruginosa* against phage infection. Further, we hypothesized that high cyclic-di-CMP levels were needed for lysate-induced phage tolerance. It was previously shown that the *retS* mutant displayed high levels of cyclic-di-GMP and exhibited a hyperbiofilm phenotype [6, 11]. As the Δ*retS* mutant used here also showed a similar hyperbiofilm phenotype and exhibited high resistance to phage infection, we introduced an inducible plasmid encoding a cyclic-di-GMP degrading phosphodiesterase (PDE) to reduce cyclic-di-GMP levels in the wild-type and Δ*retS* background. It was demonstrated that when cyclic-di-GMP levels were degraded, sensitivity to phage infection was restored, even when bacteria were exposed to cell lysate (**Fig 2-11**). Our results demonstrate the importance of high levels of cyclic-di-GMP in conferring phage resistance when exposed to cell lysate. These results also tracked with other studies that aimed to increase susceptibility to phage by lowering bacterial cyclic-di-GMP levels through activating PDEs, inhibiting DGCs, or binding and sequestering cyclic-di-GMP [72, 96]. Taken

together, we showed that lysate-induced phage tolerance needs further investigation to fully characterize.

We determined that cell lysate produced through phage-lysis or sonication released a small, water-soluble compound that conferred a transient phage tolerance to neighboring *P. aeruginosa*. This response depended on an active Gac/Rsm signaling pathway. A novel finding was that *P. aeruginosa* mounted phage tolerance responses to cell lysates from other bacterial species' lysates, suggesting that the signal was present in many bacterial species and that the active molecule acted as a danger signal. We further determined that the phage lifecycle was suppressed at the post-transcriptional level, as this compound did not affect Type-IV-pili expression, a common phage receptor. Compared to previous research, our results shared elements of previous experiments, but showed a novel signal related to responses to imminent threats by bacteriophages, rather than bacterial competition or external danger exposure, such as antibiotics.

Chapter 3: Gac/Rsm-signaling regulates intracellular polyamine levels in *P. aeruginosa*

3.1 Introduction

Polyamines are polycations that are ubiquitous in nature and are found in all living organisms, barring some Archaea [43]. The most common polyamines found in bacteria are putrescine, spermidine, and spermine. Polyamines bind to a diversity of cellular molecules, including DNA, RNA, and proteins [63]. Polyamines are important for cell homeostasis; their functions include an influence on transcription and translation, siderophore biosynthesis, cell growth stimulation, and biofilm formation [45]. Furthermore, polyamines play a role in stress responses, as they induce oxidative stress responses, SOS system activation, and spur resistance to acid and antibiotics [46]. Intracellular polyamine levels can be altered by either biosynthesis or importing from the environment [56]. Due to their pleotropic nature, polyamine levels need to be tightly controlled, as depletion stalls growth in many γ-proteobacteria and excessive

levels are cytotoxic [45]. While polyamines are crucial for γ-proteobacteria growth, there are studies showing that they are not required for normal growth in Gram-positive bacteria like *Bacillus subtilis* and *S. aureus*, as these bacteria subsist on very low levels of polyamines [45, 51, 52].

Polyamines are also vital for viral infection. Polyamines' positive charge helps condense and aggregate negatively-charged phage genomic DNA or RNA, neutralizing the charges to allow for packaging of their genomes into the new virions' proteinaceous heads [53, 55]. Much like their bacterial hosts, the concentration of polyamines impacts phage function, with low concentrations impeding replication machinery, and too much condensing their nucleic acids to the point where replication and translation machinery cannot bind [97]. Similarly, there are some phages that do not use polyamines to condense their genome [27]. Phages can manipulate bacterial polyamine levels to enhance cellular functions, thereby increasing phage protein translation [47, 55]. Thus, polyamines are crucial for both host and pathogen, leading to a tug of war for control to determine which party will survive.

While there are individual understandings of how polyamines affect the bacterial host and invading phages, the signaling cascades that polyamines induce to confer protection against phage are largely unexplored. In this chapter, we characterize the cellular responses of *P. aeruginosa* by comparing transcriptomes and employing microbial genetic techniques to parse out important and irrelevant cellular processes that lead to the phage tolerance phenotype. We determined a novel means of cellular protection against bacteriophage, where high extracellular polyamine concentrations were interpreted as a danger signal, causing upregulation of polyamine uptake to protect the host. If a phage threat is present, then polyamines are retained, causing a suppression of phage genome replication, but if no threat is detected, then levels return to normal. This is novel because many studies showed that polyamines block phage adsorption by reducing type-IV-pili expression, but our studies show that *P. aeruginosa* do not use this method of protection, but rather suppress phage at the transcriptional level to reduce phage genome replication. We confirmed that the intracellular polyamine accumulation from cellular injury is Gac/Rsm-dependent, indicating a major role for

Gac/Rsm signaling in regulating polyamine homeostasis, while ruling out the role of Gac/Rsm-linked sigma factors in mediating this response. As Gac/Rsm signaling is conserved across γ-proteobacteria and polyamines are ubiquitous in the environment, intracellular polyamine accumulation could be a conserved strategy that bacteria use to defend against phage infection, which could provide insights into bacterial immune systems in response to cellular injuries.

3.2 Materials and Methods

3.2.1 Bacterial Strains, Bacteriophages, and culture conditions

Bacterial strains, phages, and plasmids are listed in Table 3-1. Deletion mutants were constructed using allelic exchange and Gateway technology, as described previously [74]. Unless indicated otherwise, bacteria were grown in lysogeny broth (LB) at 37°C with shaking and supplemented with antibiotics (Sigma). Unless otherwise noted, antibiotics were used at the following concentrations: gentamicin (10 or 30 μg ml^{-1}), ampicillin (100 μg ml^{-1}), and carbenicillin (300 μg ml^{-1}).

Table 3-1. List of bacterial strains, phages, and plasmids used in this study

Strain	Description	Source
Escherichia coli		
DH5α	Plasmid maintenance/propagation	New England Biolabs
S17	λpir-positive strain used for conjugation	New England Biolabs
NC101	AIEC isolate	[67]
Burkholderia cenocepacia		
K56-2	Epidemic CF isolate	[69]
Staphylococcus aureus		
JP1	Serotype-8 human blood isolate	[76]
Pseudomonas aeruginosa		
PAO1	Wild type	[78]
PAO1 Δ*retS*	Clean deletion of *retS* from PAO1	[71]
PAO1 Δ*gacS*	Clean deletion of *gacS* from PAO1	[79]
PAO1 Δ*rpoH*	Clean deletion of *rpoH* from PAO1	[98]
PAO1 Δ*rpoN*	Clean deletion of *rpoN* from PAO1	[98]
PAO1 Δ*rpoS*	Clean deletion of *rpoS* from PAO1	[98]
PAO1 Δ*algU*	Clean deletion of *algU* from PAO1	[98]
PAO1 ΔPA2055	Clean deletion of PA2055 from PAO1	This study
PAK	*P. aeruginosa* strain K wild type	[73]
Bacteriophages		

Pf4	Inoviridae	[82]
JBD26	Siphoviridae	[83]
CMS1	Podoviridae	[78]
DMS3vir	Siphoviridae	[84]
F8	Myoviridae	[85]
KPP21	Podoviridae	[86]
Plasmids		
pEX18Gm	Allelic exchange suicide vector	[87]
pJN105	araC-PBAD cassette cloned in pBBR1MCS-5, GmR; empty vector	[88]
pJN105::PA2133	PA2133 in pJN105; degrades cyclic-di-GMP, GmR	This study

3.2.2 Primers table

The oligonucleotides used in this chapter are listed in Table 3-2.

Table 3-2. List of oligonucleotides used in this study.

Name	Sequence 5' - 3'
DMS3 qPCR F	TCGACTCGGAACAGCAGAAC
DMS3 qPCR R	TAGAACATCCACTGCGCCAG

3.2.3 Cell lysate preparation (sonication)

Overnight cultures of *P. aeruginosa* PAO1 cells were pelleted, washed in PBS, and resuspended in fresh LB. Bacteria were then lysed by infecting with DMS3vir (MOI = 1) or sonication. Cell debris was removed by centrifugation and any virions removed by filtering through a 100 kDa MWCO membrane. Agar plates were prepared by adding agar powder (1.5% w/vol) to the bacterial lysate and then autoclaving.

3.2.4 RNA Extraction

Total RNA was extracted from the indicated strains and conditions using TRIzol as described [99]. In summary, *P. aeruginosa* strains were cultured in LB medium under at 37°C with shaking to a specified time point (For liquid cultures, 2 hours post-phage infection; for plate-based extraction, overnight growth). Prior to sample collection, an ice-cold stop solution (90% ethanol and 10% saturated phenol) was added and the cultures were immediately placed on ice to stop all cellular processes. Bacterial pellets

were collected by centrifugation (12,000 xg, 5 min, at 4°C); flash frozen and stored in -80°C until RNA extraction. For RNA isolation, frozen pellets were thoroughly resuspended and mixed in 100µl lysozyme solution (3mg/ml in 10mM Tris-HCl and 1mM EDTA) pre-warmed to 37°C and then incubated at 37°C for 1 minute. The cells were then lysed by immediately adding 1 ml tri-reagent (Trizol) and vortexing for 10 seconds until solution turned clear. Following an incubation period of 5 minutes at room temperature, 200 µL chloroform was added and the sample was vortexed for another 10 seconds until homogeneous. The sample was incubated for 2-5 minutes at room temperature until visible phase separation was observed and then centrifuged at 12,000 xg for 10 minutes. The upper phase was gently collected (about 600 µL) and mixed at a 1:1 ratio with 100% isopropanol and then mixed by vortexing for 2-3 seconds. The sample was incubated for 1 hour at -20°C and then centrifuged (12,000 xg, 30 minutes at 4°C) to collect the RNA pellet. The solution was removed without disturbing the pellet, followed by two consecutive wash rounds using 750 µL of 70% ethanol. The pellets were air dried for 5 minutes and then dissolved in nuclease free H20 and incubated for 5 minutes at 50°C. All RNA samples were treated with TURBO deoxyribonuclease (DNase) (Life technologies).

3.2.5 RNA-seq

The integrity of the total cellular RNA was evaluated using RNA tape of Agilent TapeStation 2200 before library preparation. All RNA samples were of high integrity with a RIN score of 7.0 or more. rRNA was first depleted from 500 ng of each sample using MICROBExpress Kit (AM1905, Fisher) following the manufacture's instruction. The rRNA-depleted total RNA was subjected to library preparation using NEBNext® Ultra™ II RNA Library Prep Kit (E7700, NEB) and barcoded with NEBNext Multiplex Oligos for Illumina (E7730, NEB) following the manufacturer's instructions. The libraries were pooled with equal amount of moles, further sequenced using MiSeq Reagent V3 (MS-102-3003, Illumina) for pair-ended, 600bp reads, and de-multiplexed using the build-in bcl2fastq code in Illumina sequence analysis pipeline. Raw sequencing reads were deposited as part of BioProject PRJNA806967 in the NCBI SRA database.

3.2.6 RNA-seq data analysis

Quality control analyses of RNA-seq datasets included clustered correlation matrix of gene expression levels and multidimensional scaling analyses (**Fig 3-1**). One of the replicates (LB, replicate 4) was identified as an outlier and removed from further analysis. RNA-seq reads were aligned to the reference *P. aeruginosa* PAO1 genome (GenBank: GCA_000006765.1), mapped to genomic features, and counted using Rsubread package v1.28.1 [100]. In viral challenge assays, the DMS3 phage genome (GenBank: DQ631426.1) was concatenated with PAO1 genome and treated as a single genomic feature. Count tables produced with Rsubread were normalized and tested for differential expression using edgeR v3.34.1 [101]. Genes with ≥2-fold expression change and a false discovery rate (FDR) below 0.05 were considered significantly different. Functional classification and Gene Ontology (GO) enrichment analysis were performed using PANTHER classification system (http://www.pantherdb.org/) [102]. RNA-seq analysis results were plotted with ggplot2 and pheatmap packages in R.

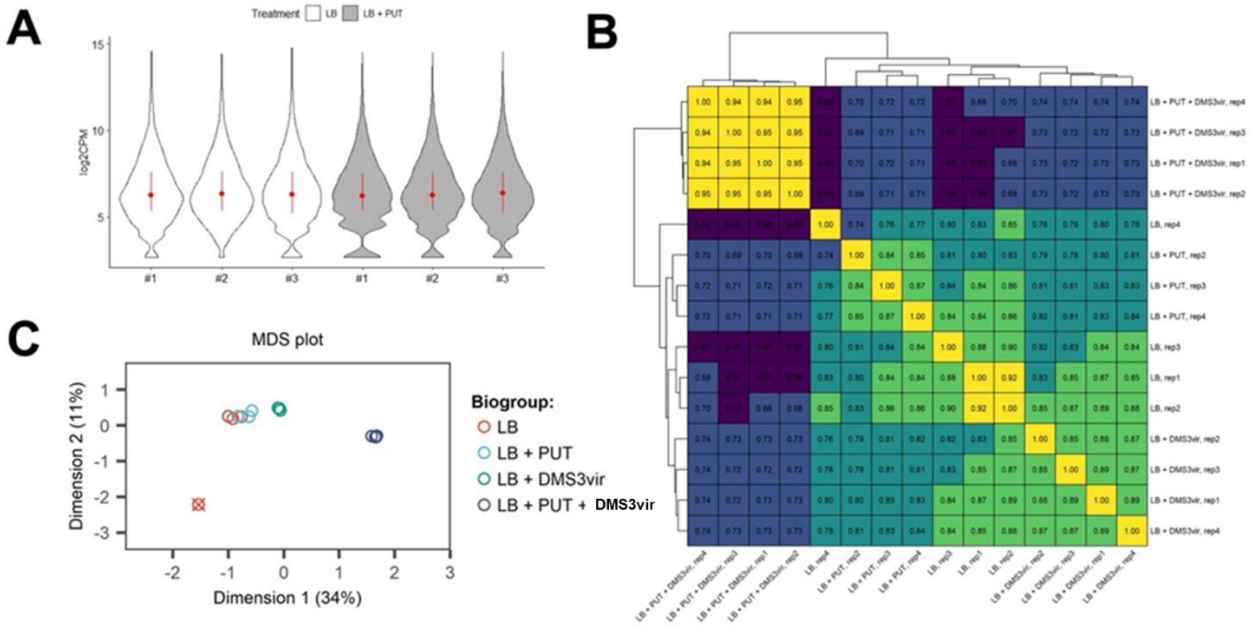

Figure 3-1. RNA-seq quality control. (A) The distribution of mapped read counts (log2 counts per million [CPM]) are shown for each replicate. Results are mean ± SD of triplicate or quadruplicate experiments. *P<0.05, **P<0.01. (B) Heatmap showing clustered correlation matrix of gene expression levels in RNA-seq samples. Pearson coefficients (numbers) were calculated from normalized log2 counts per million (log2CPM) values for all mapped genes produced with edgeR package. (C) Multidimensional scaling (MDS) plot showing variation between RNA-seq samples

based on normalized log2CPM expression data for mapped genes. One of the replicates (LB, replicate 4) was identified as an outlier (crossed) and removed from further analyses.

3.2.7 Polyamine-supplemented plate preparation

Polyamines (Putrescine dihydrochloride [MP Biomedicals] and Spermidine trihydrochloride [Sigma]) were added to sterile molten LB agar (1.5%) at the indicated final concentrations. Molten agar was mixed until polyamine powder was fully dissolved and then poured to make polyamine-supplemented agar plates.

3.2.8 Total polyamine content assay

Polyamines were measured using the Total Polyamine Assay Kit (MAK349, Sigma). A 100 µL aliquot of the indicated bacterial cultures was collected, centrifuged, washed with 1x PBS, and resuspended in PBS. Bacteria were lysed with 1:10 vol/vol chloroform, vortexed, and incubated at room temperature for 2 h. The solution was centrifuged, and the top aqueous layer was collected. 1.0 µL of the collected sample was mixed with the Total Polyamine Assay Kit reagents following the manufacturer's instructions, incubated at 37°C for 30 minutes, and then read using a CLARIOStar plate reader using end point fluorescence (λ_{ex} = 535 nm/λ_{em} = 587 nm). Polyamine concentrations were determined by comparing values to a standard curve constructed from known concentrations of putrescine. Values were then normalized to OD_{600} measurements taken from the original bacterial cultures.

3.2.9 Growth curve assay

Overnight cultures were diluted to an OD_{600} of 0.05 in 96-well plates containing LB and, if necessary, the appropriate antibiotics, cell lysate, or polyamines. Three biological replicates with three technical replicates were used per condition. After 2 h of growth, strains were infected with the indicated phage and growth measurements resumed. OD_{600} was measured using a CLARIOstar (BMG Labtech) plate reader at 37°C every 15 minutes with shaking prior to each measurement.

3.2.10 Statistical analyses

Unless specified otherwise, differences between data sets were evaluated by Student's t test, using GraphPad Prism version 5.0 (GraphPad Software, San Diego, CA). P values of < 0.05 were considered statistically significant.

3.2.11 DMS3vir genome copy number qPCR assay

Primers for qPCR were created for DMS3vir-26, a hypothetical protein (DMS3 qPCR F and R, **Table 3-1**). All samples, standards, and controls were run in triplicate in 10 μL reactions using SYBR SsoAdvanced Universal Green Supermix, 1 ng genomic DNA/reaction, and gene-specific primers (300 nM final concentration). Samples were run on a CFX Connect Real-Time System (Bio-Rad) using the following cycle conditions: 98°C for 1 min followed by 45 cycles of 98°C for 15 sec and 60°C for 30 sec, followed by a melt curve from 65°C-98°C by 0.5°C steps. Data were captured with CFX Maestro, organized in Excel, and analyzed and visualized in Prism 9. A standard curve with a linear regression trendline was created and the log copy number for each condition was calculated. A one-way ANOVA with Tukey's multiple comparison test was performed in Prism on log-transformed data to compare the mean copy number at each time point to those of each condition and strain.

3.2.12 Genomic DNA extraction

Whole genomic DNA was extracted from PAO1 pellets that had been frozen overnight at -80°C. DNA was purified using the Monarch Genomic DNA kit per the manufacturer's protocol.

3.2.13 Phage DNA extraction

Whole genome DNA was extracted from intact DSM3vir supernatants by heating the phage supernatant for 15 minutes at 100°C. Once cooled, DNA was purified using the Monarch Genomic DNA kit per the manufacturer's protocol. DNA concentrations were eluted and quantified using a Nanodrop set to dsDNA program.

3.2.14 Adsorption assay

Wild-type, Δ*retS*, or Δ*gacS P. aeruginosa* were grown to an OD_{600} of 0.2 in LB broth with or without 50 mM putrescine followed by infection with DMS3vir or CMS1 at an MOI of 0.75. At times 0.5-, 1-, and 10-minutes post infection, 500 µL aliquots were collected from each culture. Cells were removed by centrifugation (4,000 x g, 10 minutes) and virions in supernatants enumerated on lawns of *P. aeruginosa* PAO1.

3.3 Results

3.3.1 RNA-seq suggests lysate exposure upregulates polyamine catabolism genes

We mined the previous RNA-seq performed on *P. aeruginosa* PAO1 WT on LB-lysate agar and LB agar from Chapter 2.3.3 and Figure 2-6 to identify specific metabolic

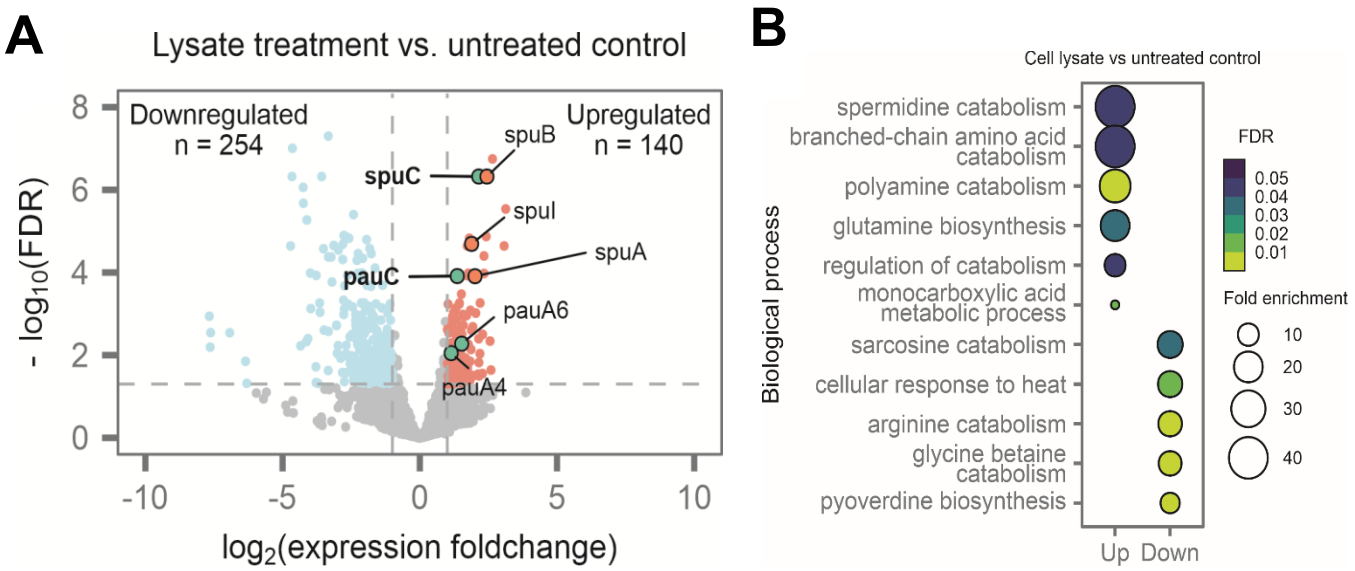

Figure 3-2. Polyamine catabolism is upregulated in *P. aeruginosa* exposed to cell lysate. (A) Volcano plot showing differentially expressed genes in wild-type cells grown on LB-lysate agar compared to cells grown on LB agar. Red indicates upregulated genes (log2[foldchange] > 1 and false discovery rate (FDR) <0.05) and blue indicates downregulated genes (log2[foldchange] <-1 and FDR<0.05). Non-significant genes are shown in gray. Polyamine metabolism and transport genes are highlighted. Data are representative of duplicate experiments. (B) Gene enrichment analysis of significant differentially expressed genes shown in (A). Dot sizes indicate fold enrichment of observed genes associated with specific Gene Ontology (GO) terms versus what is expected by random chance.

processes that were differentially expressed during LB-lysate exposure. As stated before, *P. aeruginosa* grown on LB-lysate agar showed 394 genes that were differentially regulated compared to cells grown on LB agar (**Fig 3-2 A**). Further, gene enrichment analysis showed that spermidine/polyamine catabolism genes were upregulated and overrepresented in LB-lysate agar datasets (**Fig 3-2 B**), some that are highlighted in the volcano plot in Figure 3-2 A. The results suggested that polyamines and their metabolism play a role in lysate-induced phage tolerance.

3.3.2 Extracellular polyamine concentrations spikes during a mass cell lysis event

In bacteria, the polyamines putrescine and spermidine are typically found inside the cells at concentrations ranging from 0.1-30 millimolar [43, 47]. To test whether a cell lysis event (either through phage infection or other mass lysis event) could release millimolar concentrations into the local environment, total polyamine concentrations were determined for the LB-lysate solution used to make plates. LB agar had negligible concentrations of total polyamine (~1.03 mM), whereas LB-lysate had total polyamine concentrations reaching around 27 mM and chloroform extracted LB-lysate had total polyamine concentrations reaching 35 mM (**Fig 3-3 A**). We also measured the polyamine concentrations of cell lysates from other bacterial species including within *Pseudomonas* strain K, *B. cenocepacia, E. coli*, and *S. aureus*, we found significant polyamine contents ranging from 17 to 26 mM (**Fig 3-3 B**), which aligns with our previous data showing other specie's cell lysate triggering phage tolerance. To determine whether a phage-lysis event could produce comparable polyamine concentrations to sonicated cell lysate, total polyamine concentrations were tracked over time for a culture infected with DMS3vir. DMS3vir triggered cell lysis at 4-6 hours post-infection, releasing ~20 mM total polyamine (**Fig 3-3 C-E**). When extracellular polyamine concentrations were normalized to bacterial density (OD600), a dramatic increase in polyamine release was observed at 4-6 hours post-infection (**Fig 3-3 D**)**,** indicating that phage-induced lysis of *P. aeruginosa* releases abundant polyamines into the environment.

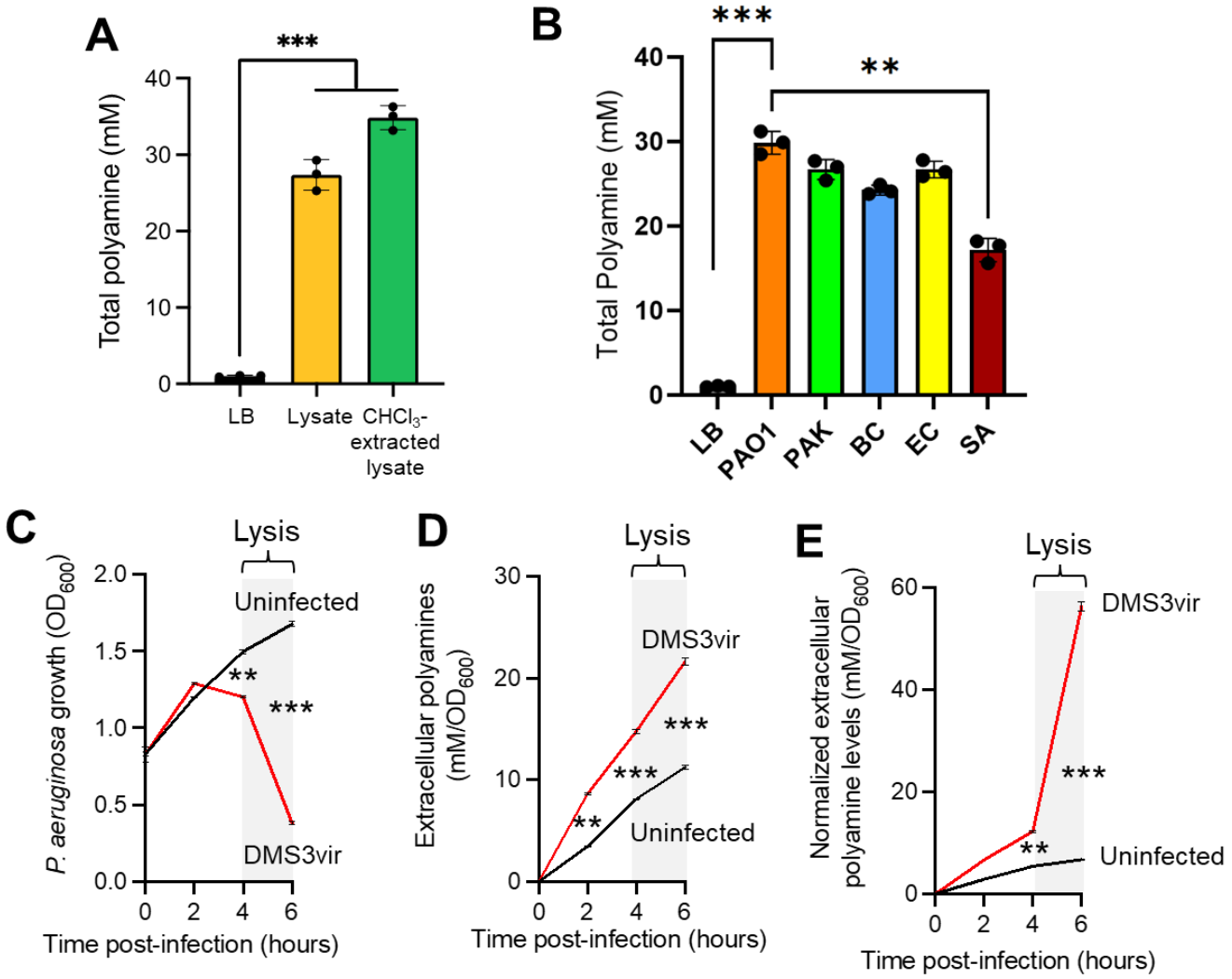

Figure 3-3. Polyamines are released into the environment during a mass-cell lysis event. (A) Total polyamine content in LB broth, cell lysate, and CHCl3-extracted cell lysate were measured by fluorometric assay. Results are means ± SD of three experiments, ***P<0.002. (B) Total polyamine content for cell lysates from other bacterial species by fluorometric assay. PAK = *Pseudomonas* strain K; BC = *B. cenocepacia*, EC = *E. coli*, SA = *S. aureus*. Results are mean ± SD of one experiment, ***P<0.002 (C) Growth of uninfected and DMS3vir-infected *P. aeruginosa* was monitored by OD600. Mass cell lysis is indicated by the gray box. Results are means ± SD of three experiments, **P<0.01, ***P<0.001. (D) Total polyamine content was measured by fluorometric assay in culture supernatants collected from cultures shown in (C). Results are means ± SD of three experiments, **P<0.01, ***P<0.001. (E) Polyamine concentration (mM from panel D) was normalized to cell density (OD600 from panel C). Results are means ± SD of three experiments, **P<0.01, ***P<0.001.

3.3.3 Polyamines in cell lysates induce a protective phage tolerance

It was hypothesized that polyamines could inhibit phage lifecycles, and to test that, commercially available putrescine or spermidine was used. *P. aeruginosa* lawns were grown on LB agar (MOPS buffered to pH 7.2) supplemented with 0 to 100-mM of polyamine and then challenged with a phage panel. Both polyamines reduced DMS3vir replication in a dose-dependent manner (**Fig 3-4 A and B**). In addition, the putrescine plates inhibited replication of phages Pf4, JBD26, and F8, but not CMS1 (**Fig 3-4 C and D**), which correlated with observations from crude bacterial cell lysate (**Fig 2-1**),

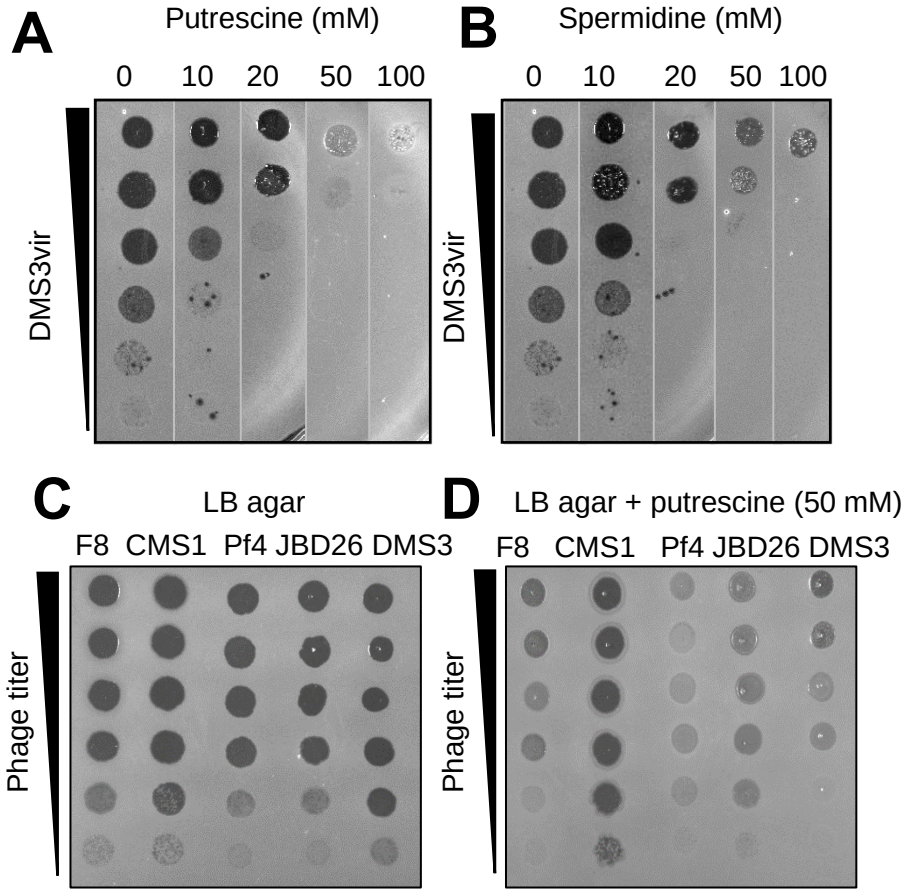

Figure 3-4. The polyamines putrescine and spermidine induce phage tolerance in *P. aeruginosa*. (A and B) The polyamines putrescine (A) or spermidine (B) were added to LB agar at the indicated concentrations. DMS3vir was spotted onto lawns of P. aeruginosa, and plaques were imaged after 18 h of growth at 37°C. (C and D) The indicated species of phage were spotted onto lawns of *P. aeruginosa* growing on LB agar or LB agar supplemented with 50 mM putrescine.

indicating that polyamines are the signal in cell lysates that induce phage tolerance.

3.3.4 Polyamines reduce phage adsorption and inhibit DNA replication in Gac/Rsm-dependent manner

To test the hypothesis that polyamine-induced phage tolerance and Gac/Rsm signaling were connected, the Gac/Rsm *P. aeruginosa* mutants were grown in LB broth supplemented with 50 mM putrescine. This polyamine concentration was used as it produced a robust phage tolerance response in wild-type *P. aeruginosa*, making it good for comparison of the response in Δ*retS*, and Δ*gacS*. Growth curve experiments showed that co-culturing with putrescine resulted in wild-type and Δ*retS P. aeruginosa* being less susceptible to DMS3vir infection (**Fig 3-5 A and B**), whereas the disabled Gac/Rsm signaling mutant, Δ*gacS*, remained susceptible to phage infection (**Fig 3-5 C**). It was noted that in liquid culture, all strains showed a lower density of growth in putrescine as compared to growth in LB broth. Wild-type cells reached a lower density once it reached stationary phase, but was still tolerant to phage (**Fig 3-5 A**). Δ*gacS* also displayed a polyamine-induced growth reduction, but remained sensitive to phage infection (**Fig 3-5 C**). This growth suppression contrasts with the lack of growth inhibition on solid agar supplemented with 50 mM putrescine (**Fig 2-7**), which could be explained by a surface-associated phenotype. Collectively, these results indicate that polyamine growth suppression is not a prerequisite for polyamine-induced phage tolerance.

To observe the effect of exogenous polyamines on DMS3vir replication, wild-type, Δ*retS*, and Δ*gacS P. aeruginosa* were co-cultured with DMS3vir and putrescine and phage titers were measured over time. In wild-type cells, putrescine reduced DMS3vir titers by ~3,500-fold compared to wild-type cells grown in LB broth after 6 hours (**Fig 3-6 A**). Similar observations were made in Δ*retS P. aeruginosa*; after 6 hours, putrescine

reduced DMS3vir replication by ~1,300 fold compared to Δ*retS* cultures without putrescine (**Fig 3-6B**). When Gac/Rsm signaling was disabled (Δ*gacS*), DMS3vir replication was not affected by putrescine and was comparable to DMS3vir replication in wild-type cells growing in LB broth (**Fig 3-6 C**). These results suggest that exogenous

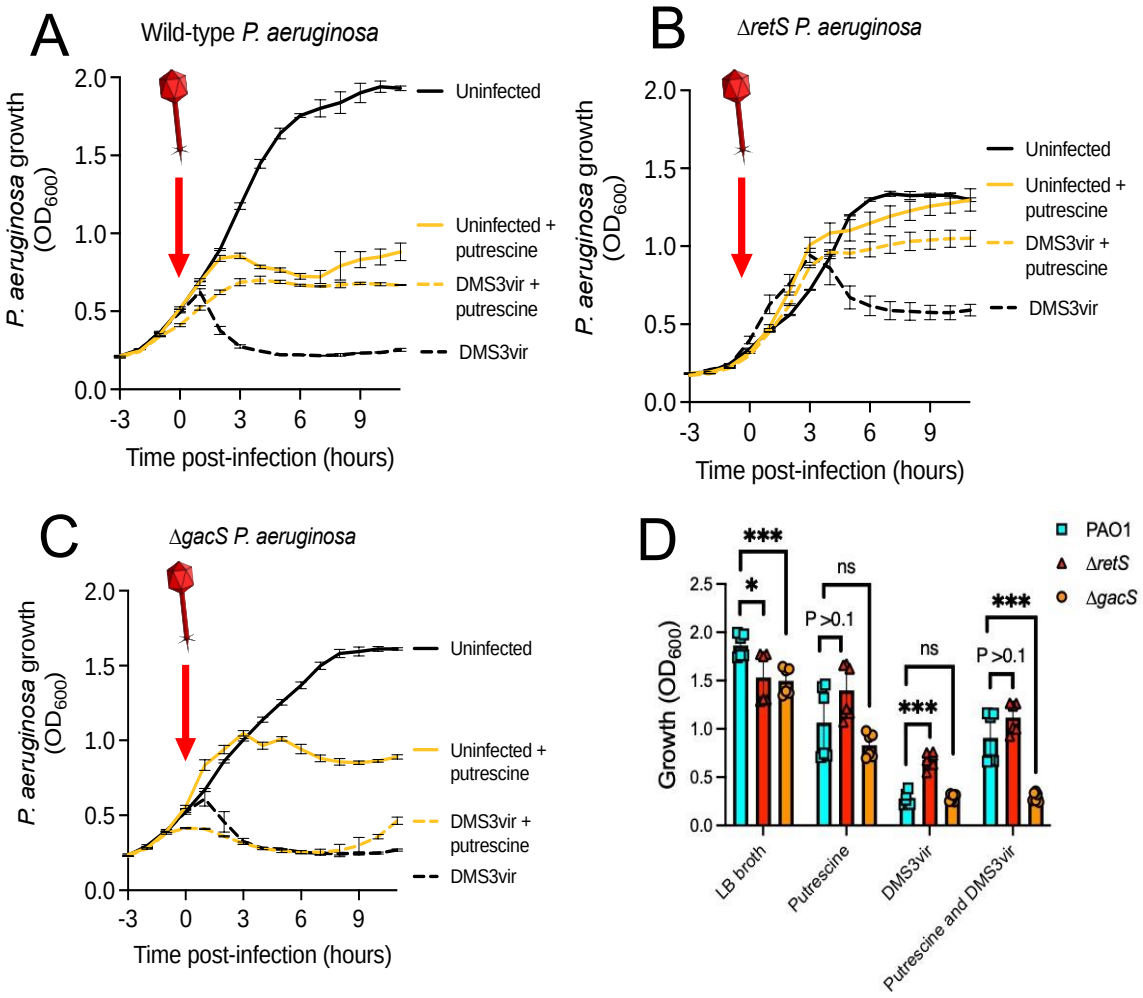

Figure 3-5. Polyamine-induced phage tolerance causes a growth reduction in liquid culture. (A-C) Growth curves of the indicated *P. aeruginosa* strains grown with (yellow) or without (black) 50 mM putrescine are shown. Cells were infected with DMS3vir at the indicated time (arrow) at a multiplicity of infection (MOI) of 1. Results are means ± SD of six experiments. (D) Statistical comparison of growth in wild-type, Δ*retS*, and Δ*gacS* strains at the 6-h timepoint shown in Figure 3-4 A-C. Growth (OD600) was measured six-hours post-infection for the indicated strains grown under the indicated conditions. Results are means ± SD of six experiments. Ns, not significant, *P<0.05, ***P<0.001.

putrescine inhibits phage replication in a Gac/Rsm-dependent manner.

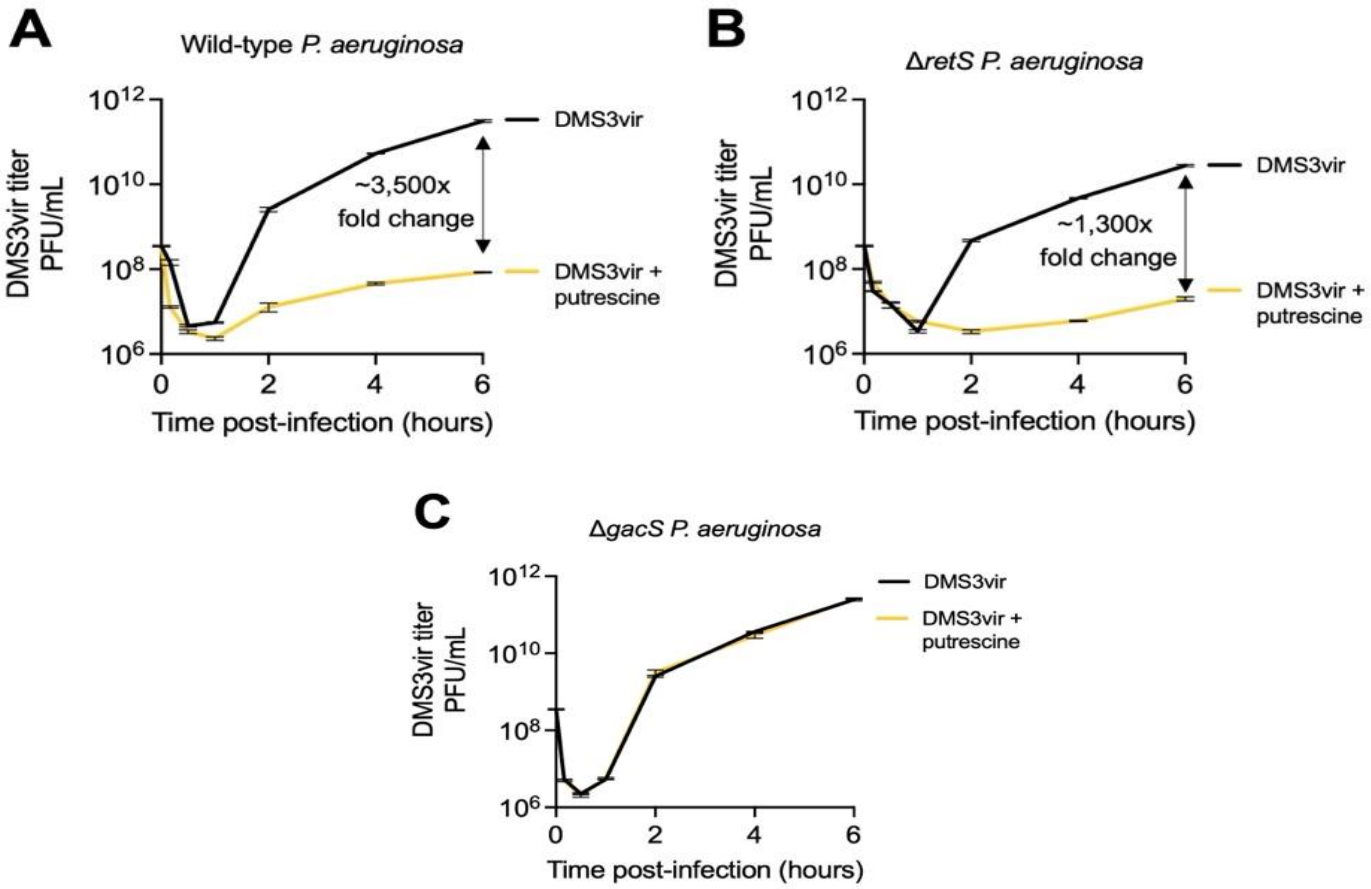

Figure 3-6. Putrescine inhibits DMS3vir replication in a Gac/Rsm-dependent manner. (A-C) DMS3vir titers in phage-infected cultures were measured at the indicated times. Results are means ± SD of three experiments.

Next, the effect of polyamines on phage lifecycle were investigated, starting with virion adsorption onto the cell. Adsorption assays were performed on wild-type, Δ*retS*, or Δ*gacS P. aeruginosa* with or without 50 mM putrescine followed by infection with DMS3vir (MOI 0.75). Samples were collected at 0.5-, 1-, and 10-minutes post-infection, before any progeny virions were produced (**Fig 3-7 A-C**). Bacteria and any adsorbed virions were removed by centrifugation at each timepoint and non-adsorbed virions in supernatants were measured via plaque assay. In wild-type cultures grown without putrescine, non-adsorbed DMS3vir titers were almost four times lower compared to cultures grown with putrescine at 10 minutes post-infection (**Fig 3-7 A**), indicating polyamines had modestly inhibited DMS3vir adsorption to *P. aeruginosa*. Adsorption of

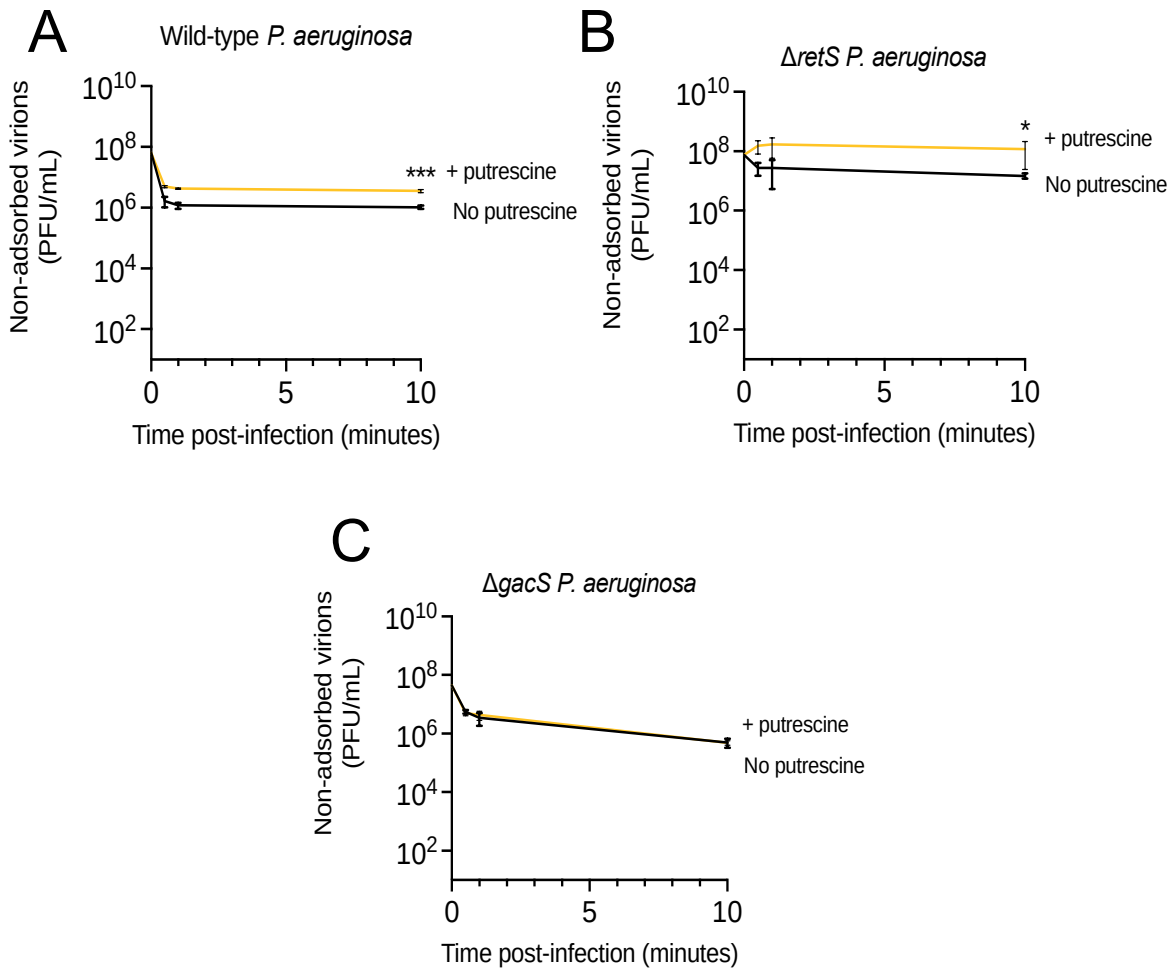

Figure 3-7. Putrescine modestly inhibits DMS3vir virion adsorption. (A-C) DMS3vir virion adsorption to host cells was measured by growing wild-type, Δ*retS*, or Δ*gacS P. aeruginosa* with (yellow) or without (black) putrescine for 3 hours at 37°C followed by infection with DMS3vir (MOI 0.75). Samples were collected at 0.5-, 1-, and 10-minutes post-infection, centrifuged to remove adsorbed virions and host cells, and phage titers in culture supernatants were measured by plaque assay. Results are means ± SD of three experiments. *P<0.05, ***P<0.001.

DMS3vir to Δ*retS* cells was also modestly impaired by putrescine (**Fig 3-7 B**). DMS3vir adsorption to Δ*gacS* cells was not affected by putrescine and was comparable to adsorption of DMS3vir to wild-type cells grown without putrescine (**Fig 3-7 C**). These results indicate that putrescine inhibited phage adsorption to a small degree to inhibit DMS3vir replication.

The effect of phage DNA replication when exposed to exogenous polyamines was investigated next. Through qPCR, DMS3vir genome copy numbers in cell pellets were assessed at 10- and 120-minutes post-infection. At 10 minutes post-infection, no significant difference in DMS3vir genome copy number was observed between strains grown with or without putrescine (**Fig 3-8 A**), indicating equivalent numbers of DMS3vir genomes were injected into cells, even when putrescine was present. After 120 minutes in a wild-type host grown without putrescine, DMS3vir genome copy numbers increased ~1,000-fold compared to the 10-minute time point (**Fig 3-8 B**). When putrescine was present, DMS3vir genome copy numbers remained static compared to the 10-minute time point (**Fig 3-8 B, yellow bar**). DMS3vir genome copy numbers were ~100-fold lower in Δ*retS P. aeruginosa* grown with putrescine whereas putrescine had no effect on DMS3vir genome copy number in Δ*gacS* bacteria grown with or without putrescine (**Fig 3-9 B**). The qPCR results indicate that putrescine significantly inhibits DMS3vir genome replication.

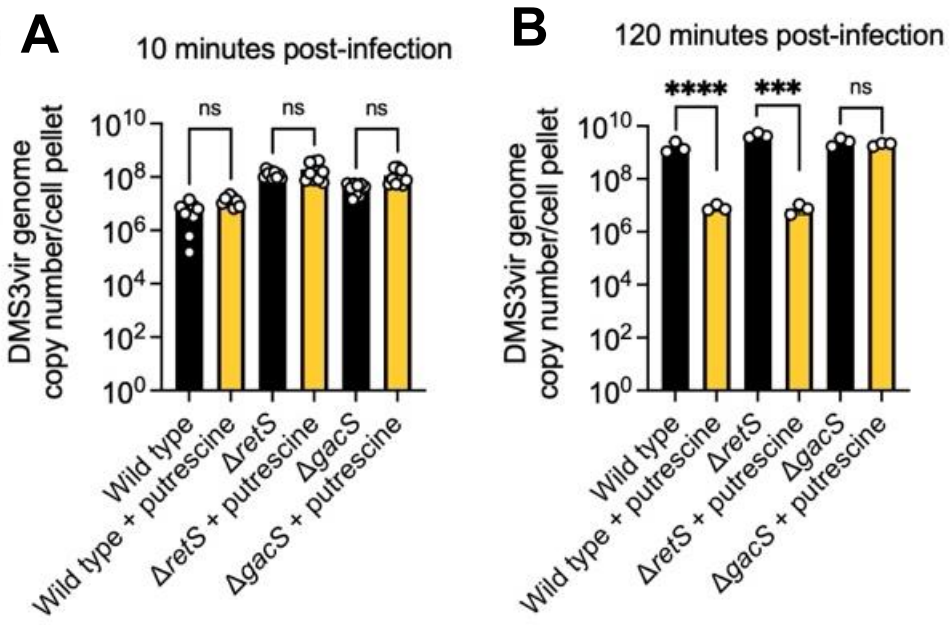

Figure 3-8. Putrescine significantly affects DMS3vir genome replication. DMS3vir genome copy number was measured by qPCR in the indicated strains at 10- or 120-minutes post-infection with or without 50 mM putrescine. Absolute copy number was determined using a standard curve generated with a cloned copy of the target sequence. Results are means ± SD of nine (J) or three (K) experiments: ****P<0.0001, ***P<0.001, ns (not significant).

3.3.5 Degradation of cyclic-di-GMP levels re-sensitized *P. aeruginosa* to DMS3vir infection in the presence of polyamines

As previous work showed that expressing PA2133 in wild-type *P. aeruginosa* on lysate agar plates restored sensitivity to DMS3vir (**Fig 2-10**), it was hypothesized that cyclic-di-GMP signaling and Gac/Rsm together would be needed for polyamine-induced phage tolerance in *P. aeruginosa*. To that end, the phosphodiesterase PA2133 was expressed in wild-type (**Fig 3-9 A-B**) and Δ*retS* (**Fig 3-9 C-D**) *P. aeruginosa* to degrade intracellular cyclic-di-GMP levels. Expression of PA2133 re-sensitized both strains to DMS3vir infection in the presence of 50 mM putrescine. These results suggest that Gac/Rsm and cyclic-di-GMP signaling are required for polyamine-induced phage tolerance in *P. aeruginosa*.

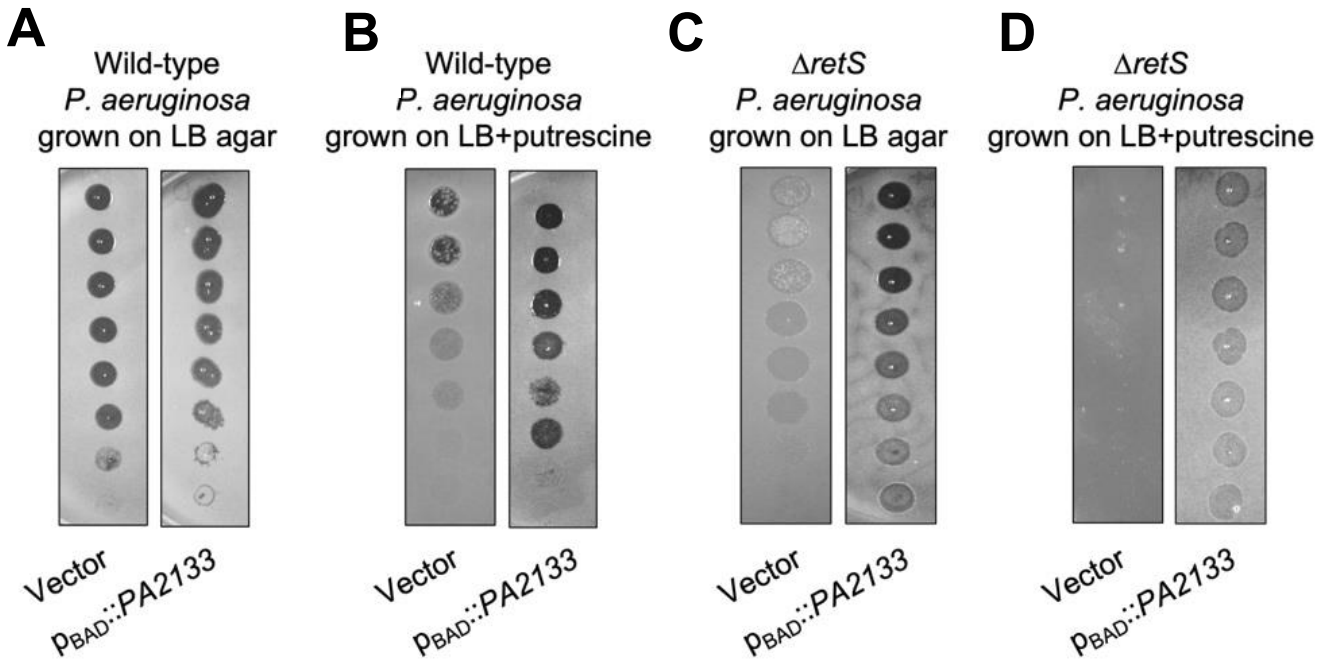

Figure 3-9. Expression of the cyclic-di-GMP degrading phosphodiesterase PA2133 restores sensitivity of *P. aeruginosa* to phage DMS3vir infection in the presence of putrescine. (A-B) Wild-type PAO1 and (C-D) Δ*retS P. aeruginosa*. Serial dilution plaque assays comparing the plating efficiency of phage DMS3vir on the indicated *P. aeruginosa* strains carrying an inducible c-di-GMP-degrading phosphodiesterase (pBAD::PA2133) or a control strain containing an empty vector. Bacterial lawns were grown on LB agar supplemented with $CHCl_3$-extracted lysate supplemented with 0.1% arabinose for 18 h.

3.3.6 DMS3vir infection induces Gac/Rsm-dependent intracellular polyamine accumulation

Another RNA-seq experiment was performed to investigate how polyamines and phage infection affected *P. aeruginosa* transcription. Wild-type cells were grown with or without putrescine for 3 hours, and then followed by infection with DMS3vir at an MOI of 1. Uninfected *P. aeruginosa* grown with putrescine shared 62 differentially regulated genes with cells grown on LB-lysate agar (**Fig 3-10 A and B**). The overlapping 62 genes were enriched for GO terms associated with polyamine catabolism (FDR = 1.81E-03, PANTHER Overrepresentation Test). Polyamine catabolism was the only GO term that was significantly enriched in the 62 overlapping genes after FDR correction with 8 out of 62 genes (13%) being related to polyamine catabolism, indicating that upregulation of polyamine catabolism genes is a common feature of cells exposed to lysate or putrescine.

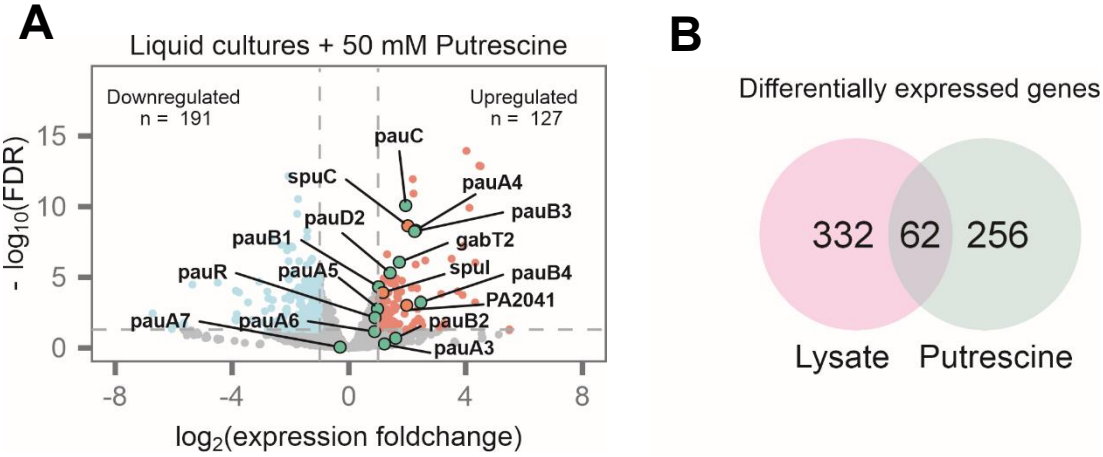

Figure 3-10. Putrescine exposure activates polyamine catabolic pathways. (A) Volcano plot showing differentially expressed genes (DEGs) in PAO1 cultured in liquid LB cultures with addition of 50 mM putrescine. Red dots indicate upregulated genes [log 2 (foldchange) > 1 and FDR<0.05], and blue indicate downregulated genes [log2(fold change) <-1 and FDR<0.05]. Non-significant genes are shown in gray. Genes involved in polyamine and putrescine breakdown are highlighted. B) Venn diagram showing DEGs overlapping between putrescine and cell lysate treatments.

DMS3vir transcription was strongly downregulated in cells grown in putrescine compared to cells grown without putrescine (**Fig 3-11 A, large blue dot**). In DMS3vir-

infected cells grown with 50 mM putrescine, we were surprised to find polyamine catabolism genes such as *spuC, pauB1, pauC*, and *pauD1* were significantly downregulated compared to uninfected cells grown with putrescine (**Fig 3-11B**).

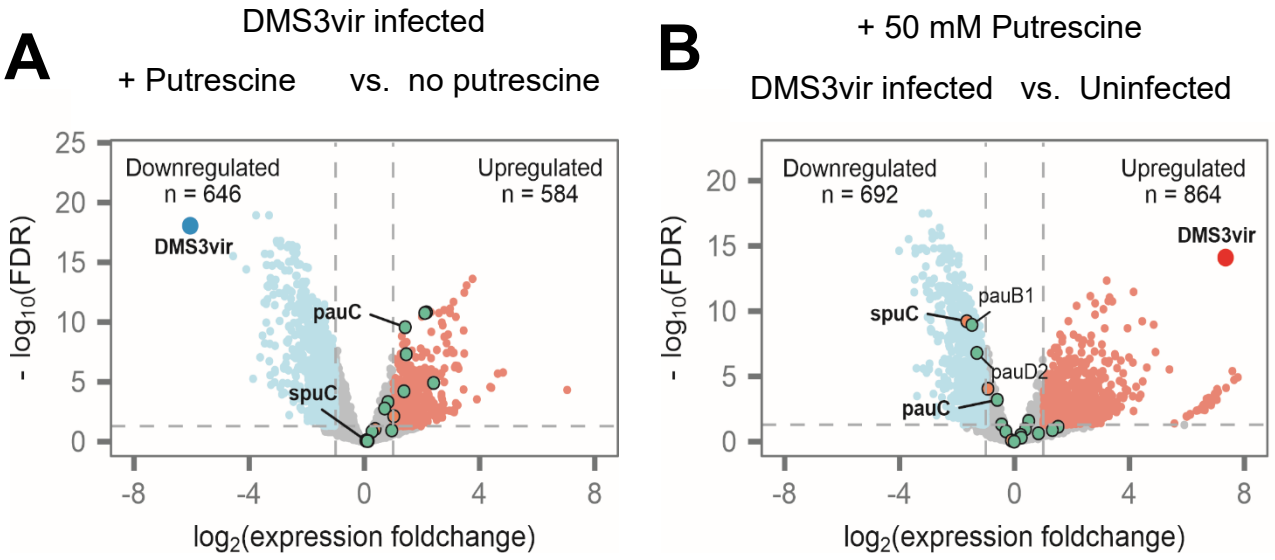

Figure 3-11. DMS3vir infection downregulates polyamine catabolism genes. Volcano plots showing differentially expressed genes in (A) DMS3vir-infected cells cultured with or without 50 mM putrescine or (B) DMS3vir-infected verses uninfected cells both grown with 50 mM putrescine. Red dots indicate upregulated genes (log2[foldchange] > 1 and FDR<0.05), and blue indicates downregulated genes (log2[fold change] < -1 and FDR<0.05). Non-significant genes are shown in gray. Genes involved in polyamine and putrescine catabolism are highlighted. Reads that mapped to the DMS3vir genome are indicated by large blue or red dots in panels A or B, respectively. Three or four biological replicates for each condition are shown.

We hypothesized that downregulated polyamine catabolism in phage-infected cells would cause intracellular polyamine levels to increase. To test this, cell pellets were harvested, washed with 1x PBS, lysed with $CHCl_3$, and total polyamines were measured using a fluorometric assay. Polyamine concentrations were then normalized to bacterial density (OD600). In uninfected wild-type, Δ*retS*, and Δ*gacS* cells growing in LB, basal intracellular polyamine levels were all approximately 8 mM/OD600 (**Fig 3-12 A-C, black lines**). In wild-type and Δ*retS P. aeruginosa* grown with putrescine, intracellular polyamine levels spiked to over 40 mM/OD600 during the first 30 minutes and returned to near basal levels after 6 hours (**Fig 3-12 A and B, yellow lines**). Intracellular

polyamine levels in the Δ*gacS* mutant did not change in the first 30 minutes and remained at 20 mM/OD600 over the course of the experiment (**Fig 3-12 C, yellow line**), indicating a role for Gac/Rsm signaling in regulating intracellular polyamine homeostasis in *P. aeruginosa*.

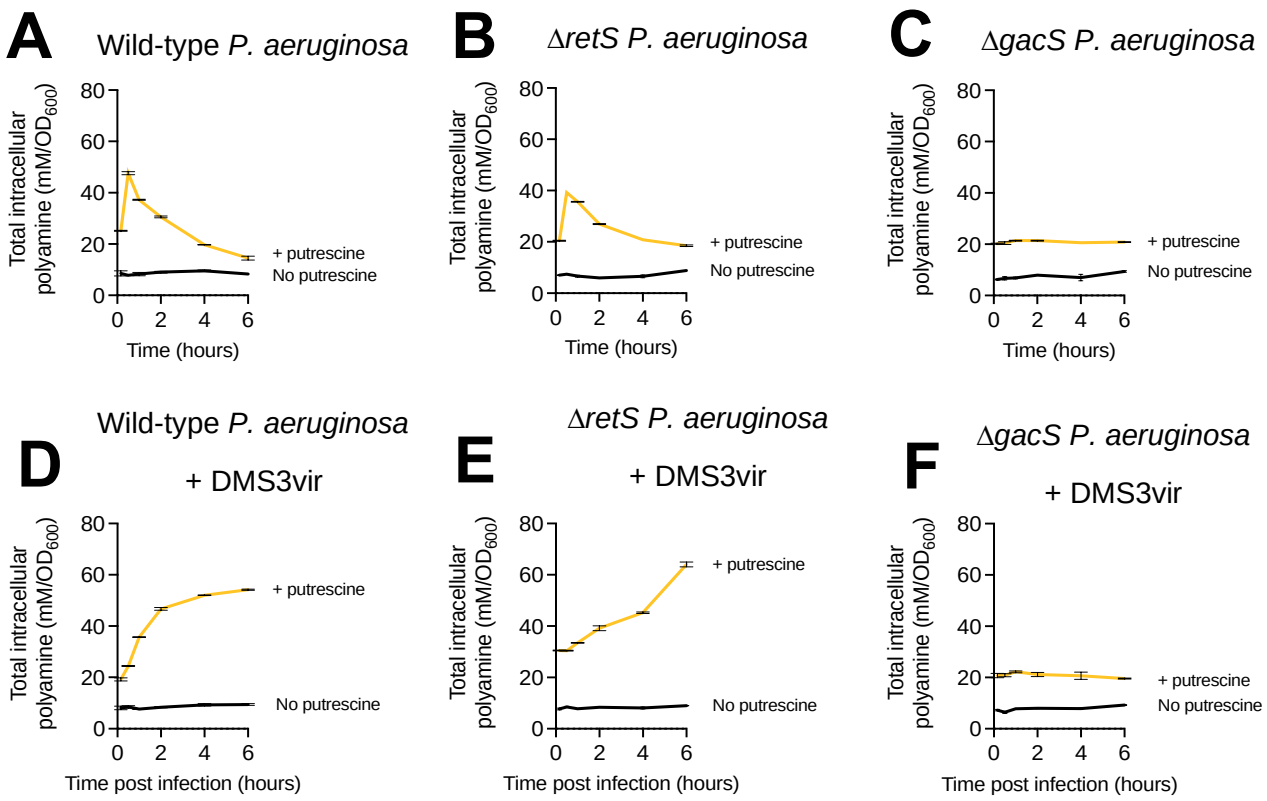

Figure 3-12. Gac/Rsm-dependent intracellular polyamine accumulation suppresses phage DMS3vir replication. Intracellular polyamines were measured and normalized to bacterial density (OD600) in (A-C) uninfected and (D-F) DMS3vir-infected cultures in the indicated strains at the indicated times with (yellow lines) or without (black lines) 50 mM putrescine. Results are means ± SD of duplicate experiments.

In *P. aeruginosa* growing in LB, DMS3vir infection did not affect intracellular polyamine levels in wild-type, Δ*retS*, or Δ*gacS* (**Fig 3-12 D-F, black lines**). In the presence of putrescine, however, DMS3vir infection caused intracellular polyamine levels to increase to and remain at ~50-60 mM/OD600 over the course of 6 hours in both wild-type and Δ*retS P. aeruginosa* (**Fig 3-12 D and E, yellow lines**). During this time, extracellular polyamine concentrations were reduced from 50 mM to ~25 mM and ~15

mM in uninfected and DMS3vir-infected cultures, respectively (**Fig 3-13**). When Δ*gacS* cells growing in putrescine were infected by DMS3vir, intracellular polyamine levels remained unchanged at ~20 mM/OD600 (**Fig 3-12 F, yellow line**), comparable to uninfected Δ*gacS* cells grown with putrescine (**Fig 3-12 C, yellow line**). This observation may explain why the Δ*gacS* strain has a polyamine-induced growth reduction but is still sensitive to phage infection (**Fig 3-5 C**); intracellular polyamine levels may be sufficiently high to affect growth, but not high enough to inhibit the phage lifecycle.

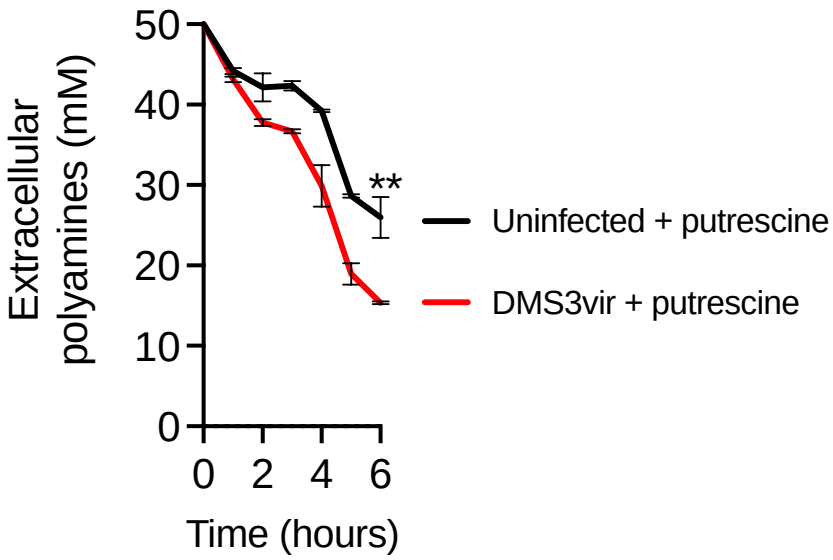

Figure 3-13: Extracellular polyamine concentrations drop faster in DMS3vir infected cells. Total polyamine concentrations in supernatants collected from uninfected (black) or DMS3vir-infected (red) P. aeruginosa PAO1 cultures growing in LB supplemented with 50 mM putrescine were measured at the indicated times. Results are means ± SD of triplicate experiments, **P<0.01.

Together, these results indicate that *P. aeruginosa* reacts to phage infection by utilizing Gac/Rsm signaling to downregulate polyamine catabolism genes, causing intracellular polyamines to accumulate, producing a transient tolerance to phage attack.

3.3.7 Deletion of differentially expressed sigma factors linked to Gac/Rsm signaling did not affect phage tolerance

Further inspection of the RNA-seq data from DMS3vir-infected PAO1 with or without 50 mM putrescine (See **Fig 3-11**), indicated that several sigma factor genes were differentially regulated (**Fig 3-14 A**). As sigma factors have roles in initiating transcription, and several sigma factors are linked to Gac/Rsm signaling [103], we tested sigma factor deletion mutants we had on hand (Δ*rpoH*, Δ*rpoS*, Δ*algU*, Δ*rpoN*) and engineered a deletion mutant for a probable sigma-70 factor (ΔPA2050). We performed plaque assays and growth curve experiments with phage DMS3vir and polyamines on all sigma factor mutants and wild-type PAO1. For three of the four sigma factor mutants (Δ*rpoH*, Δ*rpoS*, and Δ*algU*), the deletion of the sigma factor did not abolish polyamine-induced phage tolerance (**Fig 3-14 B and C**). However, for sigma factor mutant Δ*rpoN*, there was no growth decline when tested with either phage or polyamines exposure, and the mutant was resistant to all phages on LB and putrescine-supplemented plates, barring CMS1 (**Fig 3-14 D**). The panel of phages that were unable to infect were all pili-dependent phages, so we performed a twitch assay to confirm whether this mutant was tolerant to phage due to reduced phage receptor expression. Indeed, twitch assays showed that the Δ*rpoN* mutant was deficient in type IV-pili production, as it showed a similar inability to twitch like the Δ*pilA* negative control (**Fig 3-13E**). Studies have determined that the RpoN affects transcription of motility genes, which confers cross-resistance to many phages at a fitness cost [104, 105]. Thus, we concluded that Gac/Rsm-linked sigma factors were not active elements in the Gac/Rsm-dependent polyamine-induced phage tolerance.

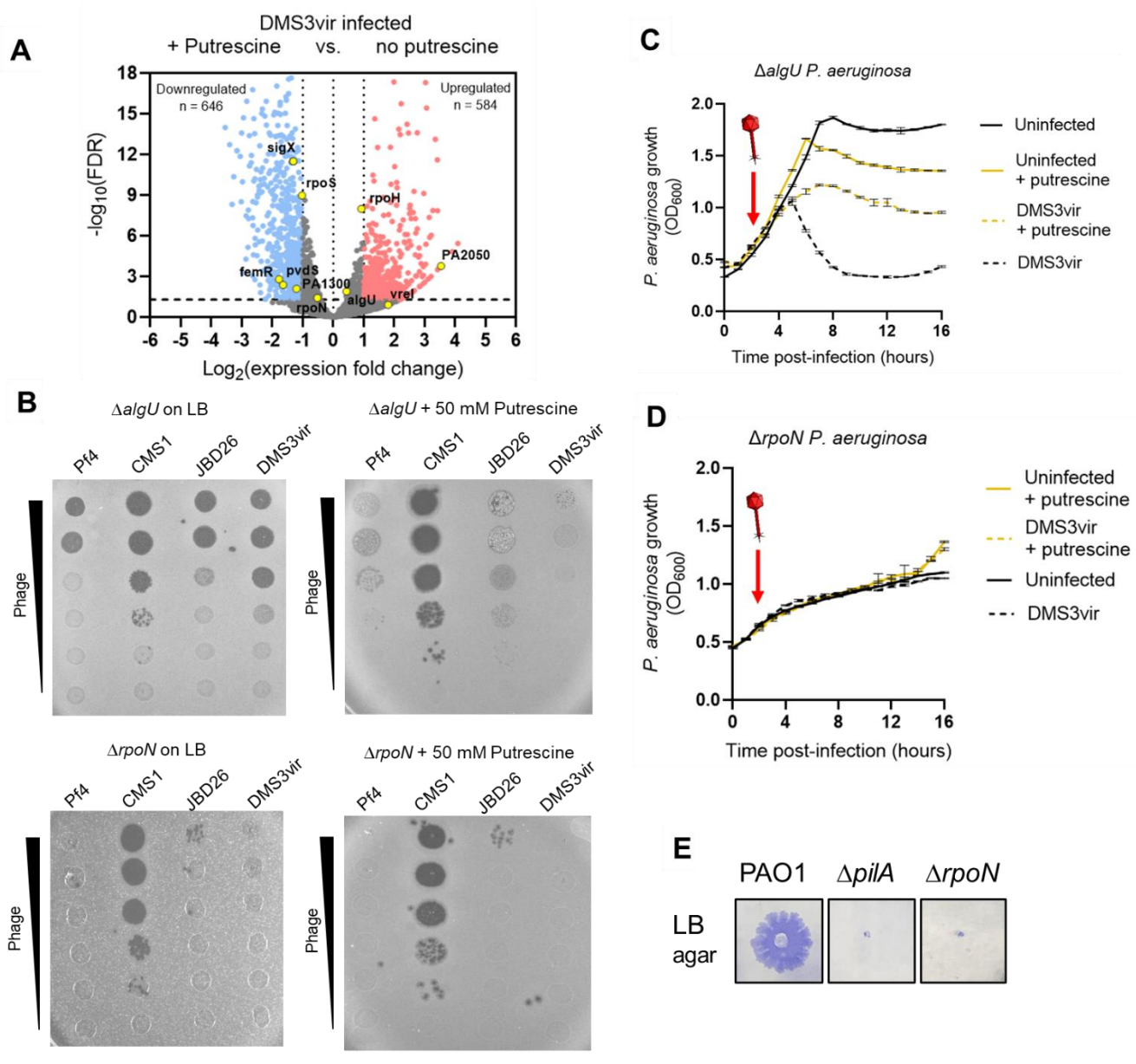
A
DMS3vir infected
+ Putrescine vs. no putrescine
Downregulated
n = 646
Upregulated
n = 584
sigX
rpoS
rpoH
PA2050
femR
pvdS
PA1300
algU
vreI
rpoN
-log10(FDR)
Log2(expression fold change)
B
ΔalgU on LB
ΔalgU + 50 mM Putrescine
ΔrpoN on LB
ΔrpoN + 50 mM Putrescine
Pf4
CMS1
JBD26
DMS3vir
Phage
C
ΔalgU P. aeruginosa
P. aeruginosa growth (OD600)
Time post-infection (hours)
Uninfected
Uninfected + putrescine
DMS3vir + putrescine
DMS3vir
D
ΔrpoN P. aeruginosa
P. aeruginosa growth (OD600)
Time post-infection (hours)
Uninfected + putrescine
DMS3vir + putrescine
Uninfected
DMS3vir
E
PAO1
ΔpilA
ΔrpoN
LB agar

Figure 3-14: Sigma factors do not play a role in polyamine-induced Gac/Rsm-dependent phage tolerance. (A) Volcano plot showing differentially expressed sigma factor genes from DMS3vir-infected cells cultured with or without 50 mM putrescine (Same conditions as Figure 3-11A). Red dots indicate upregulated genes (log2[foldchange] > 1 and FDR<0.05), and blue indicates downregulated genes (log2[fold change] < -1 and FDR<0.05). Non-significant genes are shown in gray. Sigma factor genes are highlighted. Four biological replicates for each condition are shown. (B) *P. aeruginosa* sigma factor mutants Δ*algU* (top) and Δ*rpoN* (bottom) grown on LB agar and LB-putrescine agar plates and then challenged with serially diluted phage panel. Representative images are after 18 hours of growth at 37°C (Δ*algU* plaque pattern is representative of the other *P. aeruginosa* sigma factor mutants Δ*rpoS,* Δ*rpoH, and* ΔPA2050). (C-D) Growth curves of the indicated *P. aeruginosa* strains grown with (yellow) or without (black) 50 mM putrescine. Cells were infected with DMS3vir at the indicated time (arrow) at a multiplicity of infection (MOI) of 1. Results are means ± SD of six experiments. (E) Twitch assays were performed with the indicated strains on a LB agar lawn. Bacteria were stab-inoculated through the agar to the plastic dish below and grown for 24 h at 37°C. The agar was then removed and the adherent bacteria on the dish stained with Coomassie Blue. The Δ*pilA* strain is a twitch-deficient negative control. Representative images of triplicate experiments are shown.

3.4 Discussion

Polyamines were first observed in 1678 in human semen by Antonie van Leeuwenhoek. Later in 1878, it was identified as spermine phosphate by Schreiner, and since then, a variety of polyamines were identified in nearly every living organism, barring two orders of Archaea [106]. The ubiquitous nature of polyamines underlies the importance of these small polycations in organisms in both prokaryotic and eukaryotic cells.

Experiments performed in this chapter demonstrate the significance of high polyamine concentrations in cell lysates. We showed that significant concentrations of polyamines are released upon mass phage-induced cell lysis, triggering a protective phage tolerance that was Gac/Rsm signaling and cyclic-di-GMP dependent. RNA-seq analyses showed that polyamine exposure upregulated polyamine metabolism genes when no phage threat was present, but downregulated polyamine catabolism during co-exposure to phage and polyamines, suggesting the live cells were retaining polyamines intracellularly. Furthermore, we showed that during a co-exposure to phage and extracellular polyamine event, intracellular polyamine levels are maintained at a high level, conferring a lasting protection. In addition, high intracellular polyamine levels

reduced DMS3vir phage adsorption and inhibited phage replication in a Gac/Rsm-dependent manner. Lastly, we determined that a subset of sigma factors linked to the Gac/Rsm signaling regulon was did not have a role in Gac/Rsm-dependent intracellular polyamine accumulation. In summary, we concluded that lysate-induced phage tolerance was due to a Gac/Rsm-dependent intracellular polyamine accumulation, and DMS3vir replication was suppressed at a post-transcriptional level.

Our RNA-seq data comparing *P. aeruginosa* PAO1 transcripts on LB and LB-lysate agar suggested that a significant portion of upregulated transcripts were attributed to polyamine metabolism, specifically catabolism (**Fig 3-2**). It has been shown that polyamines levels increase during times of stress [60], and that polyamines can directly bind to reactive oxygen species and nucleic acids and induce differential expression of protective enzymes, like superoxide dismutase, to shield cellular nucleic acids from harm [47]. Thus, it stands to reason that if no imminent threat is detected, catabolism would be activated to recycle the excess polyamines for use as carbon and nitrogen sources and to alleviate protein translation inhibition due to high polyamine levels [62, 96]. Further, during our purification of crude cell lysates in Chapter 2, we determined that our active signal was small and water-soluble, which aligns with the molecular characteristics of polyamines. Based on the results that commercial polyamines suppressed phage titers in the same manner as crude cell lysate (**Fig 3-6**), suggests that polyamines are being perceived as danger signals, triggering a phage stress response, and aligning with past research [96].

Literature has reported that intracellular polyamine concentrations vary for different bacterial species, ranging from 0.1 to 32 mM [43-45, 47]. Furthermore, it is known that polyamines are vital for γ-proteobacteria growth, whereas many Gram-positive species like *B. cereus* require significantly smaller concentrations of polyamines to function [45, 52]. An interesting finding was that cell lysate from *Staphylococcus aureus*, a Gram-positive bacterium that literature showed thrives in very low polyamine environments and does not possess polyamine catabolism genes, [52] triggered phage tolerance as much as other bacterial strains (**See Fig 2-5**). Polyamine levels of this bacterium's lysate were lower than other species (**Fig 3-3**). However, the polyamine levels were

enough to produce a similar reduction as seen in the dose-response phage tolerance from commercial polyamines (**Fig 3-4**). One possibility is that a subset of virulent *S. aureus* clinical strains had acquired mobile elements encoding polyamine metabolism genes that allow them to biosynthesize and breakdown polyamines, making exogenous polyamines less cytotoxic to the pathogen [51, 52]. The *S. aureus* employed in these experiments was a clinical strain, so it could possess such elements, thus it could produce enough polyamines in its lysate to trigger phage tolerance. Future experiments could compare whether non-clinical strains of other Gram-positives can produce enough polyamines to trigger lysate-induced phage tolerance. Our results demonstrated that polyamines released during cell lysis induced the transient phage tolerance.

The Gac/Rsm pathway modulates circa 300 different genes and it regulates polyamine production, specifically through arginine decarboxylase (*speA*) and ornithine decarboxylases (*speC*) being controlled at the transcriptional level by the GacS sensor in *P. chlororaphis* O6 [94]. Additionally, the two major RNA binding proteins in the Gac/Rsm pathway, RsmA and RsmN, have expansive regulons that control many polyamine metabolism genes. RsmA's regulon encompasses two periplasmic polyamine-binding proteins (PA2711 and PA0295) and acetylpolyamine aminohydrolase PA1409, whereas RsmN recognizes a 5'-CANGGAYG binding motif found in polyamine genes *spuA*, *speC*, *pauB3*, *pauA5*, and *pauC* [23, 107]. This intersection of polyamine metabolism and the Gac/Rsm signaling aligns with our results on the importance of an active Gac/Rsm system for polyamine-induced phage tolerance.

As stated previously, bacteria accumulate polyamines during times of stress, including oxidative stress, bacteriophage infection, or exposure to acid or antibiotics [55, 56, 108]. Our research turned to intracellular polyamine levels when RNA-seq indicated that polyamine catabolism was downregulated during co-exposure to polyamines and phage (**Fig 3-12**). This suggested that during concurrent exposure to phage and polyamines, polyamine catabolism was reduced, causing intracellular levels to increase in order to protect the host cell. This phenomenon is conserved in plant cells which rapidly accumulate polyamines to counteract viral activities and to spur activation of stress responses, similar to our results [55, 108]. Our results showed that polyamine

accumulation due to stress produces a protective state that can allow for bacterial cells to halt phage replication and possibly gain immunity to subsequent infections.

We examined the cellular mechanisms that might underlie polyamine-induced phage tolerance. Cyclic-di-GMP level control mechanisms are an antibacterial target, as many studies work to modulate levels to alter bacterial sensitivities to antibacterial agents, antibiotics, and bacteriophages [109]. A subset of phages requires high cyclic-di-GMP levels to successfully replicate within their hosts [109]. For example, *E. coli* phage N4 specifically stimulates cyclic-di-GMP-building diguanylate cyclase, DgcJ, to increase cyclic-di-GMP levels to complete its lifecycle [110]. The results found that our phage panel preferred low cyclic-di-GMP levels to promote host sensitivity to infection (**See Fig 2-10).** Moreover, degradation of cyclic-di-GMP levels through phosphodiesterase PA2133 in Δ*retS* and wild-type PAO1 promoted phage sensitivity despite protective polyamine exposure (**Fig 3-9**). As cyclic-di-GMP levels are controlled by many systems, including the Gac/Rsm system, this could represent diverse actions this second messenger utilizes to protect the host. Conversely, this could be subverted by the invading phages to promote phage DNA transcription and replication [11, 109].

Another area we delved into was the role of sigma factors in initiating stress responses. Sigma factors are multi-domain cofactors of bacterial RNA polymerases that have roles in transcription initiation and mediate responses to external stimuli (such as heat stress, acid exposure, and reactive oxygen species). Several sigma factors are known to be regulated by Gac/Rsm signaling being upregulated, which we saw differentially-expressed in RNA-seq analysis (**Fig 3-14 D and E**) [98, 104, 111]. We determined that a subset of sigma factors were not involved in Gac/Rsm-dependent polyamine-induced phage tolerance, although certain factors (Δ*rpoN*) could affect phage receptor expression at a fitness cost (Fig [105]. Our research ruled out the role of a subset of Gac/Rsm-linked sigma factors were not involved in this polyamine-induced phage tolerance.

Polyamines have diverse effects on phages, highlighting the molecules' pleotropic nature. For instance, many phages require polycationic polyamines to condense and neutralize their negatively-charged phage DNA to allow for packaging into

proteinaceous heads [53, 105]. It has been shown that polyamines can coat bacteria, shielding the bacterium from phage attachment and penetration; this polyamine coating also extends to protection from cationic peptides, aminoglycoside and quinolone antibiotics [46, 54, 57]. Our observations found that DMS3vir adsorption was moderately blocked by polyamines and that an active Gac/Rsm system increased the amount of non-adsorbed DMS3vir as compared to disabled cells (**Fig 3-7**). Our results shared results of another adsorption study by Xuan et. al., where their *P. aeruginosa* Δ*retS* mutants had almost no phages attached to it, but the Δ*gacS* and wild-type PAO1 had plenty attached, which was similar to our results. Xuan et. al.'s study found that the reduction in attachment was due to reduction in the type-IV-pili (a common phage receptor) production in the Δ*retS* mutant [89]. In contrast to our results, all of our Gac/Rsm mutants did not have a type-IV-pili reduction when exposed to polyamines or phage (**See Fig 2-9**). The discrepancy could be the that Xuan's strains were not exposed to polyamines and in our experiments DMS3vir phage could not bind because of interference from polyamines rather than a reduction in the phage receptor. Polyamines can indirectly and directly bind to nucleic acids and proteins, so interference from polyamines is a possibility. Whereas we saw only modest inhibition of DMS3vir adsorption, there was significant reduction in phage replication as indicated by qPCR genome copy numbers in putrescine-supplemented conditions and the importance of an active Gac/Rsm system in further reducing phage copy numbers (**Fig 3-8**). This reduction in phage genome copy numbers could be attributed to intracellular polyamines aggregating phage DNA, making it inaccessible to replication and transcriptional machinery [58, 59]. Another explanation is that polyamines could be affecting DNA replication enzymes, such as DNA gyrase. DMS3vir copies its genome through replicative transposition, which requires DNA gyrase [112]. Polyamine-induced phage tolerance was shown to halt phage replication and that the process was dependent on an active Gac/Rsm pathway.

The data support a model where *P. aeruginosa* detected extracellular polyamines as a danger signal, triggering accumulation and retention of the extracellular polyamines in anticipation of a phage threat. Phage DNA was inhibited at the post-transcriptional level by an undetermined means, leading to a significant reduction in genome replication. If

no phage threat is detected, polyamines are catabolized and polyamine levels return to basal levels. We determined there a role for cyclic-di-GMP in this mechanism, whereas sigma factors were not involved in Gac/Rsm-dependent polyamine-induced phage tolerance.

Chapter 4: Intracellular polyamine accumulation triggered by linear phage DNA and evasion by N4-like bacteriophage

4.1 Introduction

Phages pose a constant threat to bacterial persistence. As phages aim to hijack their hosts to promote their proliferation, bacteria evolved diverse bacterial immune mechanisms called anti-phage defense systems to interrupt phage replication [33]. These immune systems include innate systems, such as restriction modification and adaptive systems like CRISPR-Cas [113, 114]. Anti-phage defense systems are induced by phage-specific proteins or nucleic acids, or cellular metabolic alterations caused by an active viral infection [113]. For example, both restriction modification and CRISPR-Cas recognize viral nucleotide motifs and will bind and cleave viral DNA to interrupt the phage transcription and replication [31]. Many characterized defense systems have homologues with analogous functions to eukaryotic innate immunity, suggesting ancient sources of many immune systems [115, 116].

Previous chapters described our findings that polyamines were interpreted as a danger signal and protected *P. aeruginosa* from a diverse panel of phages, suggesting that there was a phage-associated signal that triggered polyamine accumulation. However, we also saw that co-exposure to infecting phage and exogenous polyamines were needed to trigger sustained polyamine accumulation. As such, we investigated the influence polyamine accumulation had on phage lifecycle processes, like adsorption, replication, and transcription. We also determined the form of infecting phage DNA that triggers phage tolerance. Phage DNA shifts between two forms during replication, circularized or linear DNA, so we tested whether one was more conducive to triggering polyamine uptake. In addition, we had a phage in our panel that consistently was

unaffected by polyamine-induced phage tolerance, so we investigated the effects of polyamines on phage CMS1 and another N4-like phage from the same group.

Studies described in this chapter expand our knowledge on how polyamines affect phage replication in pathogenic *P. aeruginosa*. We determined that Gac/Rsm-dependent intracellular polyamine accumulation inhibited phage genome replication and transcription. Further, we described a group of N4-like phages that subverted this response by unknown means. Presently, many phage therapies still fail due to bacterial targets evolving to become resistant to phage cocktail treatments. By understanding the varied mechanisms that bacteria use to defend themselves, we could leverage that knowledge to target those systems with the ultimate goal to optimize phage therapies to treat multidrug-resistant bacterial infections.

4.2 Materials and Methods

4.2.1 Bacterial strains, bacteriophages, and plasmids

Bacterial strains, phages, and plasmids are listed in Table 4-1. Deletion mutants were constructed using allelic exchange and Gateway technology, as described previously [74]. Unless indicated otherwise, bacteria were grown in lysogeny broth (LB) at 37°C with shaking and supplemented with antibiotics (Sigma) or 0.1% arabinose when appropriate. Unless otherwise noted, antibiotics were used at the following concentrations: gentamicin (10 or 30 μg ml^{-1}), ampicillin (100 μg ml^{-1}), and carbenicillin (300 μg ml^{-1}).

Table 4-1. List of bacterial strains, phages, and plasmids used in this study

Strain	Description	Source
Escherichia coli		
DH5α	Plasmid maintenance/propagation	New England Biolabs
S17	λpir-positive strain used for conjugation	New England Biolabs
Pseudomonas aeruginosa		
PAO1	Wild type	[78]
PAO1 Δ*retS*	Clean deletion of *retS* from PAO1	[71]
PAO1 Δ*gacS*	Clean deletion of *gacS* from PAO1	[79]
Bacteriophage		

Pf4	Inoviridae	[82]
JBD26	Siphoviridae	[83]
CMS1	Podoviridae	[78]
DMS3vir	Siphoviridae	[84]
F8	Myoviridae	[85]
KPP21	Podoviridae	[78]
Plasmids		
pMF230	constitutively expression of eGFP	[117]
pI-SceI	I-SceI nuclease cloned into pHERD30T	This study
pCut	I-SceI cut site cloned into pUCP18	This study
pEmpty	pUCP18	[118]
pEX18Gm	Allelic exchange suicide vector	[87]

4.2.2 Primers

The nucleotides used in this study are listed in Table 4-2.

Table 4-2: List of oligonucleotides used in this study

Name	Sequence 5' - 3'
pI-SceI F	GCGGAATTCatgcatatgaaaaac
pI-SceI R	GCGTCTAGAttatttcaggaaagtt
pCut F	AACAGCGGATCGTTCTGG
pCut R	CAACTTGAAGTCCTTGATCG
M13 R	CAGGAAACAGCTATGAC

4.2.3 Linearized plasmid DNA assay

pI-SceI was constructed by cloning the I-SceI nuclease from pSLTS [a gift from Shelley Copley, Addgene plasmid # 59386, [69]] cloned into the expression vector pHERD30T between the EcoRI and XbaI sites using primers I-SceI F and I-SceI R (Table 4-1). Restriction cloning sites in primer sequences are indicated by capital letters. pCut was constructed by cloning the I-SceI recognition sequence (TAGGGATAACAGGGTAAT) into pUCP18 between the HindIII and EcoRI sites. pEmpty is simply the empty pUCP18 vector. Primers used to screen for the presence/absence of circular and linear plasmid DNA are as follows: pCutF and M13R produce a 1kb product indicating the presence of circular pCut (these primers will not amplify linearized pCut DNA). pCutF and pCutR produce a 0.5 kb product indicating the presence of both linear and circular forms of pCut. Clones carrying pI-SceI and confirmed linearized pCut plasmid DNA or those carrying pEmpty were archived and used for downstream experiments.

4.2.4 Antibiotic treatment

P. aeruginosa was grown in LB broth to an OD600 of 0.6 before being treated with antibiotics (0.3 µg/mL of ciprofloxacin or 1.0 µg/mL of tobramycin) and with or without 50 mM putrescine. At 1-, 2-, and 6- hours post infection, OD600 measurements were taken and a 100 µL aliquot of each culture was collected for intracellular polyamine measurements.

4.2.5 Adsorption assay

Wild-type, Δ*retS*, or Δ*gacS P. aeruginosa* were grown to an OD_{600} of 0.2 in LB broth with or without 50 mM putrescine followed by infection with CMS1 at an MOI of 0.75. At times 0.5-, 1-, and 10-minutes post infection, 500 µL aliquots were collected from each culture. Cells were removed by centrifugation (4,000 x g, 10 minutes) and virions in supernatants enumerated on lawns of *P. aeruginosa* PAO1.

4.2.6 Total polyamine content assay

Polyamines were measured using the Total Polyamine Assay Kit (MAK349, Sigma). A 100 µL aliquot of the indicated bacterial cultures was collected, centrifuged, washed with 1x PBS, and resuspended in PBS. Bacteria were lysed with 1:10 vol/vol chloroform, vortexed, and incubated at room temperature for 2 h. The solution was centrifuged, and the top aqueous layer was collected. 1.0 µL of the collected sample was mixed with the Total Polyamine Assay Kit reagents following the manufacturer's instructions, incubated at 37°C for 30 minutes, and then read using a CLARIOStar plate reader using end point fluorescence (λ_{ex} = 535 nm/λ_{em} = 587 nm). Polyamine concentrations were determined by comparing values to a standard curve constructed from known concentrations of putrescine. Values were then normalized to OD_{600} measurements taken from the original bacterial cultures.

4.2.7 Plaque assay

Plaque assays were performed using lawn overlays of the indicated strains grown on the indicated plates. Phages in filtered supernatants were serially diluted ten-fold in PBS

and spotted onto lawns of the indicated strain. Plaques were imaged after 18 h of growth at 37°C.

4.2.8 PFU/mL assay – Determination of plaque forming units

During the course of experiments in which exogenous phage were added to the culture, a 500 µL aliquot was collected. The sample was centrifuged and the supernatant was collected and passed through a 0.22-µM filter to produce a cell-free supernatant. A bacterial lawn overlay of PAO1 WT was prepared on LB plates. The cell-free supernatant was serially diluted ten-fold and 5 µL was spotted onto the bacterial lawn. Once dried, the plaques were enumerated and PFU/mL was back calculated using the dilution factor, volume dispensed onto the plate, and the plaque count that was in the range of 20 to 200 plaques per spot. Three replicates per time point were collected and used to determine the average PFU/mL.

4.2.9 Growth curve assays

Overnight cultures were diluted to an OD_{600} of 0.05 in 96-well plates containing LB and, if necessary, the appropriate antibiotics, cell lysate, or polyamines. Three biological replicates with three technical replicates were used per condition. After 2 h of growth, strains were infected with the indicated phage and growth measurements resumed. OD_{600} was measured using a CLARIOstar (BMG Labtech) plate reader at 37°C every 15 minutes with shaking prior to each measurement.

4.3 Results

4.3.1 Circularized plasmid DNA does not trigger intracellular polyamine accumulation

Previously, it was demonstrated that polyamines inhibited DMS3vir genome replication in a Gac/Rsm-dependent manner (**Fig 3-8**). Because the DMS3vir genome replicates as a circular episome, it was hypothesized that polyamines would inhibit other episomal DNA species, like plasmids. To test this, the copy number of pMF230, a high copy number plasmid constitutively expressing GFP, was measured via qPCR [117]. Results

showed that putrescine did not affect plasmid copy number in wild-type, Δ*retS*, or Δ*gacS* *P. aeruginosa* (**Fig 4-1 A**). Additionally, transcription of *gfp* from pMF230 was not affected by putrescine and any strain tested (**Fig 4-1B**), consistent with the observation that putrescine does not affect pMF230 copy number.

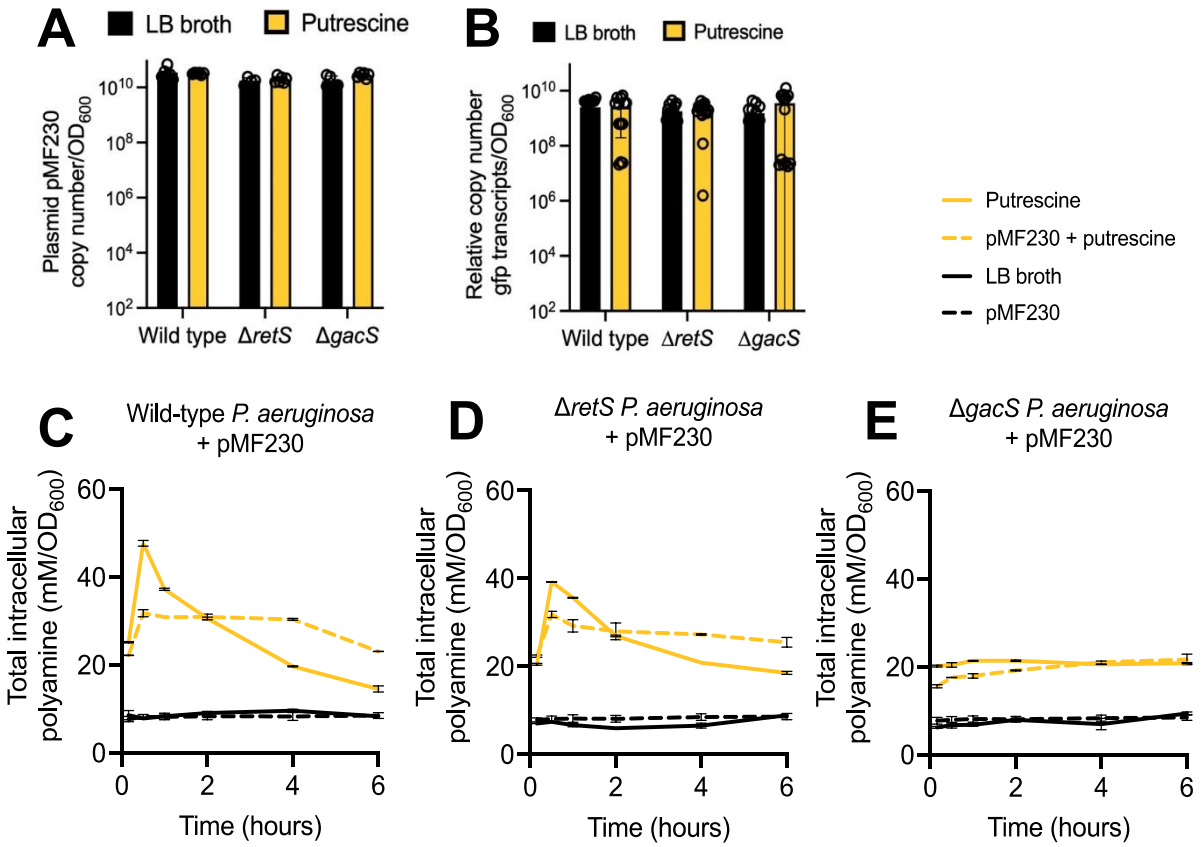

Figure 4-1. Plasmid pMF230 does not induce intracellular polyamine accumulation. (A) Plasmid pMF230 was purified from the indicated strains and copy number measured by qPCR (normalized to bacterial OD600). Absolute copy number was determined using a standard curve generated with a cloned copy of the target sequence. Results are means ± SD of six experiments: ***P<0.001. (B) RT-qPCR was used to measure *gfp* expression in the indicated conditions and strains. Results are means ± SD of at least 12 experiments. (C-E) Intracellular polyamines were measured by fluorometric assay in the indicated strains grown in the presence or absence of 50 mM putrescine with or without the plasmid pMF230. Results are means ± SD of duplicate experiments. Black lines represent cultures grown without putrescine; yellow lines represent cultures supplemented with 50 mM putrescine.

Intracellular polyamine levels in *P. aeruginosa* carrying plasmid pMF230 were also measured. As polyamines did not affect plasmid pMF230 replication or transcription, we predicted that this plasmid would not induce intracellular polyamine accumulation in *P. aeruginosa*. Indeed, in wild-type, Δ*retS*, and Δ*gacS P. aeruginosa*, pMF230 had no impact on intracellular polyamine accumulation (**Fig 4-1 C-E**). As a whole, these results

disproved our hypothesis and indicated that polyamines specifically inhibit double-stranded phage DNA replication.

4.3.2 Linear DNA induces intracellular polyamine accumulation

Intracellular polyamine accumulation was only seen in the presence of phage infection, but how bacterial cells sense that were infected was unclear. As polyamines protect *P.*

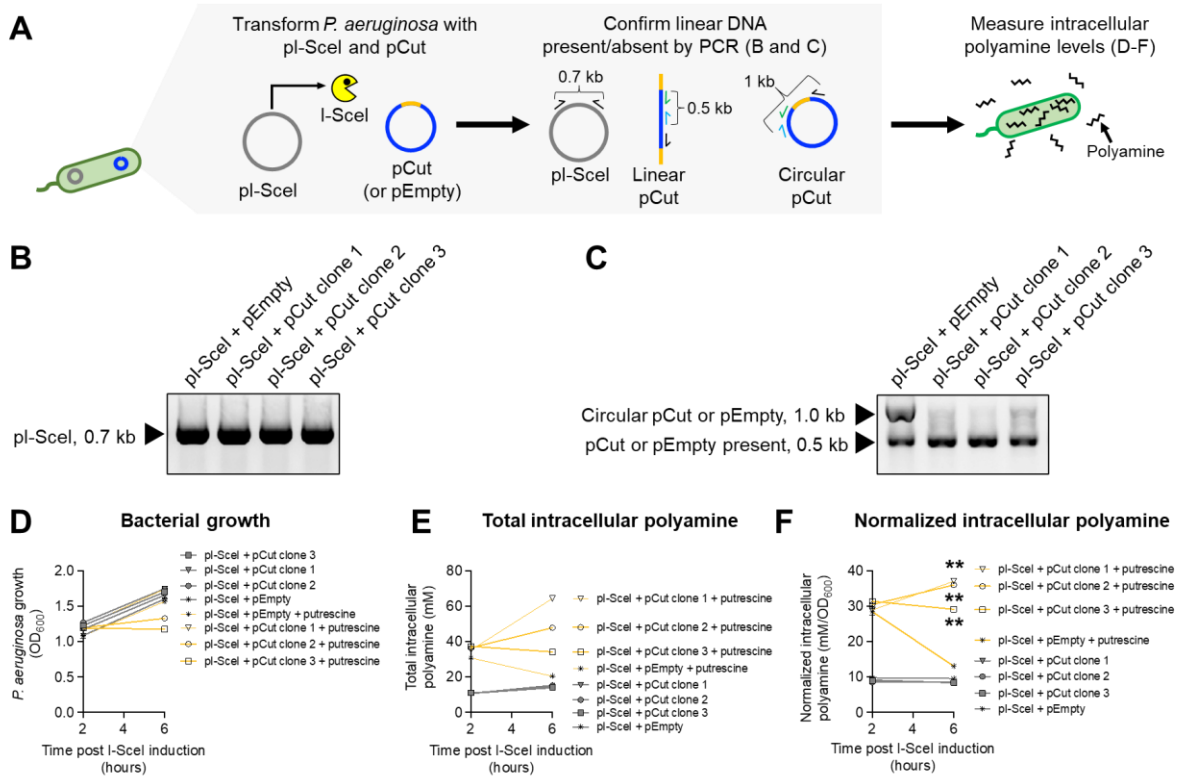

Figure 4-2. Linear DNA induces intracellular polyamine accumulation. (A) Experimental design. pI-SceI encodes the inducible homing endonuclease I-SceI. pCut encodes the 18 bp I-SceI while the empty vector control pEmpty lacks the cut site. (B) The presence of plasmid pI-SceI was confirmed by PCR in the indicated *P. aeruginosa* PAO1 transformants at 6 h post-I-SceI induction. (C) The presence or absence of linear pCut or pEmpty plasmid DNA was confirmed by PCR in the indicated transformants 6 h post I-SceI induction. Three clones containing linear pCut plasmid DNA were included in these experiments. (D-F) Transformants were grown with (yellow) or without (gray) 50 mM putrescine in LB broth for the indicated times at 37°C. (D) Bacterial density (OD_{600}) and (E) total intracellular polyamine were measured. (F) Intracellular polyamine levels were normalized to bacterial density (OD_{600}). Results are means ± SD of duplicate experiments.

aeruginosa from a variety of phage species, it suggests that there is a common phage-associated signal that triggers polyamine accumulation. A commonality of many phage species is that they either inject linear DNA into the host cell or produce linear DNA at some point during their natural replication cycle (e.g., rolling circle replication) [113]. We therefore hypothesized that linearized DNA could trigger intracellular polyamine accumulation. To address this hypothesis, *P. aeruginosa* was transformed with two plasmids—one encoding the inducible homing endonuclease I-SceI (pI-SceI) and a second high-copy plasmid encoding the 18 bp I-SceI cut site (pCut) (**Fig 4-2 A**). A plasmid not encoding the I-SceI cut site was included as a negative control (pEmpty). PCR was used to confirm the presence of pI-SceI (**Fig 4-2 B**) and the presence or absence of linear pCut plasmid DNA *in vivo* (**Fig 4-2 C**). Growth and intracellular polyamine levels were measured in *P. aeruginosa* carrying pI-SceI and pEmpty and in three clones containing pI-SceI and linearized pCut DNA. Growth of two clones containing linearized pCut was static compared to all other strains (**Fig 4-2 D, yellow circles and squares**). Inhibition of cell division associated with the induction of the SOS DNA damage response by linear plasmid DNA may explain this observation. Linear plasmid DNA induced significant ($P<0.01$) intracellular polyamine accumulation compared to cells carrying the circular pEmpty vector (**Fig 4-2 E and F**), indicating that linear DNA induced intracellular polyamine accumulation in *P. aeruginosa*.

4.3.3 DNA-damaging antibiotics induce Gac/Rsm-dependent intracellular polyamine accumulation

As linearized DNA stimulated intracellular polyamine accumulation, other ways to produce linear DNA *in vivo* were investigated. Fluoroquinolone antibiotics like ciprofloxacin induce double-strand DNA breaks by poisoning DNA gyrase at replication forks [119]. We hypothesized that double-stranded DNA breaks caused by ciprofloxacin would induce polyamine accumulation in *P. aeruginosa* (**Fig 4-3 A**). To test this, *P. aeruginosa* was treated with a sub-inhibitory concentration (0.3 µg/mL) of ciprofloxacin. As a control, *P. aeruginosa* was also cultured with a sub-inhibitory concentration of tobramycin (1.0 µg/mL), an aminoglycoside antibiotic that targets the ribosome.

Results showed that *P. aeruginosa* cultures continued to grow in the presence of subinhibitory levels of ciprofloxacin or tobramycin (**Fig 4-3 B**), suggesting that DNA

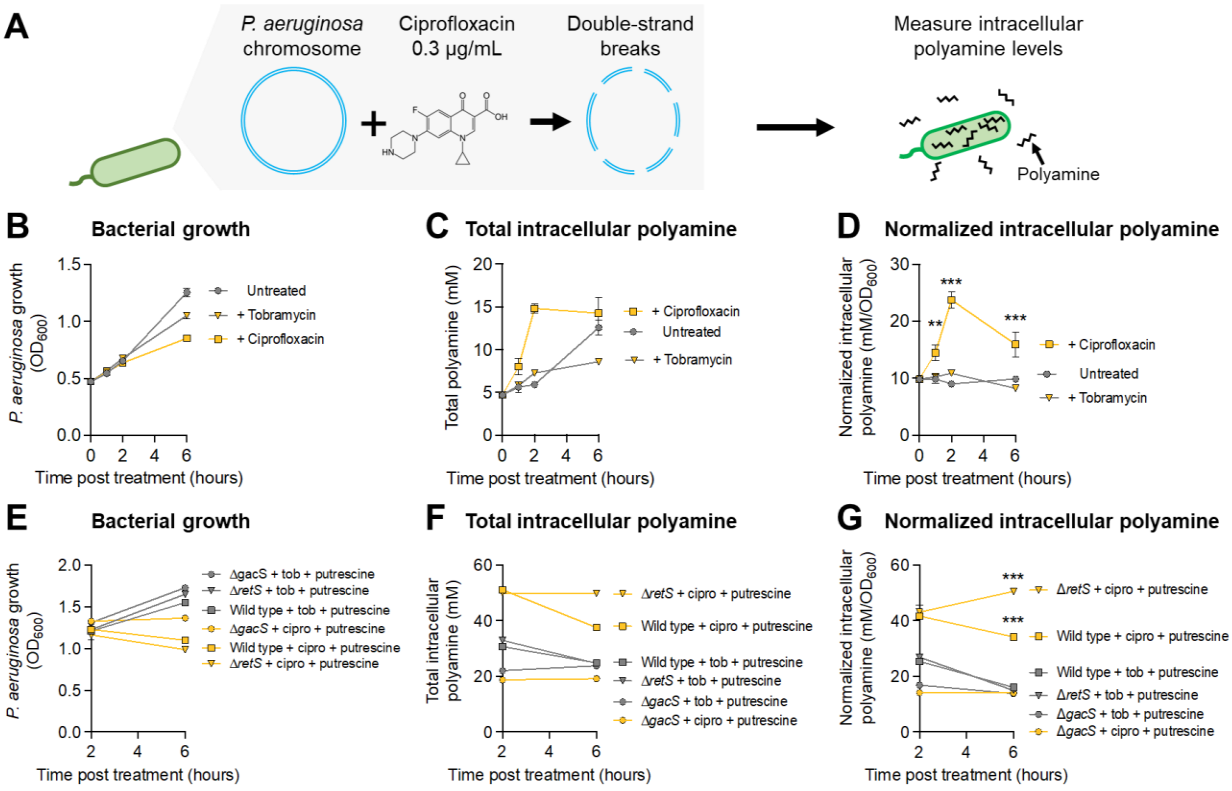

Figure 4-3. Ciprofloxacin, but not tobramycin, induces Gac/Rsm-dependent intracellular polyamine accumulation. (A) Experimental design. (B) *P. aeruginosa* was grown in LB broth to an OD_{600} of 0.5 and treated with a subinhibitory does of either the DNA damaging antibiotic ciprofloxacin (cipro, 0.3 µg/mL) or the ribosome-targeting antibiotic tobramycin (tob, 1.0 µg/mL). Bacteria continued to grow in all conditions. (C) Intracellular polyamine was measured by fluorometric assay at the indicated times. (D) Intracellular polyamine levels were normalized to bacterial density (OD_{600}). Results are means ± SD of triplicate experiments. **P<0.01, ***P<0.001 compared to untreated control. (E-G) A similar experiment was performed using wild-type, Δ*retS*, and Δ*gacS* *P. aeruginosa*. (E) Bacterial density (OD_{600}), (F) total intracellular polyamine, and (G) normalized intracellular polyamine levels were measured or calculated at 2- and 6-h post treatment. Results are means ± SD of triplicate experiments. ***P<0.001 comparing cipro-treated and tob-treated groups.

replication and protein synthesis were not completely inhibited by antibiotic treatment. Without exogenous putrescine, intracellular polyamine levels were comparable in untreated and tobramycin-treated cells at 2 hours post-treatment (**Fig 4-3 C and D,**

triangles vs. circles) while treatment with ciprofloxacin significantly (P<0.001) increased normalized intracellular polyamine levels (**Fig 4-3 D, squares**).

To link Gac/Rsm signaling to ciprofloxacin-induced polyamine accumulation, intracellular polyamine levels were measured in wild-type, Δ*retS*, and Δ*gacS P. aeruginosa* grown in LB supplemented with 50 mM putrescine. Under these conditions, growth of cells treated with ciprofloxacin was static or slightly inhibited compared to cells treated with tobramycin (**Fig 4-3 E, yellow vs. gray**). Six hours post-treatment, intracellular polyamine levels remained elevated in wild-type and Δ*retS* cells treated with ciprofloxacin while intracellular polyamine levels decreased in untreated and tobramycin-treated cells (**Fig 4-3 F and G, yellow vs. gray**). In the Δ*gacS* mutant, intracellular polyamine levels remained unchanged under all conditions tested (**Fig 4-3 G, circles**). These results suggest that ciprofloxacin triggered Gac/Rsm-dependent intracellular polyamine accumulation in *P. aeruginosa*.

4.3.4 N4-like bacteriophage like CMS1 and KPP21 do not induce IPA and are immune to polyamine suppression

It was demonstrated that cell lysate and putrescine inhibited the replication of phages F8, DMS3vir, JBD26, and Pf4, but not phage CMS1 (**Fig 2-1 and 3-4**), a lytic N4-like phage in the family Podoviridae genus Litunavirus [120]. Because CMS1 was able to replicate in wild-type, Δ*retS*, and Δ*gacS* in the presence of 50 mM putrescine (**Fig 4-4 A-C**), we reasoned polyamines would not affect CMS1 adsorption to *P. aeruginosa*. Indeed, adsorption of CMS1 to wild-type or Δ*retS P. aeruginosa* was not affected by putrescine (**Fig 4-4 D and E**) while adsorption of CMS1 virions to Δ*gacS* cells was enhanced under all conditions tested (**Fig 4-4 F**), suggesting a link between Gac/Rsm signaling and expression of the CMS1 cell surface receptor. CMS1 also did not stimulate intracellular polyamine accumulation in *P. aeruginosa*; wild-type, Δ*retS*, or Δ*gacS* grown with exogenous putrescine and infected by CMS1 produced intracellular polyamine curves comparable to uninfected cultures (**Fig 4-5 A-C, compare similarities to Fig 3-12 A-C**). To determine if CMS1 was the only N4-like bacteriophage that was not affected by polyamine accumulation, another N4-like

bacteriophage was acquired and tested for plaquing ability on polyamine plates. In a similar fashion, putrescine did not affect plaquing efficiency of N4-like phage KPP21 [86] (**Fig 4-6**), hinting that N4-like phages have evolved a mechanism(s) to subvert inhibition by Gac/Rsm-dependent intracellular polyamine accumulation.

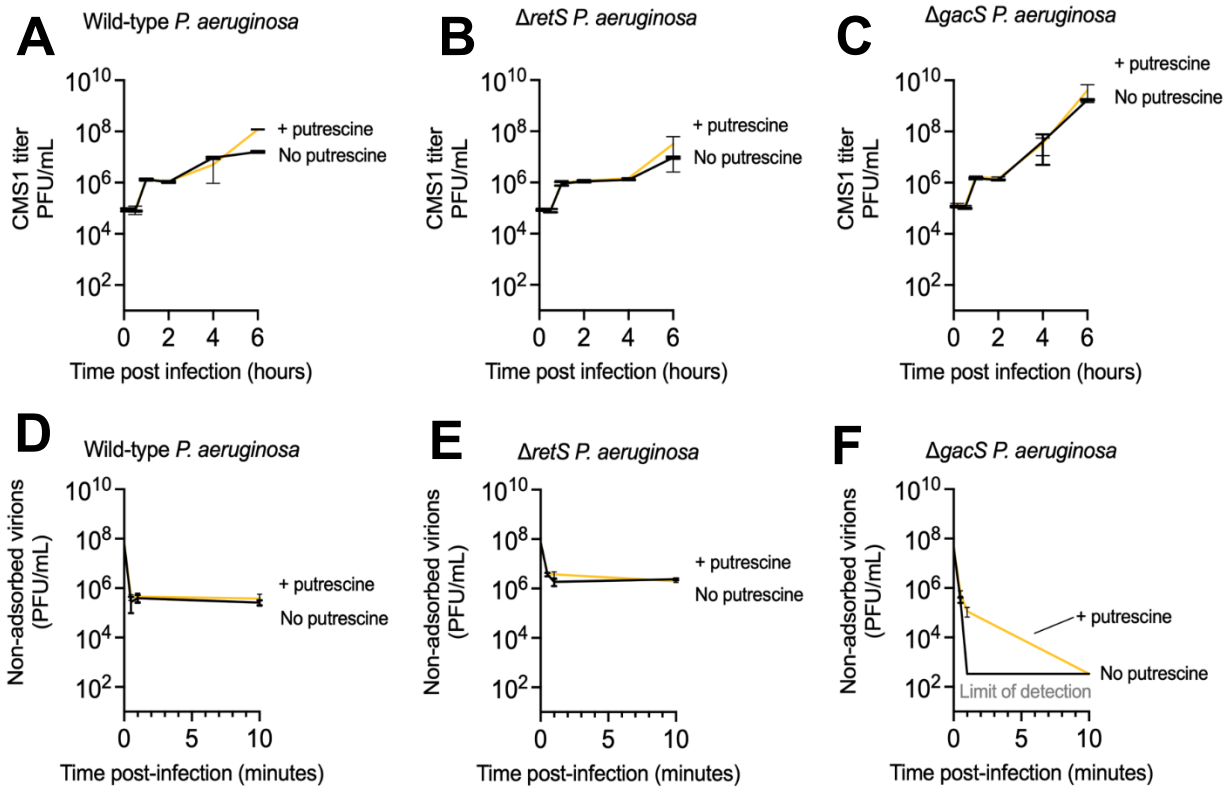

Figure 4-4. CMS1 adsorption and replication are not affected by exogenous putrescine. The indicated strains were grown to an OD_{600} of 0.3 in the presence or absence of 50 mM putrescine followed by infection with the N4-like phage CMS1 at a MOI of 1. (A-C) Phage titers, (D-F) CMS1 virion adsorption were then measured at the indicated times. Results are means ± SD of triplicate experiments.

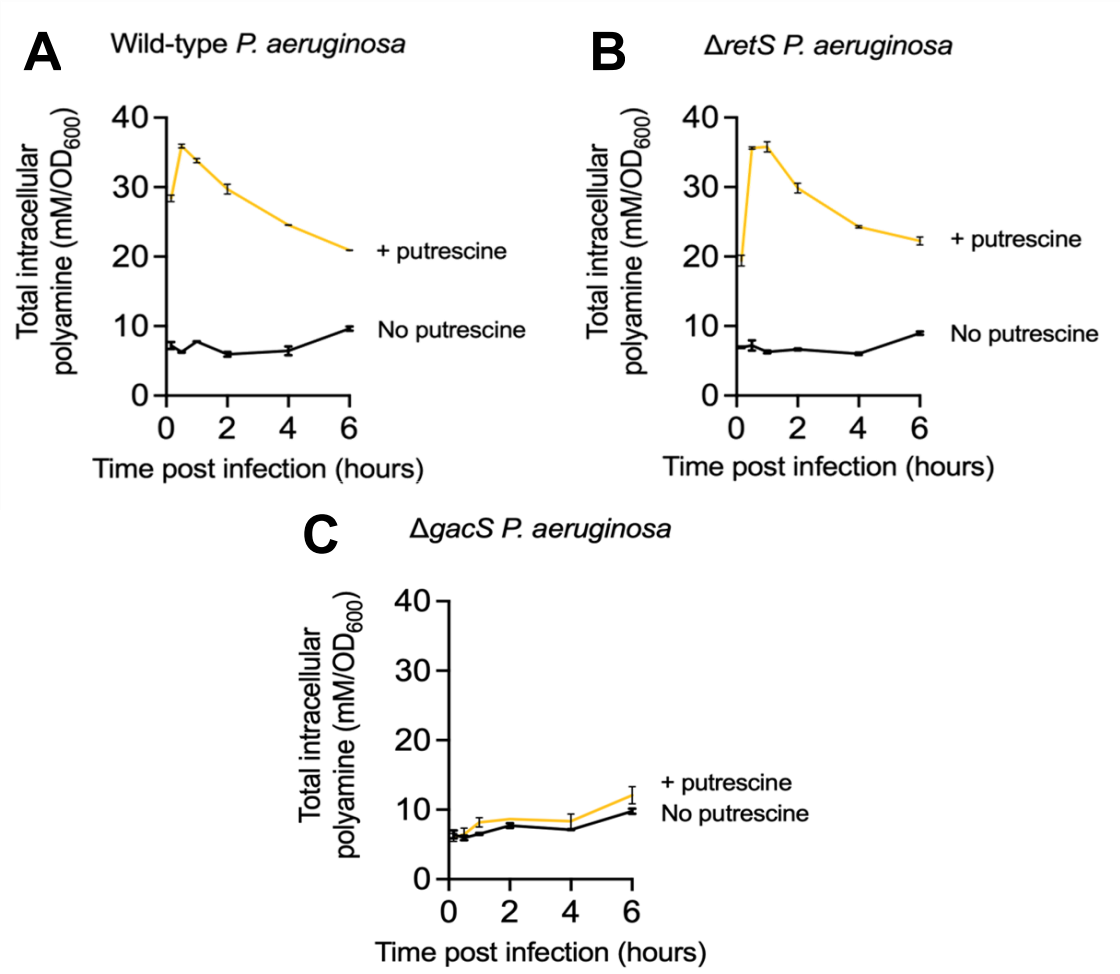

Figure 4-5. CMS1 infection does not induce Gac/Rsm-dependent intracellular polyamine accumulation. The indicated strains were grown to an OD_{600} of 0.3 in the presence or absence of 50 mM putrescine followed by infection with the N4-like phage CMS1 at a MOI of 1. (A-C) Intracellular polyamine levels were then measured at the indicated times. Polyamine levels were normalized to bacterial density (OD_{600}). Results are means ± SD of triplicate experiments.

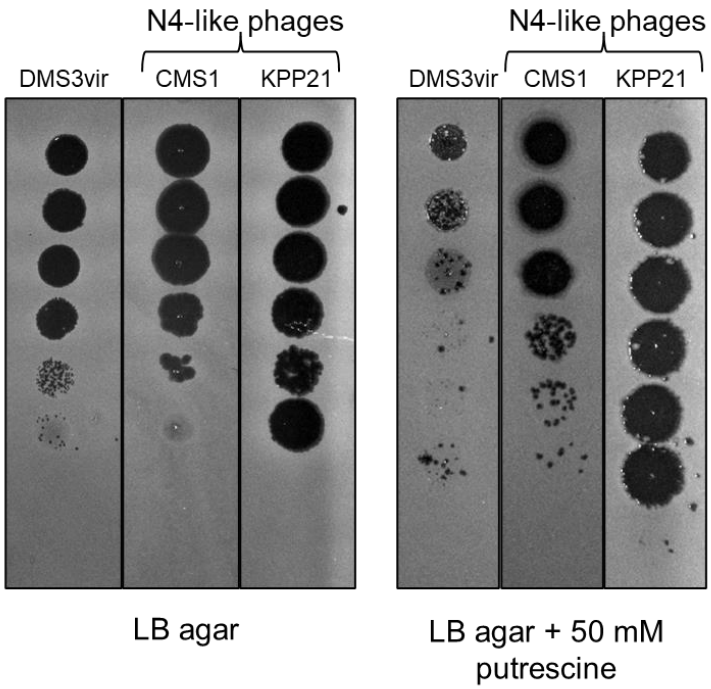

Figure 4-6. N4-like phages escape inhibition by exogenous putrescine**.** Serial dilution plaque assays comparing the plating efficiency of phage DMS3vir and the N4-like phages CMS1 and Kpp21 on lawns of *P. aeruginosa* PAO1. Bacterial lawns were grown on LB agar or LB agar supplemented with 50 mM putrescine for 18 h.

4.4 Discussion

Phages are the most abundant biological entities on the planet, with viruses outnumbering bacterial cells by a factor of 10 [27]. It is proposed that phages arose shortly after the advent of bacterial cells billions of years ago [33]. As such, the war between bacteria and phages is ever ongoing. To prevent bacterial cell death by viral infection, multiple anti-phage defense systems have evolved to interrupt the phage lifecycle. System similarities are seen today in the central components of eukaryotic cell innate immune systems [121], with examples ranging from Toll/interleukin-1 receptor (TIR)-containing pathogen sensors, cyclic GMP-AMP synthase (cGAS)-STING pathways, viperin antiviral proteins, and gasdermin proteins [28, 115, 122, 123].

Bacterial defense systems fall into two categories: systems that target viral nucleic acids and abortive infection systems. Abortive infection systems detect various phage components such as DNA and proteins, resulting in host suicide or metabolic shut down

[31]. One example of an abortive infection system called CBASS (cyclic oligonucleotide-based anti-phage signaling system) occurs when the sensing of phage infection induces the production of cyclic oligonucleotides, causing downstream effector activation to initiate cell death [34]. Further, the CBASS system is considered to be the prokaryotic ancestor to the eukaryotic cGAS-STING antiviral pathway [115]. The most abundant and well-studied are the systems targeting nucleic acids, as they are usually the first viral component to enter the cell during infection [33]. For example, restriction modification (R-M) systems seek and detect unmethylated DNA containing specific base motifs, indicating foreign DNA in the cell, leading to targeted destruction [31]. CRISPR-Cas is also well studied and involves recognition and degradation of viral nucleic acids that were acquired and archived from a previous infection [35].

Previously, it was shown that polyamines were protective against diverse phage groups, hinting that there was a common phage-associated signal that induced polyamine accumulation. To elucidate that signal, we tested a few forms phage DNA takes when it enters the host and replicates. We determined that circularized replicating DNA did not trigger polyamine accumulation, but linear DNA that would be present upon phage DNA injection was needed to induce polyamine accumulation. Furthermore, generating linear DNA within the host using DNA-damaging agents like the antibiotic ciprofloxacin also triggered polyamine accumulation. Lastly, we determined that a group of N4-like phages that included phages CMS1 and KPP21 did not induce polyamine accumulation upon infection, suggesting that these phages evolved means to overcome polyamine accumulation induced protection.

Results showed that episomally replicating plasmid DNA did not induce polyamine accumulation, nor did the host cell affect transcription and replication of said plasmid. This aligns with studies that showed that many plasmids require polyamines to replicate [124], which could indicate that some aspect about plasmid DNA is not interpreted as dangerous foreign DNA. There is evidence that some mobile genetic elements like plasmids can act “selfishly” by encoding plasmid addiction systems to ensure their survival though generations [125]. This suggests that bacterial cells do not treat plasmid DNA as threats, so no polyamine accumulation occurs. Linear DNA, however, was a

trigger for polyamine accumulation. During phage infection, linear DNA is injected into the host and for some phages linear DNA is produced at one point during replication [113]. Linear DNA is not a common occurrence during normal cellular processes, which would lead the host cell to interpret linear phage DNA as damaged host DNA in a manner similar to genotoxic stress-triggered responses like the SOS response [126]. Many phage systems are also activated by linear DNA, such as the DISARM system, restriction-modification, or abortive infection systems [34, 113, 122]. Further research will need to be done to delve into phage defense system activation. We also saw that DNA-damaging agents, like ciprofloxacin antibiotic treatment, triggered polyamine accumulation. This was a novel result, as ciprofloxacin treatment alone (without exogenous polyamines) was enough to trigger polyamine accumulation, whereas all previous experiments needed both phage infection and polyamine exposure to polyamine accumulation. A few reasons may shed light on why. Polyamines are known to be protective against reactive oxygen species and DNA damaging UV radiation by scavenging reactive oxygen species or reducing accessibility of attack sites [127, 128], so ciprofloxacin exposure caused enough damage to trigger polyamine accumulation in a bid to protect the genome. Further, ciprofloxacin could be a more potent inducer of polyamine accumulation that phage infection or linear DNA by the amount of linearized DNA in the host cell caused by ciprofloxacin treatment vs. phage infection. The exact trigger and mechanism that mediates the Gac/Rsm-dependent polyamine accumulation was not determined, but clues into the characteristics of the trigger were elucidated in this chapter.

The results suggested a significant role for Gac/Rsm signaling in modulating intracellular polyamine levels in *P. aeruginosa*. The Gac/Rsm signaling pathway includes two RNA binding proteins, RsmA and RsmN, both of which bind to genes involved in polyamine metabolism (**Fig 1-3**) [23, 107]. The RsmA regulon includes genes encoding two periplasmic polyamine-binding proteins (PA2711 and PA0295) and the acetylpolyamine aminohydrolase PA1409 [23]. Polyamine catabolism genes are also in the RsmN regulon, as the 5′-CANGGAYG motif recognized by RsmN include polyamine metabolism genes like *spuA*, *speC*, *pauB3*, *pauA5*, and *pauC* [107].

Lastly, we demonstrated that N4-like bacteriophages have evolved a yet uncharacterized mechanism to overcome Gac/Rsm-dependent polyamine accumulation. N4-like phage are characterized by the presence of virion-associated RNA polymerase that is co-injected with the viral DNA upon phage infection [129]. The polymerase then initiates RNA synthesis and helps pull the phage genome into the host cell. Injection of the remaining genome is carried out by a phage-encoded RNA polymerase [130]. These RNA polymerases then begin transcription before the cell detects the phage DNA, inhibiting threat detection mechanisms. Furthermore, multiple N4-like phage species have been shown to encode proteins that bind to *P. aeruginosa* polyamine metabolism genes, which could give support to the suggestion that N4-like phages modulate host polyamine metabolism to subvert inhibition by polyamine accumulation [131, 132]. One the N4-like phage proteins described in these studies, gp30, targets the host's spermidine acetyltransferase, a regulator of intracellular polyamine levels. The study suggests that this protein modulated the concentration of polyamines within the host to allow the phage to utilize the polyamines for phage DNA condensation and packaging [131]. However, based on the partially annotated genome sequencing for phage CMS1, this phage does not encode a protein similar to gp30, hinting that there are other means this phage overcame polyamine accumulation [120]. Further annotation of the CMS1 genome and investigation into how other N4-like phages control host polyamine levels would give more insight into how polyamine-induced protection is achieved mechanistically.

Experiments determined that linear DNA is sufficient to trigger Gac/Rsm-dependent polyamine accumulation. Linear DNA can be in a few forms, such as linear phage DNA or host linearized DNA caused by genome damage (in this case DNA targeting antibiotic treatment). Danger signal detection is an important aspect of innate immune systems. Our data support a model where *P. aeruginosa* senses polyamines and linear DNA as a danger signal, initiating threat assessments of cellular injury. Future studies include identifying the exact mechanisms by which linear DNA is sensed, how Gac/Rsm signaling adjusts intracellular polyamine levels, and whether other molecules act as

danger signals would provide novel insights into bacterial immune systems. Our results also highlight danger sensing as a collective behavior across biological kingdoms, which may unveil universal principles of cellular responses to viral infection and cellular injury.

Chapter 5: Conclusions

5.1 Current model

Cellular injury or infection by pathogens release intracellular contents into the environment, with certain molecules being seen as danger signals by neighboring cells. Based on the identity and concentration of the active molecule, both eukaryotic and prokaryotic cells can make threat assessments and initiate appropriate responses. Bacteria are able to sense a variety of danger signals from lysed neighbor cells and orchestrate a greater assortment of defensive responses [26, 36, 40, 67]. These responses are deemed anti-phage defense systems, and their effects range from targeting phage-specific molecules to interrupt its lifecycle (such as CRISPR-Cas, DISARM, and R-M systems) to programmed cell death, as a last resort, during progressed phage infection (abortive infection systems) [34, 113].

In this dissertation, we determined that phage infection causes lysed bacterial cells to release high concentrations of polyamines into the extracellular space. In neighboring *P. aeruginosa*, high extracellular polyamines are detected by undescribed means, triggering an upregulation in polyamine uptake and reduction in polyamine catabolism, causing intracellular polyamine levels to rise in anticipation of an imminent phage infection (**Fig 5-1**). If linear DNA is detected within the neighbor cell while polyamine levels are high, the high polyamines will be maintained and the intracellular polyamines will inhibit phage transcription and replication in a post-transcriptional manner, ultimately interrupting the phage lifecycle. Further, it was determined that Gac/Rsm signaling is paramount for *P. aeruginosa* to mediate the increase and maintenance of high intracellular polyamine levels. If linearized DNA is not detected during the period of high polyamine accumulation, polyamine catabolism will reinitiate and intracellular concentrations will return to basal levels. Additionally, genotoxic stressors that produce

linear DNA fragments are enough to trigger polyamine accumulation, indicating that linear DNA is also seen as a danger signal that triggers bacterial defenses. This study also highlighted the importance of the two-component system Gac/Rsm in mediating polyamine levels. Finally, as polyamines are ubiquitous in the environment, the phage tolerance phenotype may be a conserved strategy employed by γ-proteobacteria to defend against phage infection.

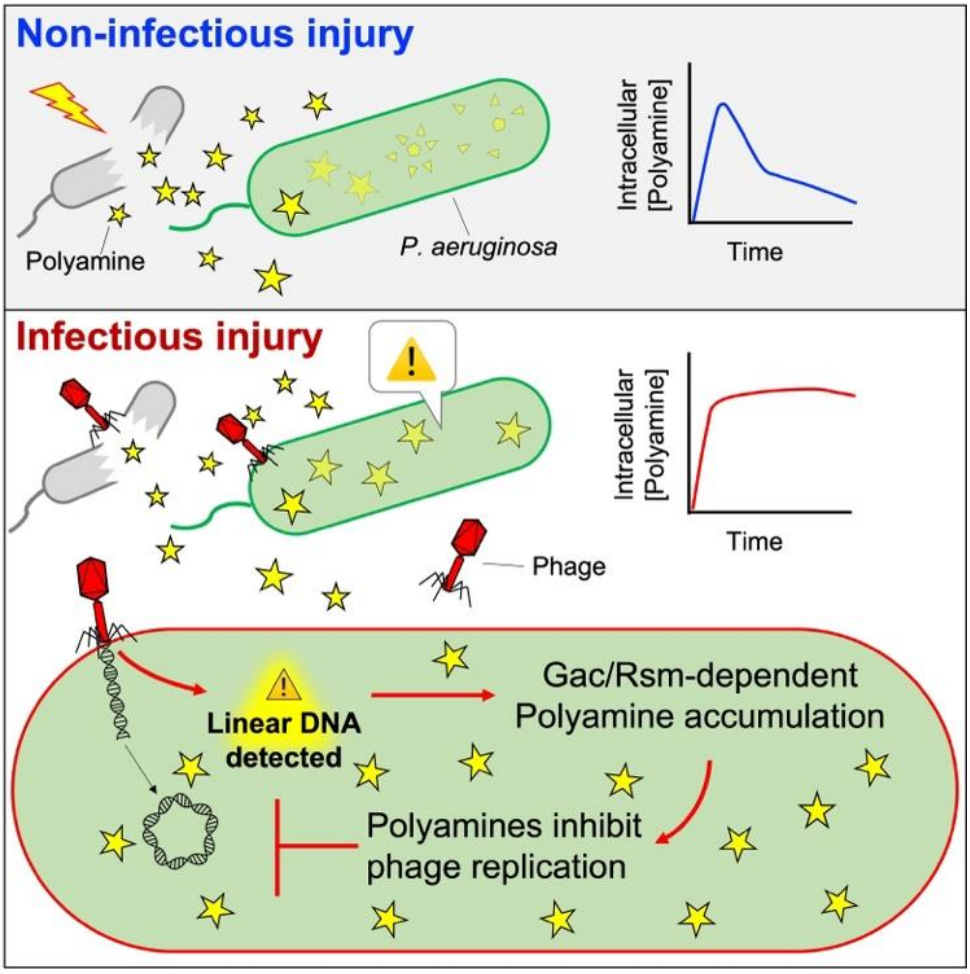

Figure 5-1: Model schematic of Gac/Rsm-dependent intracellular polyamine accumulation Released polyamines and linear phage DNA trigger a Gac/Rsm-dependent polyamine accumulation that inhibits phage replication. If a non-infectious injury occurs near a live cell (top), polyamine levels will spike and then rapidly decrease as no phage threat is detected. If linear DNA is detected within the cell when polyamine accumulating (bottom), levels will remain high, inhibiting phage replication and proliferation.

We present a model in which *P. aeruginosa* detects polyamines and linear DNA as danger signals to make a threat determination of cellular injury. Future research to

tease out the detailed mechanisms in which linear DNA is sensed, how Gac/Rsm signaling modulates polyamine metabolism, how cyclic-di-GMP signaling fits into the mechanism, and what other molecules serve as danger signals will lay the groundwork for understanding bacterial immune systems. Intracellular polyamine accumulation was triggered by DMS3vir phage infection and linear DNA, which is analogous to how some phage defense systems detect infection. For example, the DrmAB complex of DISARM systems binds to linear DNA substrates with a 5'-overhang, allowing this defense system to detect infection by a wide range of phage species [113]. How linear DNA induces intracellular polyamine accumulation is not known, but it may involve DNA-binding protein(s) analogous to DrmAB that discriminate DNA targets based on structure as opposed to sequence.

5.2 Future directions and summary

One observation of interest that needs future research is that during visualization of cells using fluorescence microscopy, wild-type and Δ*gacS* cells infected by DMS3vir were significantly longer than uninfected cells and cells supplemented with putrescine did not exhibit cell elongation during a DMS3vir infection (**Fig 5-2**). *P. aeruginosa* Δ*retS* cell length did not change under any condition tested. These results suggest that successful infection by DMS3vir prevents *P. aeruginosa* cell division and septum formation, resulting in cell elongation. These results also suggest that putrescine disrupted DMS3vir replication before the phage can prevent *P. aeruginosa* cell division—so long as Gac/Rsm signaling was intact. Polyamines can inhibit or enhance DNA gyrase activity [43], so it is possible that high intracellular polyamine levels inhibited DNA gyrase, halting DMS3vir replication in *P. aeruginosa*. This might explain our fluorescence imaging results of *P. aeruginosa* Gac/Rsm mutants exposed to putrescine and DMS3vir phage. Polyamine exposure could have halted DMS3vir transcription through DNA aggregation before the phage could affect the host's cell division processes.

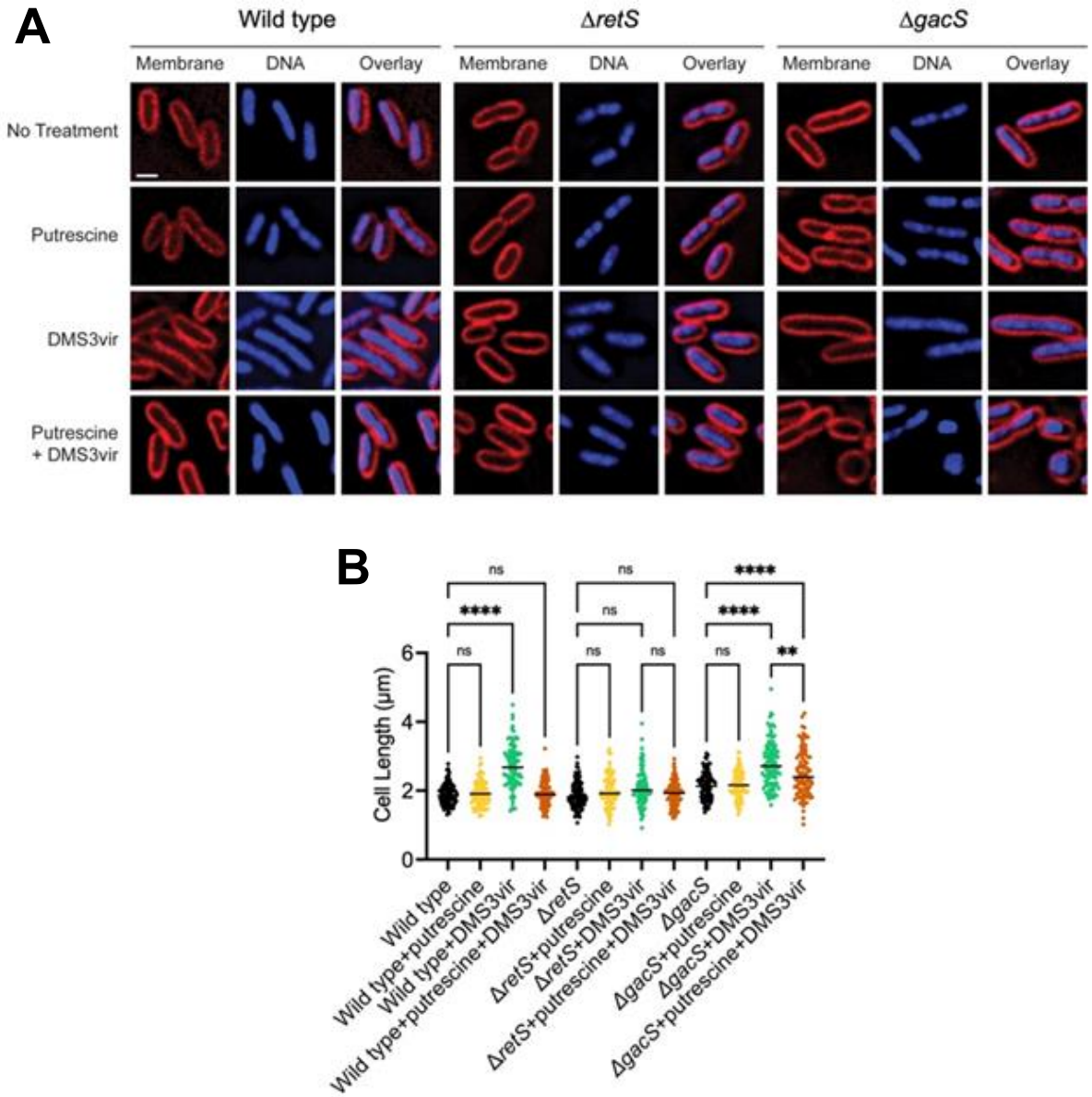

Figure 5-2. Putrescine prevents cell elongation caused by DMS3vir infection. (A and B) Fluorescence micrographs of wild-type, Δ*retS*, or Δ*gacS P. aeruginosa* strains stained with SynaptoRed (membrane; red) and DAPI (DNA; blue) 2 hours post-treatment with putrescine, phage DMS3vir, both, or neither. Scale bar is 1 μm. (B) Quantification of cell length of cells in each treatment condition shown in panel D. n = 100 cells; **** $P < 0.0001$, ** $P < 0.06$, and ns = not statistically significant.

Polyamine metabolism involves biosynthesis, catabolism, and transport mechanisms in *P. aeruginosa*. To identify the specific mechanisms of Gac/Rsm-dependent polyamine accumulation, polyamine biosynthesis, catabolism, and transport should be investigated through genetic techniques like Gateway technology or other cloning methods. Disabling certain systems could provide insights into the role of polyamines in mediating phage tolerance. Future studies to determine the precise mechanisms by which Gac/Rsm and cyclic-di-GMP signaling regulates intracellular polyamine accumulation and how bacterial cells sense phage infection will provide valuable new insights into phage-bacteria interactions. Another aspect to investigate is how N4-like bacteriophage undermine polyamine accumulation to replicate unimpeded. There is preliminary evidence that N4-like phage encode proteins that bind to polyamine metabolism-linked enzymes in *P. aeruginosa*, suggesting that these phages have means to manipulate bacterial polyamine levels. To summarize, there are still many mechanistic questions how polyamines are interpreted as a danger signal and how that defense response is mediated, but further studies could reveal broad principles of responses to viral infection and cellular injury.

5.3 Methods for Fluorescence microscopy

P. aeruginosa strains of wild-type, Δ*gacS*, and Δ*retS* were back-diluted from overnight cultures and grown until OD600 = 0.2-0.3. Cells were then treated with putrescine to a final concentration of 50mM, DMS3vir, both, or neither. In the cultures that were treated with both, cells were pre-treated for 10 min with putrescine prior to the addition of phage. Cultures were then allowed to grow for an additional 2 hours. UV fluorescence microscopy was then performed as previously described [133]. Briefly, cells from culture aliquots of each strain in different treatment condition were stained with 1 µg/ml SynaptoRed (FM4-64) and 1 µg/ml DAPI to visualize the membrane and DNA respectively. Aliquots (5 µl) of the stained samples were then spotted onto glass-bottom dishes (Mattek) and covered with a 1% agarose pad. Samples were imaged on a DeltaVision Elite microscope (Applied Precision/GE Healthcare/Leica Microsystems) equipped with a Photometrics CoolSnap HQ2 camera. Seventeen planes were acquired every 200 nm. The images were subsequently deconvolved using the manufacturer-

supplied software, SoftWorx. Cell length was measured using ImageJ and analyzed in GraphPad Prism 9.

References

1. Holger, D., et al., *Clinical Pharmacology of Bacteriophage Therapy: A Focus on Multidrug-Resistant Pseudomonas aeruginosa Infections.* Antibiotics (Basel), 2021. **10**(5).
2. Stover, C.K., et al., *Complete genome sequence of Pseudomonas aeruginosa PAO1, an opportunistic pathogen.* Nature, 2000. **406**(6799): p. 959-64.
3. Malhotra, S., D. Hayes, Jr., and D.J. Wozniak, *Cystic Fibrosis and Pseudomonas aeruginosa: the Host-Microbe Interface.* Clin Microbiol Rev, 2019. **32**(3).
4. Pang, Z., et al., *Antibiotic resistance in Pseudomonas aeruginosa: mechanisms and alternative therapeutic strategies.* Biotechnology Advances, 2019. **37**(1): p. 177-192.
5. Mulani, M.S., et al., *Emerging Strategies to Combat ESKAPE Pathogens in the Era of Antimicrobial Resistance: A Review.* Front Microbiol, 2019. **10**: p. 539.
6. Moscoso, J.A., et al., *The diguanylate cyclase SadC is a central player in Gac/Rsm-mediated biofilm formation in Pseudomonas aeruginosa.* J Bacteriol, 2014. **196**(23): p. 4081-8.
7. Zuber, S., et al., *GacS sensor domains pertinent to the regulation of exoproduct formation and to the biocontrol potential of Pseudomonas fluorescens CHA0.* Mol Plant Microbe Interact, 2003. **16**(7): p. 634-44.
8. Turner, K.H., et al., *Requirements for Pseudomonas aeruginosa acute burn and chronic surgical wound infection.* PLoS Genet, 2014. **10**(7): p. e1004518.
9. Goodman, A.L., et al., *Direct interaction between sensor kinase proteins mediates acute and chronic disease phenotypes in a bacterial pathogen.* Genes Dev, 2009. **23**(2): p. 249-59.
10. Rossi, E., et al., *Pseudomonas aeruginosa adaptation and evolution in patients with cystic fibrosis.* Nat Rev Microbiol, 2021. **19**(5): p. 331-342.
11. Moscoso, J.A., et al., *The Pseudomonas aeruginosa sensor RetS switches type III and type VI secretion via c-di-GMP signalling.* Environ Microbiol, 2011. **13**(12): p. 3128-38.
12. Papon, N. and A.M. Stock, *Two-component systems.* Curr Biol, 2019. **29**(15): p. R724-R725.
13. Bhagirath, A.Y., et al., *Two Component Regulatory Systems and Antibiotic Resistance in Gram-Negative Pathogens.* Int J Mol Sci, 2019. **20**(7).
14. Liu, C., et al., *Two-Component Signal Transduction Systems: A Major Strategy for Connecting Input Stimuli to Biofilm Formation.* Frontiers in Microbiology, 2019. **9**.
15. Tierney, A.R. and P.N. Rather, *Roles of two-component regulatory systems in antibiotic resistance.* Future Microbiol, 2019. **14**: p. 533-552.
16. Zschiedrich, C.P., V. Keidel, and H. Szurmant, *Molecular Mechanisms of Two-Component Signal Transduction.* J Mol Biol, 2016. **428**(19): p. 3752-75.
17. Chambonnier, G., et al., *The Hybrid Histidine Kinase LadS Forms a Multicomponent Signal Transduction System with the GacS/GacA Two-Component System in Pseudomonas aeruginosa.* PLoS Genet, 2016. **12**(5): p. e1006032.
18. Sultan, M., R. Arya, and K.K. Kim, *Roles of Two-Component Systems in Pseudomonas aeruginosa Virulence.* Int J Mol Sci, 2021. **22**(22).
19. Latour, X., *The Evanescent GacS Signal.* Microorganisms, 2020. **8**(11).
20. Lapouge, K., et al., *Gac/Rsm signal transduction pathway of gamma-proteobacteria: from RNA recognition to regulation of social behaviour.* Mol Microbiol, 2008. **67**(2): p. 241-53.

21. Shang, L., et al., *A regulatory network involving Rpo, Gac and Rsm for nitrogen-fixing biofilm formation by Pseudomonas stutzeri.* NPJ Biofilms Microbiomes, 2021. **7**(1): p. 54.
22. Ventre, I., et al., *Multiple sensors control reciprocal expression of Pseudomonas aeruginosa regulatory RNA and virulence genes.* Proc Natl Acad Sci U S A, 2006. **103**(1): p. 171-6.
23. Brencic, A. and S. Lory, *Determination of the regulon and identification of novel mRNA targets of Pseudomonas aeruginosa RsmA.* Mol Microbiol, 2009. **72**(3): p. 612-32.
24. Brencic, A., et al., *The GacS/GacA signal transduction system of Pseudomonas aeruginosa acts exclusively through its control over the transcription of the RsmY and RsmZ regulatory small RNAs.* Mol Microbiol, 2009. **73**(3): p. 434-45.
25. Jing, X., et al., *Crystal structure and oligomeric state of the RetS signaling kinase sensory domain.* Proteins, 2010. **78**(7): p. 1631-40.
26. LeRoux, M., et al., *Kin cell lysis is a danger signal that activates antibacterial pathways of Pseudomonas aeruginosa.* Elife, 2015. **4**.
27. Comeau, A.M., et al., *Exploring the prokaryotic virosphere.* Res Microbiol, 2008. **159**(5): p. 306-13.
28. Bernheim, A. and R. Sorek, *The pan-immune system of bacteria: antiviral defence as a community resource.* Nat Rev Microbiol, 2020. **18**(2): p. 113-119.
29. Kasman, L.M. and L.D. Porter, *Bacteriophages*, in *StatPearls*. 2022: Treasure Island (FL).
30. Samson, J.E., et al., *Revenge of the phages: defeating bacterial defences.* Nature Reviews Microbiology, 2013. **11**(10): p. 675-687.
31. Fineran, P.C., *Resistance is not futile: bacterial 'innate' and CRISPR-Cas 'adaptive' immune systems.* Microbiology (Reading), 2019. **165**(8): p. 834-841.
32. Vasu, K. and V. Nagaraja, *Diverse functions of restriction-modification systems in addition to cellular defense.* Microbiol Mol Biol Rev, 2013. **77**(1): p. 53-72.
33. Abedon, S.T., *Bacterial 'immunity' against bacteriophages.* Bacteriophage, 2012. **2**(1): p. 50-54.
34. Lopatina, A., N. Tal, and R. Sorek, *Abortive Infection: Bacterial Suicide as an Antiviral Immune Strategy.* Annu Rev Virol, 2020. **7**(1): p. 371-384.
35. Loureiro, A. and G.J. da Silva, *CRISPR-Cas: Converting A Bacterial Defence Mechanism into A State-of-the-Art Genetic Manipulation Tool.* Antibiotics (Basel), 2019. **8**(1).
36. LeRoux, M., S.B. Peterson, and J.D. Mougous, *Bacterial danger sensing.* J Mol Biol, 2015. **427**(23): p. 3744-53.
37. Matzinger, P., *The danger model: a renewed sense of self.* Science, 2002. **296**(5566): p. 301-5.
38. Zhivaki, D. and J.C. Kagan, *Innate immune detection of lipid oxidation as a threat assessment strategy.* Nat Rev Immunol, 2021.
39. Cioffi, W.G., D.G. Burleson, and B.A. Pruitt, Jr., *Leukocyte responses to injury.* Arch Surg, 1993. **128**(11): p. 1260-7.
40. Johnson, L., et al., *Extracellular DNA-induced antimicrobial peptide resistance in Salmonella enterica serovar Typhimurium.* BMC Microbiol, 2013. **13**: p. 115.
41. Childs, A.C., D.J. Mehta, and E.W. Gerner, *Polyamine-dependent gene expression.* Cell Mol Life Sci, 2003. **60**(7): p. 1394-406.
42. Sarkar, N.K., S. Shankar, and A.K. Tyagi, *Polyamines exert regulatory control on mycobacterial transcription: a study using RNA polymerase from Mycobacterium phlei.* Biochem Mol Biol Int, 1995. **35**(6): p. 1189-98.
43. Duprey, A. and E.A. Groisman, *DNA supercoiling differences in bacteria result from disparate DNA gyrase activation by polyamines.* PLoS Genet, 2020. **16**(10): p. e1009085.
44. Banerji, R., et al., *Polyamines in the virulence of bacterial pathogens of respiratory tract.* Mol Oral Microbiol, 2021. **36**(1): p. 1-11.

45. Krysenko, S. and W. Wohlleben, *Polyamine and Ethanolamine Metabolism in Bacteria as an Important Component of Nitrogen Assimilation for Survival and Pathogenicity.* Medical Sciences, 2022. **10**(3): p. 40.
46. Kwon, D.H. and C.D. Lu, *Polyamines induce resistance to cationic peptide, aminoglycoside, and quinolone antibiotics in Pseudomonas aeruginosa PAO1.* Antimicrob Agents Chemother, 2006. **50**(5): p. 1615-22.
47. Shah, P. and E. Swiatlo, *A multifaceted role for polyamines in bacterial pathogens.* Mol Microbiol, 2008. **68**(1): p. 4-16.
48. Ahator, S.D. and L. Zhang, *Small Is Mighty-Chemical Communication Systems in Pseudomonas aeruginosa.* Annu Rev Microbiol, 2019. **73**: p. 559-578.
49. Igarashi, K., et al., *Formation of a compensatory polyamine by Escherichia coli polyamine-requiring mutants during growth in the absence of polyamines.* J Bacteriol, 1986. **166**(1): p. 128-34.
50. Kusano, T. and H. Suzuki, *Polyamines*, in *Polyamine catabolism in plants*. 2015, Springer. p. 77-88.
51. Joshi, G.S., et al., *Arginine catabolic mobile element encoded speG abrogates the unique hypersensitivity of Staphylococcus aureus to exogenous polyamines.* Mol Microbiol, 2011. **82**(1): p. 9-20.
52. Li, B., et al., *Polyamine-independent growth and biofilm formation, and functional spermidine/spermine N-acetyltransferases in Staphylococcus aureus and Enterococcus faecalis.* Molecular Microbiology, 2019. **111**(1): p. 159-175.
53. Ames, B.N. and D.T. Dubin, *The role of polyamines in the neutralization of bacteriophage deoxyribonucleic acid.* J Biol Chem, 1960. **235**: p. 769-75.
54. Reiter, H., *The Location of the Inhibitory Action of Kcn and Several Polyamines on Bacteriophage Replication.* Virology, 1963. **21**: p. 636-41.
55. Firpo, M.R. and B.C. Mounce, *Diverse Functions of Polyamines in Virus Infection.* Biomolecules, 2020. **10**(4).
56. Fukuma, I. and S.S. Cohen, *Polyamine synthesis and accumulation in Escherichia coli infected with bacteriophage R17.* J Virol, 1973. **12**(6): p. 1259-64.
57. Harrison, D.P. and V.C. Bode, *Putrescine and certain polyamines can inhibit DNA injection from bacteriophage lambda.* J Mol Biol, 1975. **96**(3): p. 461-70.
58. Osland, A. and K. Kleppe, *Influence of polyamines on the activity of DNA polymerase I from Escherichia coli.* Biochim Biophys Acta, 1978. **520**(2): p. 317-30.
59. Ouameur, A.A. and H.A. Tajmir-Riahi, *Structural analysis of DNA interactions with biogenic polyamines and cobalt(III)hexamine studied by Fourier transform infrared and capillary electrophoresis.* J Biol Chem, 2004. **279**(40): p. 42041-54.
60. Miller-Fleming, L., et al., *Remaining Mysteries of Molecular Biology: The Role of Polyamines in the Cell.* J Mol Biol, 2015. **427**(21): p. 3389-406.
61. Chou, H.T., et al., *Molecular characterization of PauR and its role in control of putrescine and cadaverine catabolism through the gamma-glutamylation pathway in Pseudomonas aeruginosa PAO1.* J Bacteriol, 2013. **195**(17): p. 3906-13.
62. Chou, H.T., et al., *Transcriptome analysis of agmatine and putrescine catabolism in Pseudomonas aeruginosa PAO1.* J Bacteriol, 2008. **190**(6): p. 1966-75.
63. Lu, C.D., et al., *Functional analysis and regulation of the divergent spuABCDEFGH-spuI operons for polyamine uptake and utilization in Pseudomonas aeruginosa PAO1.* J Bacteriol, 2002. **184**(14): p. 3765-73.

64. Yao, X., W. He, and C.D. Lu, *Functional characterization of seven gamma-Glutamylpolyamine synthetase genes and the bauRABCD locus for polyamine and beta-Alanine utilization in Pseudomonas aeruginosa PAO1.* J Bacteriol, 2011. **193**(15): p. 3923-30.
65. Zhang, Y., et al., *A Potent Anti-SpuE Antibody Allosterically Inhibits Type III Secretion System and Attenuates Virulence of Pseudomonas Aeruginosa.* J Mol Biol, 2019. **431**(24): p. 4882-4896.
66. Fukuchi, J., et al., *Properties and structure of spermidine acetyltransferase in Escherichia coli.* J Biol Chem, 1994. **269**(36): p. 22581-5.
67. Bhattacharyya, S., D.M. Walker, and R.M. Harshey, *Dead cells release a 'necrosignal' that activates antibiotic survival pathways in bacterial swarms.* Nat Commun, 2020. **11**(1): p. 4157.
68. Tzipilevich, E., et al., *Bacteria elicit a phage tolerance response subsequent to infection of their neighbors.* The EMBO Journal, 2022. **41**(3): p. e109247.
69. Kim, J., et al., *A versatile and highly efficient method for scarless genome editing in Escherichia coli and Salmonella enterica.* BMC Biotechnol, 2014. **14**: p. 84.
70. Francis, V.I., et al., *Multiple communication mechanisms between sensor kinases are crucial for virulence in Pseudomonas aeruginosa.* Nat Commun, 2018. **9**(1): p. 2219.
71. Mougous, J.D., et al., *A virulence locus of Pseudomonas aeruginosa encodes a protein secretion apparatus.* Science, 2006. **312**(5779): p. 1526-30.
72. Valentini, M. and A. Filloux, *Biofilms and Cyclic di-GMP (c-di-GMP) Signaling: Lessons from Pseudomonas aeruginosa and Other Bacteria.* J Biol Chem, 2016. **291**(24): p. 12547-12555.
73. Jimenez, P.N., et al., *The multiple signaling systems regulating virulence in Pseudomonas aeruginosa.* Microbiol Mol Biol Rev, 2012. **76**(1): p. 46-65.
74. Fazli, M., et al., *In-Frame and Unmarked Gene Deletions in Burkholderia cenocepacia via an Allelic Exchange System Compatible with Gateway Technology.* Appl Environ Microbiol, 2015. **81**(11): p. 3623-30.
75. Gogokhia, L., et al., *Expansion of Bacteriophages Is Linked to Aggravated Intestinal Inflammation and Colitis.* Cell Host Microbe, 2019. **25**(2): p. 285-299 e8.
76. Chaffin, D.O., et al., *Changes in the Staphylococcus aureus transcriptome during early adaptation to the lung.* PLoS One, 2012. **7**(8): p. e41329.
77. Spiewak, H.L., et al., *Burkholderia cenocepacia utilizes a type VI secretion system for bacterial competition.* Microbiologyopen, 2019: p. e774.
78. Schmidt, A.K., et al., *A Filamentous Bacteriophage Protein Inhibits Type IV Pili To Prevent Superinfection of Pseudomonas aeruginosa.* mBio, 2022: p. e0244121.
79. Davies, J.A., et al., *The GacS sensor kinase controls phenotypic reversion of small colony variants isolated from biofilms of Pseudomonas aeruginosa PA14.* FEMS Microbiol Ecol, 2007. **59**(1): p. 32-46.
80. Okuda, J., et al., *Type IV pilus protein PilA of Pseudomonas aeruginosa modulates calcium signaling through binding the calcium-modulating cyclophilin ligand.* Journal of Infection and Chemotherapy, 2013. **19**(4): p. 653-664.
81. Cain, A.K., et al., *Complete Genome Sequence of Pseudomonas aeruginosa Reference Strain PAK.* Microbiol Resour Announc, 2019. **8**(41).
82. Secor, P.R., et al., *Filamentous Bacteriophage Promote Biofilm Assembly and Function.* Cell Host Microbe, 2015. **18**(5): p. 549-59.
83. Bondy-Denomy, J., et al., *Prophages mediate defense against phage infection through diverse mechanisms.* ISME J, 2016. **10**(12): p. 2854-2866.
84. Cady, K.C., et al., *The CRISPR/Cas adaptive immune system of Pseudomonas aeruginosa mediates resistance to naturally occurring and engineered phages.* J Bacteriol, 2012. **194**(21): p. 5728-38.

85. Mendoza, S.D., et al., *A bacteriophage nucleus-like compartment shields DNA from CRISPR nucleases.* Nature, 2020. **577**(7789): p. 244-248.
86. Shigehisa, R., et al., *Characterization of Pseudomonas aeruginosa phage KPP21 belonging to family Podoviridae genus N4-like viruses isolated in Japan.* Microbiol Immunol, 2016. **60**(1): p. 64-7.
87. Hmelo, L.R., et al., *Precision-engineering the Pseudomonas aeruginosa genome with two-step allelic exchange.* Nature protocols, 2015. **10**(11): p. 1820-41.
88. Yeom, D.H., et al., *Activation of multiple transcriptional regulators by growth restriction in Pseudomonas aeruginosa.* Mol Cells, 2014. **37**(6): p. 480-6.
89. Xuan, G., et al., *RetS Regulates Phage Infection in Pseudomonas aeruginosa via Modulating the GacS/GacA Two-Component System.* J Virol, 2022. **96**(8): p. e0019722.
90. Hickman, J.W., D.F. Tifrea, and C.S. Harwood, *A chemosensory system that regulates biofilm formation through modulation of cyclic diguanylate levels.* Proc Natl Acad Sci U S A, 2005. **102**(40): p. 14422-7.
91. Dalebroux, Z.D. and S.I. Miller, *Salmonellae PhoPQ regulation of the outer membrane to resist innate immunity.* Curr Opin Microbiol, 2014. **17**: p. 106-13.
92. Korgaonkar, A.K. and M. Whiteley, *Pseudomonas aeruginosa enhances production of an antimicrobial in response to N-acetylglucosamine and peptidoglycan.* J Bacteriol, 2011. **193**(4): p. 909-17.
93. Janssen, K.H., et al., *Functional Analyses of the RsmY and RsmZ Small Noncoding Regulatory RNAs in Pseudomonas aeruginosa.* J Bacteriol, 2018. **200**(11).
94. Park, J.Y., et al., *Polyamine is a critical determinant of Pseudomonas chlororaphis O6 for GacS-dependent bacterial cell growth and biocontrol capacity.* Mol Plant Pathol, 2018. **19**(5): p. 1257-1266.
95. Pesavento, C. and R. Hengge, *Bacterial nucleotide-based second messengers.* Current Opinion in Microbiology, 2009. **12**(2): p. 170-176.
96. He, Y., et al., *Correlation between the inhibition of cell growth by accumulated polyamines and the decrease of magnesium and ATP.* Eur J Biochem, 1993. **217**(1): p. 89-96.
97. Bloomfield, V.A., *Condensation of DNA by multivalent cations: considerations on mechanism.* Biopolymers, 1991. **31**(13): p. 1471-81.
98. Potvin, E., F. Sanschagrin, and R.C. Levesque, *Sigma factors in Pseudomonas aeruginosa.* FEMS Microbiol Rev, 2008. **32**(1): p. 38-55.
99. Dar, D. and R. Sorek, *Extensive reshaping of bacterial operons by programmed mRNA decay.* PLoS Genet, 2018. **14**(4): p. e1007354.
100. Liao, Y., G.K. Smyth, and W. Shi, *The R package Rsubread is easier, faster, cheaper and better for alignment and quantification of RNA sequencing reads.* Nucleic Acids Res, 2019. **47**(8): p. e47.
101. Robinson, M.D., D.J. McCarthy, and G.K. Smyth, *edgeR: a Bioconductor package for differential expression analysis of digital gene expression data.* Bioinformatics, 2010. **26**(1): p. 139-40.
102. Mi, H., et al., *Protocol Update for large-scale genome and gene function analysis with the PANTHER classification system (v.14.0).* Nature Protocols, 2019. **14**(3): p. 703-721.
103. Paget, M.S., *Bacterial Sigma Factors and Anti-Sigma Factors: Structure, Function and Distribution.* Biomolecules, 2015. **5**(3): p. 1245-65.
104. Viducic, D., et al., *RpoN Promotes Pseudomonas aeruginosa Survival in the Presence of Tobramycin.* Front Microbiol, 2017. **8**: p. 839.
105. Wright, R.C.T., et al., *Cross-resistance is modular in bacteria-phage interactions.* PLoS Biol, 2018. **16**(10): p. e2006057.
106. Gevrekci, A.Ö., *The roles of polyamines in microorganisms.* World Journal of Microbiology and Biotechnology, 2017. **33**(11): p. 204.

107. Romero, M., et al., *Genome-wide mapping of the RNA targets of the Pseudomonas aeruginosa riboregulatory protein RsmN.* Nucleic Acids Res, 2018. **46**(13): p. 6823-6840.
108. Mo, H. and E.C. Pua, *Up-regulation of arginine decarboxylase gene expression and accumulation of polyamines in mustard (Brassica juncea)in response to stress.* Physiol Plant, 2002. **114**(3): p. 439-449.
109. De Smet, J., et al., *Bacteriophage-mediated interference of the c-di-GMP signalling pathway in Pseudomonas aeruginosa.* Microb Biotechnol, 2021. **14**(3): p. 967-978.
110. Sellner, B., et al., *A New Sugar for an Old Phage: a c-di-GMP-Dependent Polysaccharide Pathway Sensitizes Escherichia coli for Bacteriophage Infection.* mBio, 2021. **12**(6): p. e0324621.
111. Martinez-Granero, F., et al., *The Gac-Rsm and SadB signal transduction pathways converge on AlgU to downregulate motility in Pseudomonas fluorescens.* PLoS One, 2012. **7**(2): p. e31765.
112. Pato, M.L., M.M. Howe, and N.P. Higgins, *A DNA gyrase-binding site at the center of the bacteriophage Mu genome is required for efficient replicative transposition.* Proc Natl Acad Sci U S A, 1990. **87**(22): p. 8716-20.
113. Bravo, J.P.K., et al., *Structural basis for broad anti-phage immunity by DISARM.* Nature Communications, 2022. **13**(1): p. 2987.
114. Wright, A.V., J.K. Nunez, and J.A. Doudna, *Biology and Applications of CRISPR Systems: Harnessing Nature's Toolbox for Genome Engineering.* Cell, 2016. **164**(1-2): p. 29-44.
115. Cohen, D., et al., *Cyclic GMP-AMP signalling protects bacteria against viral infection.* Nature, 2019. **574**(7780): p. 691-695.
116. Doron, S., et al., *Systematic discovery of antiphage defense systems in the microbial pangenome.* Science, 2018. **359**(6379).
117. Nivens, D.E., et al., *Role of alginate and its O acetylation in formation of Pseudomonas aeruginosa microcolonies and biofilms.* J Bacteriol, 2001. **183**(3): p. 1047-57.
118. Schweizer, H.P., *Escherichia-Pseudomonas shuttle vectors derived from pUC18/19.* Gene, 1991. **97**(1): p. 109-21.
119. Ponder, R.G., N.C. Fonville, and S.M. Rosenberg, *A switch from high-fidelity to error-prone DNA double-strand break repair underlies stress-induced mutation.* Mol Cell, 2005. **19**(6): p. 791-804.
120. Faith, D., et al., *Complete Genome Sequence of the N4-like Pseudomonas aeruginosa Bacteriophage vB_PaeP_CMS1.* Microbiol Resour Announc, 2022. **11**(7): p. e0023922.
121. Wein, T. and R. Sorek, *Bacterial origins of human cell-autonomous innate immune mechanisms.* Nat Rev Immunol, 2022. **22**(10): p. 629-638.
122. Johnson, A.G., et al., *Bacterial gasdermins reveal an ancient mechanism of cell death.* Science, 2022. **375**(6577): p. 221-225.
123. Ofir, G., et al., *Antiviral activity of bacterial TIR domains via immune signalling molecules.* Nature, 2021. **600**(7887): p. 116-120.
124. Tyagi, A.K., et al., *Specificity of polyamine requirements for the replication and maintenance of different double-stranded RNA plasmids in Saccharomyces cerevisiae.* Proceedings of the National Academy of Sciences, 1984. **81**(4): p. 1149-1153.
125. Tsang, J., *Bacterial plasmid addiction systems and their implications for antibiotic drug development.* Postdoc J, 2017. **5**(5): p. 3-9.
126. Cirz, R.T., et al., *Defining the Pseudomonas aeruginosa SOS response and its role in the global response to the antibiotic ciprofloxacin.* J Bacteriol, 2006. **188**(20): p. 7101-10.
127. Khan, A.U., et al., *Spermine and spermidine protection of plasmid DNA against single-strand breaks induced by singlet oxygen.* Proc Natl Acad Sci U S A, 1992. **89**(23): p. 11428-30.
128. Oh, T.J. and I.G. Kim, *Polyamines protect against DNA strand breaks and aid cell survival against irradiation in Escherichia coli.* Biotechnology Techniques, 1998. **12**(10): p. 755-758.

129. Ceyssens, P.J., et al., *Molecular and physiological analysis of three Pseudomonas aeruginosa phages belonging to the "N4-like viruses".* Virology, 2010. **405**(1): p. 26-30.
130. Carter, R.H., et al., *Phage N4 RNA polymerase II recruitment to DNA by a single-stranded DNA-binding protein.* Genes Dev, 2003. **17**(18): p. 2334-45.
131. Wagemans, J., et al., *Functional elucidation of antibacterial phage ORFans targeting Pseudomonas aeruginosa.* Cell Microbiol, 2014. **16**(12): p. 1822-35.
132. Wagemans, J., et al., *Antibacterial phage ORFans of Pseudomonas aeruginosa phage LUZ24 reveal a novel MvaT inhibiting protein.* Front Microbiol, 2015. **6**: p. 1242.
133. Brzozowski, R.S., et al., *Deciphering the Role of a SLOG Superfamily Protein YpsA in Gram-Positive Bacteria.* Frontiers in Microbiology, 2019. **10**.